REPUBLIC OF TURKEY
YILDIZ TECHNICAL UNIVERSITY
GRADUATE SCHOOL OF NATURAL AND APPLIED SCIENCES

OUTPUT FEEDBACK SYNCHRONIZATION OF EULER-LAGRANGE SYSTEMS

Elif ÇİÇEK

DOCTOR OF PHILOSOPHY THESIS
Department of Control and Automation Engineering
Program of Control and Automation Engineering

Advisor
Assist. Prof. Dr. Janset DAŞDEMİR

May, 2019

REPUBLIC OF TURKEY
YILDIZ TECHNICAL UNIVERSITY
GRADUATE SCHOOL OF NATURAL AND APPLIED SCIENCES

OUTPUT FEEDBACK SYNCHRONIZATION OF EULER-LAGRANGE SYSTEMS

A thesis submitted by Elif ÇİÇEK in partial fulfillment of the requirements for the degree of **DOCTOR OF PHILOSOPHY** is approved by the committee on 22.05.2019 in Department of Control and Automation Engineering, Program of Control and Automation Engineering.

Assist. Prof. Dr. Janset DAŞDEMİR
Yildiz Technical University
Advisor

Approved By the Examining Committee

Assist. Prof. Dr. Janset DAŞDEMİR, Advisor
Yildiz Technical University

Prof. Dr. Galip CANSEVER, Member
Yildiz Technical University

Prof. Dr. Erkan ZERGEROĞLU, Member
Gebze Technical University

Assist. Prof. Dr. Levent UCUN, Member
Yildiz Technical University

Assoc. Prof. Dr. Volkan SEZER, Member
İstanbul Technical University

I hereby declare that I have obtained the required legal permissions during data collection and exploitation procedures, that I have made the in-text citations and cited the references properly, that I haven't falsified and/or fabricated research data and results of the study and that I have abided by the principles of the scientific research and ethics during my Thesis Study under the title of Output Feedback Synchronization of Euler-Lagrange Systems supervised by my supervisor, Assist. Prof. Dr. Janset DAŞDEMİR. In the case of a discovery of false statement, I am to acknowledge any legal consequence.

Elif ÇİÇEK

Signature

This study was supported by the Scientific and Technological Research Council of Turkey (TUBITAK) Project No: 217E084.

Dedicated to the loving memory of
Naime ÖZADAK
and
Nazire ÇİÇEK

ACKNOWLEDGEMENTS

First of all, I would like to express my profound gratitude to my advisor Assist. Prof. Dr. Janset DAŞDEMİR for her endless support and patience. This PhD study would not have been possible without her immense guidance.

I would also like to thank my committee members, Prof. Dr. Galip CANSEVER, Prof. Dr. Erkan ZERGEROĞLU (GTU), Assist. Prof. Dr. Levent UCUN and Assoc. Prof. Dr. Volkan SEZER (ITU), for their valuable comments.

I appreciate TUBITAK (Turkish Scientific and Technological Research Council of Turkey) for its financial support. (Project Number: 217E084)

I would like to express my thanks to all my colleagues for their support and I am particularly thankful to Res. Asst. Buse TACAL for her endless positive energy.

I wish to thank Tuğçe OFLAZ SIRÖREN for being a true friend and I consider myself lucky to know her.

A very special thank you to my friend and my sister Assoc. Prof. Dr. Elçin TADIHAN ÖZKAN, whose presence, support and guidance I feel at every moment of my life.

Lastly, I am immensely grateful to my mother Rezzan ÇİÇEK, my father Remzi ÇİÇEK and my aunt Suzan ÖZADAK for everything. I would not be where I am today without their unconditional love and support.

Elif ÇİÇEK

TABLE OF CONTENTS

LIST OF SYMBOLS

$q_i(t)$	Actual Position
$\dot{q}_i(t)$	Actual Velocity
$\ddot{q}_i(t)$	Actual Acceleration
$\chi_i(t)$	Auxiliary Variable for Nonlinear Terms
$\tilde{N}_i(t)$	Auxiliary Variable for Nonlinear Terms
$C_i(q_i, \dot{q}_i)$	Centripetal-Coriolis Matrix
k_{1i}	Controller and Filter Gain
$\tau_i(t)$	Control Input (Torque)
$F_i(t)$	Control Input (Force)
k_{2i}	Controller and Filter Gain
$q_{di}(t)$	Desired Position
$\dot{q}_{di}(t)$	Desired Velocity
$\ddot{q}_{di}(t)$	Desired Acceleration
$x_i(t)$	End-Effector Actual Position
$x_{di}(t)$	End-Effector Desired Position
$\dot{x}_{di}(t)$	End-Effector Desired Velocity
$\ddot{x}_{di}(t)$	End-Effector Desired Acceleration
$b_i(t)$	External Disturbance Values
$\hat{b}_i(t)$	External Disturbance Estimations
$\eta_i(t)$	Filtered Tracking Error-like Signal
F_{di}	Friction Effects
$G_i(q_i)$	Gravitational Forces
$M_i(q_i)$	Inertia Matrix

$p_i(t)$	Linear-Filter Auxiliary Signal
$r_{fi}(t)$	Linear-Filter Auxiliary Signal
$\dot{p}_i(t)$	Linear-Filter Auxiliary Signal Dynamics
k_{fi}	Linear-Filter Gain
α	Linear-Filter Gain
e_{fi}	Linear-Filter Output Signal
N	Number of Agents in the Network
$e_i(t)$	Position Tracking Error
$Y_i(t)$	Regression Matrix
j	Represents Agents, that i^{th} Agent Receives Information
l	Represents Agents, that i^{th} Agent Sends Information
$\mathscr{S}$	Set, Containing all Agents in the Network
$\mathscr{S}_i$	Subset of $\mathscr{S}$, Containing all Agents, that i^{th} Agent Receives Information
$\mathscr{S}_l$	Subset of $\mathscr{S}$, Containing all Agents, that i^{th} Agent Sends Information
δ_{ij}	Symbol of Communication
k_{3ij}	Synchronization Gain
k_{4ij}	Synchronization Gain
$\theta_i(t)$	System Parameter Values
$\hat{\theta}_i(t)$	System Parameter Estimations
$T_{ij}(t)$	Time-varying Communication Delay
$\dot{e}_i(t)$	Velocity Tracking Error

LIST OF ABBREVIATIONS

EMK	Exact Model Knowledge
FSFB	Fullstate Feedback
RISE	Robust Integral Sign of the Error

LIST OF FIGURES

LIST OF TABLES

ABSTRACT

Output Feedback Synchronization of Euler-Lagrange Systems

Elif ÇİÇEK

Department of Control and Automation Engineering
Doctor of Philosophy Thesis

Advisor: Assist. Prof. Dr. Janset DAŞDEMİR

This dissertation is devoted to offer a comprehensive control structure for tracking synchronization of Euler-Lagrange systems. For this purpose, three different output-feedback control mechanisms are developed for uncertain systems. Assuming that only position measurement is available, a linear-filter is suggested to obtain a surrogate signal, instead of actual velocity errors. Linear-filter output signals and the position errors are shared over a directed communication, in the presence of variable time-delay. In the first part of the study, a Lyapunov-based stability analysis using Lyapunov-Krasovskii functionals is performed to show that designed adaptive output-feedback controller yields a semi-global asymptotic convergence of error signals to zero. In the second part, it is proven that suggested robust output-feedback controller ensures semi-global asymptotic convergence of error signals to an adjustable hyperball around zero. The synchronization of kinematically redundant systems is also considered. It is shown that the suggested output feedback controller provides tracking synchronization on Cartesian space. The analysis results are supported by presented simulation and experimental studies.

Keywords: Synchronization, uncertain systems, output-feedback control, Euler-Lagrange systems, time-varying communication delay.

YILDIZ TECHNICAL UNIVERSITY
GRADUATE SCHOOL OF NATURAL AND APPLIED SCIENCES

ÖZET

Euler-Lagrange Sistemlerin Çıkış Geribeslemeli Senkronizasyonu

Elif ÇİÇEK

Kontrol ve Otomasyon Mühendisliği Anabilim Dalı
Doktora Tezi

Danışman: Dr. Öğr. Üyesi Janset DAŞDEMİR

Bu doktora çalışmasında, Euler-Lagrange sistemlerin yörünge takip senkronizasyonu için kapsamlı bir denetleyici yapısının tasarımı ele alınmıştır. Bu amaçla, belirsizlik içeren sistemler için üç farklı çıkış geri beslemeli denetim mekanizması geliştirilmiştir. Tüm denetleyici yapılarında yalnızca konum bilgisinin ölçülebildiği varsayılmış, gerçek hız hataları yerine kullanılması için yardımcı sinyal üreten doğrusal bir filtre önerilmiştir. Doğrusal filtre çıkış sinyalleri ve konum hataları, değişken zaman gecikmesi varlığında tek yönlü bir haberleşme ağı üzerinden paylaşılmıştır. Lyapunov-Krasovskii fonksiyonelleri içeren kararlılık analizi sonucunda, tasarlanan uyarlamalı denetleyicinin hata sinyallerini yarı küresel asimptotik olarak sıfıra sürdüğü gösterilmiştir. Önerilen dayanıklı denetleyici ise, hata sinyallerinin yarı küresel asimptotik olarak orijin çevresinde boyutları ayarlanabilir bir küre çevresine yakınsamasını sağlamıştır. Kartezyen uzay üzerinde kinematik açıdan fazla serbestlik derecesi içeren sistemlerin senkronizasyonu konusunda ise, geliştirilen dayanıklı denetleyicinin elemanlar arasında senkronizasyonu sağladığı gösterilmiştir. Sunulan yapıların uygulanabilirliği, benzetim ve deneysel çalışma sonuçları ile gösterilmiştir.

Anahtar Kelimeler: Senkronizasyon, belirsiz sistemler, çıkış geribeslemeli denetim, Euler-Lagrange sistemler, değişken zaman gecikmesi.

YILDIZ TEKNİK ÜNİVERSİTESİ
FEN BİLİMLERİ ENSTİTÜSÜ

1
Introduction

1.1 Literature Review

Synchronization is one of the major areas of interest in the control of electromechanical systems. Fundamentally, synchronization can be defined as the mutual time conformity (agreement in time) of the multiple interacting systems [1]. Most complex processes (assembling, transporting, underway replenishment, geological surveying, towing large and heavy units, etc) can not be executed efficiently and safely by a single system. On the other hand, cooperative synchronization algorithms can bring advantage on flexibility, manipulability and maneuverability. Historically, many studies associated with synchronization has focused on single or double integrator dynamic models [2]. It is worth pointing out that due to the complexity of dynamic (time-varying) systems in real applications, it is exigence to use nonlinear models to ensure high-precision and accurate tracking synchronization [3]. As the most frequently used method, the Euler-Lagrange formulation finds place in distributed synchronization of electromechanical systems, as illustrated in [4], [5] and [6].

According to the information type and exchange structure between each member (agent) of the system, synchronization can be investigated under the general definitions given below:

- *Consensus:*[7] The aim of the consensus control structure is to ensure "an agreement" between states/outputs of agents in the system and let them to reach to an unspecified common value, which is usually the average value of initial states of agents.
- *Tracking Synchronization:*[8] The control structure for tracking synchronization ensures all of the agents follow the given bounded desired trajectory, simultaneously.

In the literature, existing studies investigate the synchronization problem of electromechanical systems as a conventional tracking problem with multiple agents, connected to each other via an appropriate topology. In Leader-Follower approach, as in [9] and [10], a FSFB PD-type and RISE type controllers are presented, respectively. In [9] variable time-delay issue is considered. For the consensus structure, [11] suggests an EMK FSFB controller, that does not need initial condition knowledge and deals with constant time-delays on the communication topology.

In [12], global asymptotic tracking synchronization is ensured by using a FSFB adaptive controller. In [13] FSFB velocity-based and acceleration-based control structures is presented for the synchronization of a system under constant time-delay effect. In another work [8], synchronization of non-identical agents modeled by Euler-Lagrange equations is considered and a global asymptotic synchronization result under constant time-delay effect is provided.

Presented adaptive neural network controller in [14] provides synchronization in a system with uncertainty and offers a robust term to cope with neural network approximation errors and additive disturbances.

Studies in [15], [16], [17], [18] and [19] deal with task-space synchronization (i.e. end-effector synchronization) of robot manipulators. Under the assumption of kinematic and dynamic uncertainty, [15], [17] and [18] provide adaptive controllers. These controllers need the measurement of joint velocities and estimate the end-effector velocities with the help of estimated Jacobian matrix. In addition, [17] and [18] take constant time-delay on a switching topology and strongly connected topology into consideration, respectively. Unlike these three works, [16] deals with variable time-delay problem using a FSFB adaptive controller and also mentions kinematically redundant robot manipulator structure. A recent study [19] presents a sliding mode controller and uses a low-pass filter to reduce the chattering effect on the control signal.

In study [20], the effects of constant time delay on a strongly connected and directed communication topology is considered and an adaptive FSFB control for multiple vessels is offered. In [21], synchronization of spacecrafts with a directed spanning tree communication topology is addressed and an adaptive controller is suggested to deal with constant time delay and external disturbance. As a recent work, [22] proposes a robust controller for synchronization of multiple mobile robot manipulators. In the same study, the effects of constant delay and obstacle avoidance problem are also considered.

It is worth noting that all control mechanisms mentioned above require FSFB structure, i.e. velocity measurement. To reduce the cost and bring robustness against measurement noise, it is beneficial to use observer or filter structure combining with synchronization/tracking controller as in a single electromechanical system.

In this sense, [23] suggests an observer-based EMK controller for a master-slave structure, while [24] presents an EMK controller, for Leader-Follower coordination in task-space, that requires the velocity information provided by a virtual leader. In other studies of the authors, [25] and [26], they redefine Leader-Follower problem structures for underway replenishment problem of vessels.

Considering the robot manipulator synchronization, [27], [28] and [29] offer observer-based EMK controllers. As the communication topology [27] suggests all-to-all connection, while [28] uses directed structure and allows only a subset of followers have the knowledge of desired trajectory.

The observer-based EMK controller presented in [30], provides synchronization of multiple vessels, under the effects of external disturbances. In [31], the synchronization problem of multiple mobile robot manipulators is solved by using an adaptive control structure. In the designed controller, joint velocities of manipulator parts are directly measured and used, while the end-effector velocity information is maintained by a global state observer.

All these studies on synchronization require exact dynamic model knowledge, which is not always possible to obtain. In this context, as the most related work with the aim of this thesis, an observer-based EMK control mechanism only for consensus under the effects of variable time-delay is presented in [32].

1.2 Objective of the Thesis

The aim of this dissertation is to design output-feedback control structures in adaptive and robust approaches for the distributed tracking synchronization of Euler-Lagrange systems.

The general problem is handled in two parts; tracking problem to the given desired trajectory for each agent and synchronization problem between agents in the system. For this purpose, three different control mechanisms are offered and in all cases it is assumed that velocity measurement is not available. Inspired by the studies in [33] and [34], linear-filter structures are suggested to obtain a surrogate signal, instead actual velocity error. General structures of suggested output-feedback controllers can be presented as follows

$$\tau_i(t) = \tau_{tracking}(t) + \sum_{j\in\mathscr{S}_i} \delta_{ij} k_{3ij}(e_i(t) - e_j(t - T_{ij}(t))) \\ - \sum_{j\in\mathscr{S}_i} \delta_{ij} k_{4ij}(e_{fi}(t) - e_{fj}(t - T_{ij}(t))) \tag{1.1}$$

where $\tau_i(t)$ represents the control input of each agent in the system. In the given formulation, $\tau_{tracking}(t)$ symbolizes tracking control structure. It is assumed that there exist uncertainties and external disturbances in the system. To this end, an adaptive and a robust controller are suggested for the tracking problem. Last two terms given in (1.1) stand for synchronization, where communication between agents is denoted by δ_{ij}, i.e. $\delta_{ij} = 1$ or 0. As can be seen from the formulation, position error $e_j(t - T_{ij}(t))$ and surrogate signal $e_{fj}(t - T_{ij}(t))$ of neighbor agent, that are shared over a directed communication topology with a variable time-delay $T_{ij}(t)$, are included into the proposed tracking control laws. As a result, the presented control structure regulates the transient period of operation and ensures simultaneous convergence of position errors to zero.

Hence, as a result of performed the Lyapunov-based stability analysis with Lyapunov-Krasovskii functionals, the suggested adaptive output-feedback controller guarantees the semi-global asymptotic convergence of tracking errors of each agent and synchronization errors between agents to zero, under the effects of variable time-delay on communication topology and external disturbances. Besides, proposed robust output-feedback control mechanism ensures semi-global asymptotic convergence of error signals to an adjustable hyperball around the origin. Presented simulation and experimental results show that the proposed linear-filter based control structures are applicable for synchronization.

Synchronization of kinematically redundant robot manipulators in task-space is also examined. To this end, a new output-feedback robust controller is presented, that ensures uniform ultimate boundedness of tracking errors for each agent and synchronization errors between agents, when there exists variable time delay on communication topology.

1.3 Hypothesis

This dissertation sought to offer solutions on synchronization in the following senses:

a. Similar to a single Euler-Lagrange formulated system, velocity measurement may not be always available or may cause problems, like measurement noise.

To overcome this issue, linear-filter based controllers are suggested.

b. Considering the real-time applications, it is hard to implement EMK based controllers. Sometimes uncertainties on physical parameters (mass, length, etc.) or lack of information on dynamic equations of the system model cause performance degradation. To this end, proposed linear-filters are designed without using dynamic model information. In Section 3, an adaptive controller is suggested for the case that physical parameters of agents are not known. The presented robust control structure in Section 4 provides synchronization without model information, only with the assumption, that the system can be formulated by Euler-Lagrange equations, theoretically. In Section 5, it is shown that task-space synchronization under kinematic redundancy can be obtained with bounded position errors, when there exists partial uncertainty on system parameters.

c. Based on the existing literature on synchronization, time-delay effects experienced during the transmission of information is an important problem. Effects of time-delay in real implementation can not be neglected, because these effects may cause deterioration or even instability [35, 36]. In this sense, with the help of Lyapunov-Krasovskii functionals, it is proved that the introduced control laws cope with the effects of variable time-delays.

Suggested output-feedback control laws differ from the existing literature presented in Section 1.1, since the effects of lack of velocity measurements, time-varying delay on a directed communication topology, dynamic model uncertainties and external disturbances are taken into account, simultaneously.

For the sake of presentation integrity, the prior controller design published in [37], which suggests solution for the synchronization of Euler-Lagrange systems by using a linear-filter based adaptive controller with undirected interconnection topology, is not included in this dissertation due to differences in structures and conditions.

2
Preliminaries

In this chapter some useful definitions and theorems, related with mathematical aspect of this dissertation, are presented. After introducing the Euler-Lagrange formulation, detailed information about the experimental setup, used during the test of the proposed control structures, is given.

2.1 Mathematical Background

2.1.1 Norm Definitions

Definition 2.1. (**Vector Norm**) [38] Consider a vector x, defined in real or complex vector space X. The norm function $||\cdot||$ symbolizes the mapping of X into $\mathbb{R}$ with the following conditions as

- $||x|| \geq 0$ for $\forall x \in X$ and $||x|| = 0$ iff $x = 0$.
- $||\alpha x|| = |\alpha|||x||$ for $\forall x \in X$ and all scalars α.
- $||x + y|| \leq ||x|| + ||y||$ for $\forall x, y \in X$.

For a vector set $X \in \mathbb{R}^n$, following norms can be defined as

- $||x||_1 = \sum_{i=1}^{n} |x_i|$ $\quad 1 - norm$
- $||x||_2 = \sum_{i=1}^{n} \left(|x_i|^2\right)^{1/2}$ $\quad 2 - norm$
- $||x||_p = \sum_{i=1}^{n} (|x_i|^p)^{1/p}$ $\quad p - norm$
- $||x||_\infty = max_{1 \leq i \leq n} |x_i|$ $\quad \infty - norm$

Definition 2.2. (**Matrix Norm**) [39] A matrix norm $||\cdot||$ of $A \in \mathbb{R}^{nxn}$ satisfies the following conditions

- $||A|| \geq 0$ and $||A|| = 0$ iff $A = 0$.
- $||\alpha A|| = |\alpha| ||A||$ for all scalar values α.
- $||A + B|| \leq ||A|| + ||B||$ for all matrices with same size.
- For matrices with appropriate size $||AB|| \leq ||A|| ||B||$.

Considering a symmetrical matrix $A \in \mathbb{R}^{nxn}$

- For all $x \in \mathbb{R}^n$ and $x \neq 0$, if $x^T Ax > 0$, then A is positive definite.
- For all $x \in \mathbb{R}^n$, if $x^T Ax \geq 0$, then A is positive semi-definite.
- For all $x \in \mathbb{R}^n$ and $x \neq 0$, if $x^T Ax < 0$, then A is negative definite.
- For all $x \in \mathbb{R}^n$, if $x^T Ax \leq 0$, then A is negative semi-definite.
- If for some $x \in \mathbb{R}^n$ $x^T Ax > 0$ and $x^T Ax < 0$ for other $x \in \mathbb{R}^n$, then A is indefinite.

Definition 2.3. (**Function Norms**) [39] For a function $f : \mathbb{R} \rightarrow \mathbb{R}$, $\mathscr{L}_p$ norm of f can be defined as

$$||f(t)||_p = \left(\int_0^{\inf} |f(\omega)|^p d\omega \right)^{1/p}$$

where $p = [1, \infty)$. If $p = \infty$, then $\mathscr{L}_\infty$ norm of function f is $||f(t)|| = max_{i\geq 0}|f(t)|$

2.1.2 Theorems and Lemmas

Theorem 2.1. *(**Lyapunov Stability Theorem**) [40] Consider a system defined as $\dot{x} = f(t,x), x(0) = x_0$ with an equilibrium point at the origin as $f(t,0) = 0$ and let B_{R0} be a ball around equilibrium point. Then,*

- *The origin is stable in the sense of Lyapunov, if, for all $x \in B_{R0}$, there exists a scalar function $V(t,x) > 0$ and $\dot{V}(t,x) \leq 0$.*
- *The origin is asymptotically stable if $V(t,x) > 0$ and $\dot{V}(t,x) < 0$ for all $x \in B_{R0}$.*
- *The origin is globally asymptotically stable, if B_{R0} is replaced by $\mathbb{R}^n$ and if $V(x,t)$ is positive definite, $\dot{V}(t,x)$ is negative definite and $V(t,x)$ is radially unbounded, i.e. $||x|| \rightarrow \infty$ when $t \rightarrow \infty$.*

Lemma 2.2. *(**Barbalat Lemma**) [40] Consider a differentiable function $f(t)$ and it has a finite limit as $t \rightarrow \infty$. Then,*

- $\lim_{t\to\infty} \dot{f}(t) = 0$, *if* $\dot{f}(t)$ *is uniformly continuous and* $\lim_{t\to\infty} f(t) = k < \infty$.
- $\lim_{t\to\infty} f(t) = 0$, *if* $f(t)$ *is uniformly continuous and* $\lim_{t\to\infty} \int_0^\infty f(\omega)d\omega = k < \infty$.
- $\lim_{t\to\infty} \dot{V}(t,x) = 0$, *if* $V(t,x)$ *is lower bounded,* $\dot{V}(t,x)$ *is negative semi-definite and uniformly continuous along the trajectory* $\dot{x} = f(t,x)$.
- $\lim_{t\to\infty} \dot{g}(t) = 0$, *if* $g, \dot{g} \in \mathscr{L}_\infty$ *and* $g(t) \in \mathscr{L}_p$ *for* $p = [1,\infty)$ *where* $f(t) = |g(t)|^p$.

Theorem 2.3. ***(Lyapunov-Krasovskii Theorem)*** *[41] Consider a function* $f : \mathbb{R}^+ \times \mathbb{C} \to \mathbb{R}^n$ *for the system* $\dot{x} = f(t,x_t)$ *and there exist scalar, continuous, positive and non-decreasing functions* $u(s)$*,* $v(s)$ *and* $w(s)$*. The following conditions are satisfied if there exists a continuous functional* $V : \mathbb{R}^+ \times \mathbb{C} \to \mathbb{R}^n$ *as*

$$u(|x_t(0)|) \leq V(t,x_t) \leq v(\|x_t\|)$$
$$\dot{V}(t,x_t) < -w(|x_t(0)|)$$

then, $x_t = 0$ *is uniformly asymptotically stable, where* x_t *(for a given time instant* t*) is a function defined as* $x_t(\theta) = x(t+\theta)$ *for* $\theta \in [-T(t), 0]$ *with the finite time-delay* $T(t) \in \mathbb{R}^+$ *and* $\dot{T}(t) < 1$.

2.1.3 Euler-Lagrange Based Dynamic Model Formulation

For electromechanical systems, the general equation of motion can be obtained by using Euler-Lagrange formulation as

$$\tau = \frac{d}{dt}\frac{\partial L}{\partial \dot{q}} - \frac{\partial L}{\partial q} \tag{2.1}$$

where $q \in \mathbb{R}^n$ is the generalized coordinates, $\tau \in \mathbb{R}^n$ is the generalized forces and L symbolizes the Lagrange equation as

$$L(q,\dot{q}) \triangleq T(q,\dot{q}) - U(q) \tag{2.2}$$

with $T(q,\dot{q})$ and $U(q)$ stand for kinetic and potential energies, respectively.

In a multi-agent system consisting N networked electromechanical systems, the Euler-Lagrange based dynamic model of i^{th} agent can be described as

$$M_i(q_i)\ddot{q}_i + C_i(q_i,\dot{q}_i)\dot{q}_i + F_{di}\dot{q}_i + G_i(q_i) = \tau_i + b_i \tag{2.3}$$

where the subscript i is an element of the set $\mathscr{S}$, i.e. $\mathscr{S} \triangleq \{1,...,N\}$. In the equation given in (2.3), $q_i(t) \in \mathbb{R}^n$ symbolizes the generalized coordinates, with its time derivatives $\dot{q}_i(t)$ and $\ddot{q}_i(t)$. The positive definite, symmetric matrix $M_i(q_i) \in \mathbb{R}^{nxn}$ expresses the inertia effects, the matrix $C_i(q_i,\dot{q}_i) \in \mathbb{R}^{nxn}$ stands for the Centripetal-Coriolis forces, $F_{di} \in \mathbb{R}^{nxn}$ denotes the friction effects, vector $G_i(q_i) \in \mathbb{R}^n$ represents gravitational forces and $\tau_i \in \mathbb{R}^n$ denotes the control/torque input. $b_i \in \mathbb{R}^n$ is the unknown external forces and assumed as constant or slowly time-varying [42].

It is assumed that the following properties are valid for the dynamic model given in (2.3).

Property 1: [39] The inertia matrix $M_i(q_i)$ is bounded in the sense

$$m_{1i}||\varsigma_i||^2 \leq \varsigma_i^T M_i(q_i)\varsigma_i \leq m_{2i}||\varsigma_i||^2 \qquad \forall \varsigma_i \in \mathbb{R}^n. \tag{2.4}$$

The scalars m_{1i} and m_{2i} are positive and $||\cdot||$ is the Euclidean Norm operator.

Property 2: [39] The skew-symmetry condition holds for the Coriolis matrix $C_i(q_i,\dot{q}_i)$ and the time derivative of $M_i(q_i)$ as

$$\varsigma_i^T\left(\dot{M}_i(q_i) - 2C_i(q_i,\dot{q}_i)\right)\varsigma_i = 0 \qquad \forall \varsigma_i \in \mathbb{R}^n. \tag{2.5}$$

Property 3: [43] For the vectors $\varsigma_i, \upsilon_i \in \mathbb{R}^n$, the Coriolis matrix satisfies the following condition

$$C_i(q_i,\upsilon_i)\varsigma_i = C_i(q_i,\varsigma_i)\upsilon_i. \tag{2.6}$$

Property 4: [39] The norms of Coriolis and Friction matrices and Gravity vector can be bounded as

$$||C_i(q_i,\varsigma_i)|| \leq \zeta_{C_{2i}}||\varsigma_i||, \qquad ||F_{di}|| \leq \zeta_{F_{di}}, \qquad ||G_i(q_i)|| \leq \zeta_{G_{2i}} \tag{2.7}$$

where $\zeta_{C_{2i}}$, $\zeta_{F_{di}}$ and $\zeta_{G_{2i}}$ are positive scalars.

Property 5: [39] The dynamic model given in (2.3) is linearly parametrizable in the sense

$$Y_i(q_i, \dot{q}_i, \ddot{q}_i)\theta_i = M_i(q_i)\ddot{q}_i + C_i(q_i, \dot{q}_i)\dot{q}_i + F_{di}\dot{q}_i + G_i(q_i) \tag{2.8}$$

with $\theta_i \in \mathbb{R}^p$ the parameter vector and $Y_i(q_i, \dot{q}_i, \ddot{q}_i) \in \mathbb{R}^{nxp}$ the regression matrix depending on variables $q_i(t), \dot{q}_i(t), \ddot{q}_i(t)$.

2.1.4 The Jacobian Matrix

As an electromechanical system, the dynamic model of a robot manipulator can be expressed as given in (2.3).

The end-effector position $x_i \in \mathbb{R}^m$ can be defined in Cartesian space with dimension m, as

$$x_i = f_i(q_i) \tag{2.9}$$

where $f_i(q_i) \in \mathbb{R}^m$ represents the direct kinematics as the function of joint angles $q_i(t) \in \mathbb{R}^n$. The generalized Cartesian velocity can be obtained by taking the time derivation of (2.9) as

$$\dot{x}_i = J_i(q_i)\dot{q}_i \tag{2.10}$$

where the Jacobian matrix, denoted by $J_i(q_i) \in \mathbb{R}^{nxm}$, has the definition

$$J_i(q_i) = \frac{\partial f_i(q_i)}{\partial q_i}. \tag{2.11}$$

The Jacobian matrix given in (2.10) is invertible, as long as the robot manipulator is kinematically non-redundant, in other words the dimension of link position variables n is equal to the dimension of Cartesian space m.

On the other hand, when the robot manipulator is kinematically redundant (i.e. $n > m$), the Jacobian matrix is not square and thus, it does not has an inverse. Under these circumstances, the pseudo-inverse of $J_i(q_i)$ is defined as

$$J_i^+ = J_i^T \left(J_i J_i^T\right)^{-1} \tag{2.12}$$

with the following condition

$$J_i J_i^+ = I_m \tag{2.13}$$

where $I_m \in \mathbb{R}^{mxm}$ represents the identity matrix. The pseudo-inverse term given in (2.12) satisfies the following Moore-Penrose Conditions [44]

$$\begin{aligned} J_i J_i^+ J_i &= J_i \\ J_i^+ J_i J_i^+ &= J_i^+ \\ \left(J_i^+ J_i\right)^T &= J_i^+ J_i \\ \left(J_i J_i^+\right)^T &= J_i J_i^+ \end{aligned} \tag{2.14}$$

Also, the matrix $(I_n - J_i^+ J_i)$ satisfies the conditions presented below

$$\begin{aligned} J_i(I_n - J_i^+ J_i) &= 0 \\ (I_n - J_i^+ J_i)J_i^+ &= 0 \\ (I_n - J_i^+ J_i)(I_n - J_i^+ J_i) &= (I_n - J_i^+ J_i) \\ (I_n - J_i^+ J_i)^T &= (I_n - J_i^+ J_i). \end{aligned} \tag{2.15}$$

2.2 Experimental Setup

To examine the applicability of output-feedback control structures given in Section 3 and Section 4, experimental studies have been conducted on a system consisting 3 three-link *Touch*^{TM} robot manipulators (Figure 2.1), produced by 3D Systems®. The robot manipulators have the specifications given Table 2.1 [45].

Table 2.1 Touch^{TM} Specifications

Specifications	**Touch^{TM}**
Workspace	> 160W x 120H x 70D mm
Nominal position resolution	-0.055 mm
Maximum exertable force and torque at nominal position	3.3 N
Position sensing	x,y,z (digital encoders)
Interface	USB 2.0

The experiment setup can be seen in Figure 2.2. Each manipulator has been controlled

Figure 2.1 3D Systems Touch^{TM} robot manipulator

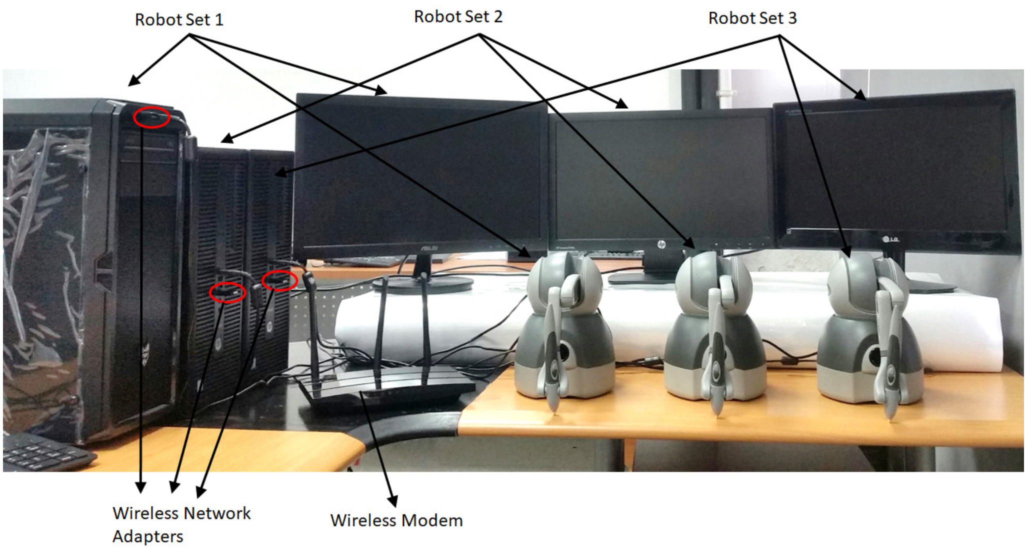

Figure 2.2 Experimental setup

with a separate computer, in the sense of distributed control structure. Encoder data of manipulators has been collected by using OpenHaptics SDK [46] software from the control cards of $Touch^{TM}$. All the work on computers has been carried out using $MATLAB^{TM}/Simulink^{TM}$ and Phansim Toolkit [47]. As an open source library, Phansim Toolkit collects encoder data with the help of OpenHaptics SDK codes and makes them readable for $MATLAB^{TM}/Simulink^{TM}$. Similarly, the control signal produced by the model conducted on $MATLAB^{TM}/Simulink^{TM}$, is applied to manipulators through Phansim Toolkit and OpenHaptics SDK. In order to share the position errors of the manipulators and the linear filter output signals via the communication topology given in Chapters 3 and 4, three wireless network adapters have been installed in the computers that communicate with each other via the wireless modem and the data has been sent / received using $MATLAB^{TM}/Simulink^{TM}$ blocks *UDP Send/Receive*, from the *Instrument Control Toolbox*. All experiments were conducted with *ODE2 (Heun)* solver for a sampling frequency $1kHz$.

3
Adaptive Output Feedback Synchronization

In this section, an output-feedback adaptive control structure for position synchronization problem of Euler-Lagrange formulated systems is provided. After the problem definition, suggested filter and controller designs are given, in detail. Then, Lyapunov-based convergence analysis using Lyapunov-Krasovskii functionals is utilized to show semi-global asymptotic convergence of all errors, including synchronization errors, to zero, under the effects of parametric uncertainty, external disturbances and variable communication delay. Lastly, simulation and experimental results of proposed filter based adaptive controller are presented.

3.1 Problem Definition

This study focuses on to ensure the trajectory tracking and position synchronization of each agent in a system, simultaneously. In this manner, the position tracking error $e_i(t) \in \mathbb{R}^n$ ($i \in \mathscr{S} \triangleq \{1, .., N\}$) can be defined for each agent with the dynamical model given in (2.3), as

$$e_i(t) = q_{di} - q_i. \tag{3.1}$$

In (3.1), $q_{di}(t)$ represents the desired trajectory and for the sake of subsequent stability analysis, it is assumed that it is a bounded function of time as well as its first three time derivatives.

3.2 Filter Design

To deal with the lack of velocity measurement, by using position error information the following linear filter is constructed to provide position tracking with the output $e_{fi} \in \mathbb{R}^n$ as

$$e_{fi}(t) = -(k_{1i} + 1)e_i + p_i \tag{3.2}$$

where $p_i(t) \in \mathbb{R}^n$ is an auxiliary signal with the dynamics

$$\begin{aligned} \dot{p}_i(t) =& -(k_{1i}+1+\alpha)p_i + ((k_{1i}+1)^2 - (k_{1i}+1) + \alpha(k_{1i}+1) + k_{2i})e_i \\ p_i(0) =& (k_{1i}+1)e_i(0). \end{aligned} \tag{3.3}$$

In equations (3.2) and (3.3), $k_{1i}, k_{2i} \in \mathbb{R}^{nxn}$, $\alpha \in \mathbb{R}^1$ are positive constant gains and α is same for all agents. The proposed design for the linear filter, mainly based on the work of [33], is similar to a high-pass filter with the position error $e_i(t)$ as the input and the surrogate signal $e_{fi}(t)$ as the output. The given filter definition is useful because it does not require any measurements or exact knowledge of dynamic model other than the position error.

The dynamic model of the linear filter can be obtained by taking the time derivative of (3.2) and inserting (3.3) as follows

$$\dot{e}_{fi}(t) = -\alpha e_{fi} - (k_{1i}+1)\eta_i + k_{2i}e_i \tag{3.4}$$

where the filtered tracking error-like signal $\eta_i(t) \in \mathbb{R}^n$ defined to ease the presentation

$$\eta_i(t) = \dot{e}_i + e_{fi} + e_i. \tag{3.5}$$

Also, by rearranging (3.5) the dynamics of position error for each agent can be represented mathematically as

$$\dot{e}_i(t) = \eta_i - e_{fi} - e_i \tag{3.6}$$

as well as the velocity

$$\dot{q}_i(t) = \dot{q}_{di} - \eta_i + e_{fi} + e_i. \tag{3.7}$$

3.3 Error System Dynamics

As the first step of the process, time derivative of (3.5) is pre-multiplied by $M_i(q_i)$ and the open loop dynamics is established as

$$M_i(q_i)\dot{\eta}_i = M_i(q_i)(\ddot{q}_{di} - \ddot{q}_i) + M_i(q_i)\dot{e}_{fi} + M_i(q_i)\dot{e}_i. \tag{3.8}$$

Substituting (3.4), (3.6) and inserting for $\ddot{q}_i$ from (2.3), it yields

$$\begin{aligned} M_i(\eta_i)\dot{\eta}_i =& M_i(q_i)\ddot{q}_{di} - C_i(q_i,\dot{q}_i)\eta_i - C_i(q_i,\eta_i)(\dot{q}_{di}+e_{fi}+e_i) + F_{di}(\dot{q}_{di}-\eta_i+e_{fi}+e_i) \\ &+ C_i(q_i,\dot{q}_{di}+e_{fi}+e_i)(\dot{q}_{di}+e_{fi}+e_i) + G_i(q_i) \\ &- M_i(q_i)(-k_{1i}\eta_i-(\alpha+1)e_{fi}+(k_{2i}-1)e_i) + Y_{di}\theta_i - \tau_i - b_i - Y_{di}\theta_i \end{aligned} \tag{3.9}$$

where $\dot{q}_i = \dot{q}_{di} - \dot{e}_i$ and the Equation (3.6) are used with the *Property 3* in Section 2.1.3. $Y_{d_i}\theta_i$, given in *Property 5*, is added and subtracted as a step to adaptive control.

For the simplicity, an auxiliary variable, consisting some of the nonlinear terms, $\chi_i(e_i(t),e_{fi}(t)) \in \mathbb{R}^n$ is defined and upper-bounded as

$$\|\chi_i\| \leq \rho_{1i}(\|e_i\|,\|e_{fi}\|)\|e_i\| + \rho_{2i}(\|e_i\|,\|e_{fi}\|)\|e_{fi}\|. \tag{3.10}$$

Details on the bound of χ_i is presented in Appendix A.1. What is notable about this definition is $\chi_i(e_i(t),e_{fi}(t))$ has an upper-bound with measurable signals.

Then, the open loop error dynamics is obtained in the following form

$$\begin{aligned} M_i(q_i)\dot{\eta}_i =& -C_i(q_i,\dot{q}_i)\eta_i - F_{di}\eta_i - \tau_i - b_i - F_{di}\eta_i - M_i(q_i)k_{1i}\eta_i \\ &- C_i(q_i,\eta_i)(\dot{q}_{di}+e_{fi}+e_i) + Y_{di}\theta_i + \chi_i. \end{aligned} \tag{3.11}$$

3.4 The Proposed Controller Scheme

As previously explained in the concept of this work, to ensure the position tracking and synchronization of agents in the system and based on the subsequent stability analysis, filter-based adaptive controller is designed as

$$\begin{aligned} \tau_i =& Y_{d_i}\hat{\theta}_i - \hat{b}_i - \gamma_i(k_{1i}+1)e_{fi} + \gamma_i k_{2i}e_i + \sum_{j\in\mathcal{S}_i}\delta_{ij}k_{3ij}(e_i(t)-e_j(t-T_{ij}(t))) \\ &-(k_{1i}+1)\sum_{j\in\mathcal{S}_i}\delta_{ij}k_{4ij}(e_{fi}(t)-e_{fj}(t-T_{ij}(t))) \end{aligned} \tag{3.12}$$

with the positive and diagonal control gain matrices $\gamma_i, k_{3ij}, k_{4ij} \in \mathbb{R}^{nxn}$, the estimated parameter vector $\hat{\theta}_i \in \mathbb{R}^p$ and external disturbances $\hat{b}_i \in \mathbb{R}^n$, with the update functions

$$\begin{aligned} \hat{\theta}_i(t) =& \Gamma_{1i}Y_{d_i}^T(t)e_i(t) - \Gamma_{1i}\int_0^t \frac{d}{d\omega}\{Y_{d_i}^T(\omega)\}e_i(\omega)d\omega + \Gamma_{1i}\int_0^t Y_{d_i}^T(\omega)(e_{fi}(\omega)+e_i(\omega))d\omega \\ \hat{b}_i(t) =& -\Gamma_{2i}e_i(t) - \Gamma_{2i}\int_0^t (e_{fi}(\omega)+e_i(\omega))d\omega \end{aligned} \tag{3.13}$$

where $\Gamma_{1i} \in \mathbb{R}^{pxp}$ and $\Gamma_{2i} \in \mathbb{R}^{nxn}$ are the positive definite, constant and diagonal adaptation gain matrices. Also, by using (3.5), dynamic definitions for (3.13) can be presented as

$$\begin{aligned} \dot{\hat{\theta}}_i =& \Gamma_{1i} Y_{d_i}^T \eta_i \\ \dot{\hat{b}}_i =& -\Gamma_{2i} \eta_i. \end{aligned} \tag{3.14}$$

The proposed control structure (3.12) can be evaluated in two parts. The first part, consisting first four terms, deal with the tracking problem of each individual agent. The second part with the last two terms of (3.12) stands for the position and velocity synchronization problem, respectively. δ_{ij} given in these terms, represents the communication between agents, i.e. $\delta_{ij} = 1$ if agent j sends information to agent i, otherwise $\delta_{ij} = 0$, and $\mathscr{S}_i$ is a subset of $\mathscr{S}$ consisting all agents that send information to agent i.

The signals $e_j(t-T_{ij}(t))$ and $e_{fj}(t-T_{ij}(t))$ are the versions of $e_j(t)$ and $e_{fj}(t)$ subjected to the time-varying communication delay $T_{ij}(t)$.

Based on the subsequent Lyapunov-based convergence analysis using Lyapunov-Krasovskii functionals [41], the mentioned time-varying delay $T_{ij}(t)$ is a continuously differentiable function and satisfies the condition $\dot{T}_{ij}(t) = d_{ij} < 1$.

Considering a real communication system, it can not be expected that the magnitude of time delay for each interconnection link in the network is same. It will be clearly seen in the stability analysis, that equal-valued time delay $T_{ij}(t)$ for each link is not required to provide synchronization.

Finally, the closed loop dynamics for the filtered tracking error-like signal $\eta_i(t)$ can be obtained by using (3.11) and (3.12) as,

$$\begin{aligned} M_i(q)\dot{\eta}_i =& Y_{di}\tilde{\theta}_i + \tilde{b}_i - C_i(q_i,\dot{q}_i)\eta_i - F_{di}\eta_i - M_i(q_i)k_{1i}\eta_i - C_i(q_i,\eta_i)(\dot{q}_{di} + e_{fi} + e_i) \\ & + \chi_i + \gamma_i(k_{1i}+1)e_{fi} - \gamma_i k_{2i} e_i - \sum_{j\in\mathscr{S}_i} k_{3ij}(e_i(t) - e_j(t - T_{ij}(t))) \\ & + (k_{1i}+1)\sum_{j\in\mathscr{S}_i} k_{4ij}(e_{fi}(t) - e_{fj}(t - T_{ij}(t))) \end{aligned} \tag{3.15}$$

where $\tilde{\theta}_i \in \mathbb{R}^p$ and $\tilde{b}_i \in \mathbb{R}^n$ represent the difference between the real values and estimated values of agents' parameters and external disturbances, respectively, as in the form of $\tilde{\theta}_i = \theta_i - \hat{\theta}_i$ and $\tilde{b}_i = \hat{b}_i - b_i$.

3.5 Stability Analysis

Theorem 3.1. *The filter structure of* (3.2)-(3.3) *and the output feedback control law given by* (3.12) *with the estimation rules in* (3.13) *ensure semi-global asymptotic convergence of all errors to zero and synchronization of the system, that consists of N agents with the dynamic structure given in* (2.3)*, in the following sense*

$$\lim_{t\to\infty} y_i(t) = 0 \tag{3.16}$$

where

$$y_i(t) = \begin{bmatrix} \eta_i(t)^T & e_{fi}(t)^T & e_i(t)^T & s_{ij}(t)^T \end{bmatrix}^T$$

and

$$s_{ij}(t) = \begin{bmatrix} \delta_{ij}(e_i(t) - e_j(t - T_{ij}(t)))^T & \delta_{ij}(e_{fi}(t) - e_{fj}(t - T_{ij}(t)))^T \end{bmatrix}^T.$$

All closed-loop signals remain bounded, as long as following gain conditions hold

$$\alpha = \frac{k_{5ij}}{\lambda_{min}\{k_{4ij}\}} + \frac{\lambda^2_{max}\{k_{1j}+1\}(1-d_{ij})}{4\lambda_{min}\{k_{4ij}\}} + \frac{\lambda^2_{max}\{k_{2i}\}}{\lambda_{min}\{k_{4ij}\}} + \frac{\lambda^2_{max}\{k_{2j}\}(1-d_{ij})}{4\lambda_{min}\{k_{4ij}\}d^2_{ij}} + \frac{\lambda^2_{max}\{k_{4ij}\}(1-d_{ij})}{4\lambda_{min}\{k_{4ij}\}}$$

$$\lambda_{min}\{k_{1i}\} + \zeta_{F_{di}} > \zeta_{C_{2i}}\left(\zeta_{di} + \|e_{fi}(0)\| + \|e_i(0)\|\right) + 2 + \sum_{i\in\mathcal{S}_l} \delta_{li} z_{1li}$$

$$k_{2i} = \frac{k_{6i}}{\gamma_i} + \frac{\rho^2_{1i}}{4\gamma_i} + \frac{\lambda^2_{max}\{k_{4ij}\}}{4\gamma_i}$$

$$\gamma_i = \frac{k_{7i}}{\alpha} + \frac{\lambda^2_{max}\{k_{3ij}\}}{4\alpha} + \frac{\rho^2_{2i}}{4\alpha}$$

$$\lambda_{min}\{k_{3ij}\} > 1 + \frac{1-d_{ij}}{4} + \frac{(1-d_{ij})}{4d^2_{ij}} + \frac{1}{4(1-d_{ij})}$$

$$k_{5ij} > 1 + \frac{1}{4(1-d_{ij})}$$

$$k_{6i} > \sum_{i\in\mathcal{S}_l} \delta_{li} z_{1li} d^2_{li}$$

$$k_{7i} > \sum_{i \in \mathscr{S}_l} \delta_{li} z_{2li} d_{li}^2$$

where

$$z_{1li} = (\lambda_{max}^2\{k_{3li}\} + \lambda_{max}^2\{k_{4li}\}), \quad z_{2li} = \lambda_{max}^2\{k_{3li}\} + \lambda_{max}^2\{k_{4li}\}\alpha^2$$

and the subindice l symbolizes other agents in the system, that receive information from agent i. Additionally, it is possible to show that the synchronization error between $q_i(t)$ and $q_j(t)$ satisfies

$$\lim_{t \to \infty} q_i(t) - q_j(t) = 0 \tag{3.17}$$

if all agents have the same desired trajectory q_d, or

$$\lim_{t \to \infty} q_i(t) - q_j(t) = q_{di}(t) - q_{dj}(t) \tag{3.18}$$

in case of different desired trajectories.

Proof. For each agent in the system, a non-negative function $V_{1i}(t)$ can be defined and the sum of these functions can be used to prove the stability of whole system as

$$\begin{aligned} V_1(t) =& \sum_{i \in \mathscr{S}} V_{1i}(t) \\ =& \frac{1}{2} \sum_{i \in \mathscr{S}} \Big\{ \eta_i^T M_i(q_i) \eta_i + e_i^T k_{2i} \gamma_i e_i + e_{f_i}^T \gamma_i e_{f_i} + \tilde{\theta}_i^T \Gamma_{1i}^{-1} \tilde{\theta}_i \\ & + \tilde{b}_i^T \Gamma_{2i}^{-1} \tilde{b}_i + \sum_{j \in \mathscr{S}_i} \delta_{ij} (e_i(t) - e_j(t - T_{ij}(t)))^T k_{3ij} (e_i(t) - e_j(t - T_{ij}(t))) \\ & + \sum_{j \in \mathscr{S}_i} \delta_{ij} (e_{fi}(t) - e_{fj}(t - T_{ij}(t)))^T k_{4ij} (e_{fi}(t) - e_{fj}(t - T_{ij}(t))) \Big\} \end{aligned} \tag{3.19}$$

which can be bounded as

$$\lambda_1 \|y(t)\|^2 \leq \lambda_1 \|h(t)\|^2 \leq V_1(t) \leq \lambda_2 \|h(t)\|^2 \tag{3.20}$$

where

$$h(t) = \begin{bmatrix} y^T(t) & \tilde{b}^T(t) & \tilde{\theta}^T(t) \end{bmatrix}^T \tag{3.21}$$

and

$$
\begin{aligned}
\lambda_{1i} =& \frac{1}{2} min\Big\{m_{1i}, \lambda_{min}\{\gamma_i\}, \lambda_{min}\{k_{2i}\}, \lambda_{min}\{k_{3ij}\}, \lambda_{min}\{k_{4ij}\}, \lambda_{min}\{\Gamma_{1i}^{-1}\}, \lambda_{min}\{\Gamma_{2i}^{-1}\}\Big\} \\
\lambda_{2i} =& \frac{1}{2} max\Big\{m_{2i}, \lambda_{max}\{\gamma_i\}, \lambda_{max}\{k_{2i}\}, \lambda_{max}\{k_{3ij}\}, \lambda_{max}\{k_{4ij}\}, \lambda_{max}\{\Gamma_{1i}^{-1}\}, \lambda_{max}\{\Gamma_{2i}^{-1}\}\Big\}.
\end{aligned}
\tag{3.22}
$$

Taking the time derivative of (3.19), the following equation can be obtained

$$
\begin{aligned}
\dot{V}_1(t) =& \sum_{i=1}^{N} \Big\{ \eta_i^T \Big[Y_{di}\tilde{\theta}_i + \tilde{b}_i - C_i(q_i, \dot{q}_i)\eta_i - F_{di}\eta_i - M_i(q_i)k_{1i}\eta_i \\
& - C_i(q_i, \eta_i)(\dot{q}_{di} + e_{fi} + e_i) + M_i(q_i)\eta_i + \chi_i + \gamma_i(k_{1i}+1)e_{fi} - \gamma_i k_{2i} e_i \\
& - \sum_{j\in\mathscr{S}_i} k_{3ij}(e_i(t) - e_j(t - T_{ij}(t))) + (k_{1i}+1) \sum_{j\in\mathscr{S}_i} k_{4ij}(e_{fi}(t) - e_{fj}(t - T_{ij}(t))) \Big] \\
& + \frac{1}{2}\eta_i^T \dot{M}_i(q_i)\eta_i - \tilde{\theta}_i^T \Gamma_{1i}^{-1}\Gamma_{1i} Y_{di}^T \eta_i - \tilde{b}_i^T \Gamma_{2i}^{-1}\Gamma_{2i}\eta_i + e_i^T k_{2i}\gamma_i \Big[\eta_i - e_{fi} - e_i \Big] \\
& + e_{fi}^T \gamma_i \Big[-\alpha e_{fi} - (k_{1i}+1)\eta_i + k_{2i}e_i \Big] + \sum_{j\in\mathscr{S}_i} \delta_{ij}(e_i(t) - e_j(t - T_{ij}(t)))^T \\
& \times k_{3ij} \Big[\eta_i(t) - e_{fi}(t) - e_i(t) - (1 - d_{ij})\eta_j(t - T_{ij}(t)) \\
& + (1 - d_{ij})e_{fj}(t - T_{ij}(t)) + (1 - d_{ij})e_j(t - T_{ij}(t)) \Big] \\
& + \sum_{j\in\mathscr{S}_i} \delta_{ij}(e_{f_i}(t) - e_{f_j}(t - T_{ij}(t)))^T \\
& \times k_{4ij} \Big[-\alpha e_{fi}(t) - (k_{1i}+1)\eta_i(t) + k_{2i}e_i(t) + (1 - d_{ij})(k_{1j}+1)\eta_j(t - T_{ij})) \\
& + (1 - d_{ij})\alpha e_{fj}(t - T_{ij}(t)) - (1 - d_{ij})k_{2j}e_j(t - T_{ij}(t)) \Big] \Big\}
\end{aligned}
\tag{3.23}
$$

where (3.4), (3.6), (3.14), (3.15) were utilized. By employing the upper-bound in (3.10) and making some algebraic manipulations (3.23) can be reformulated as

$$
\begin{aligned}
\dot{V}_1(t) \leq \sum_{i=1}^{N} \Bigg\{ & -\Big[\zeta_{F_{di}} + m_{1i}\lambda_{min}\{k_{1i}\}\Big]\|\eta_i\|^2 + \Big[\zeta_{C2i}(\zeta_{di} + \|e_{fi}\| + \|e_i\|)\Big]\|\eta_i\|^2 \\
& + \rho_{1i}\|\eta_i\|\|e_i\| + \rho_{2i}\|\eta_i\|\|e_{fi}\| - k_{2i}\gamma_i\|e_i\|^2 - \gamma_i\alpha\|e_{fi}\|^2 \\
& - \sum_{j\in\mathscr{S}_i}\delta_{ij}\lambda_{min}\{k_{3ij}\}\|e_i(t) - e_j(t - T_{ij}(t))\|^2 \\
& - \sum_{j\in\mathscr{S}_i}\delta_{ij}\lambda_{min}\{k_{4ij}\}\alpha\|e_{fi}(t) - e_{fj}(t - T_{ij}(t))\|^2 \\
& + \sum_{j\in\mathscr{S}_i}\delta_{ij}(1-d_{ij})\lambda_{max}\{k_{3ij}\}\|e_i(t) - e_j(t - T_{ij}(t))\|\|\eta_j(t - T_{ij}(t))\| \\
& + \sum_{j\in\mathscr{S}_i}\delta_{ij}(1-d_{ij})\lambda_{max}\{k_{4ij}\}\lambda_{max}\{k_{1j}\} + 1\|e_{fi}(t) - e_{fj}(t - T_{ij}(t))\|\|\eta_j(t - T_{ij}(t))\| \\
& + \sum_{j\in\mathscr{S}_i}\delta_{ij}\lambda_{max}\{k_{3ij}\}\|e_i(t) - e_j(t - T_{ij}(t))\|\|e_{fi}(t)\| \\
& + \sum_{j\in\mathscr{S}_i}\delta_{ij}(1-d_{ij})\lambda_{max}\{k_{3ij}\}\|e_i(t) - e_j(t - T_{ij}(t))\|\|e_{fj}(t - T_{ij}(t))\| \\
& + \sum_{j\in\mathscr{S}_i}\delta_{ij}d_{ij}\lambda_{max}\{k_{3ij}\}\|e_i(t) - e_j(t - T_{ij}(t))\|\|e_j(t - T_{ij}(t))\| \\
& + \sum_{j\in\mathscr{S}_i}\delta_{ij}d_{ij}\lambda_{max}\{k_{4ij}\}\alpha\|e_{fi}(t) - e_{fj}(t - T_{ij}(t))\|\|e_{fj}(t - T_{ij}(t))\| \\
& + \sum_{j\in\mathscr{S}_i}\delta_{ij}\lambda_{max}\{k_{4ij}\}\lambda_{max}\{k_{2i}\}\|e_{fi}(t) - e_{fj}(t - T_{ij}(t))\|\|e_i(t)\| \\
& + \sum_{j\in\mathscr{S}_i}\delta_{ij}(1-d_{ij})\lambda_{max}\{k_{4ij}\}\lambda_{max}\{k_{2j}\}\|e_{fi}(t) - e_{fj}(t - T_{ij}(t))\|\|e_j(t - T_{ij}(t))\| \Bigg\}.
\end{aligned}
\tag{3.24}
$$

If we select α, γ_i and k_{2i} as given in the Theorem (3.1) with adding and subtracting $2\|\eta_i(t)\|^2$, $\sum_{j\in\mathscr{S}_i}\delta_{ij}(1-d_{ij})(\lambda^2_{max}\{k_{3ij}\}+\lambda^2_{max}\{k_{4ij}\})\|\eta_j(t-T_{ij}(t))\|^2$, $\sum_{j\in\mathscr{S}_i}\delta_{ij}(1-d_{ij})d^2_{ij}(\lambda^2_{max}\{k_{3ij}\}+\lambda^2_{max}\{k_{4ij}\})\|e_j(t-T_{ij}(t))\|^2$, $\sum_{j\in\mathscr{S}_i}\delta_{ij}\frac{1}{4(1-d_{ij})}\|e_{fi} - e_{fj}(t-T_{ij}(t))\|^2$, $\sum_{j\in\mathscr{S}_i}\delta_{ij}(1-d_{ij})d^2_{ij}(\lambda^2_{max}\{k_{4ij}\} + \alpha^2\lambda^2_{max}\{k_{5ij}\})\|e_{fj}(t-T_{ij}(t))\|^2$ and $\sum_{j\in\mathscr{S}_i}\delta_{ij}\left(1+\frac{(1-d_{ij})}{4}+\frac{(1-d_{ij})}{4d^2_{ij}}+\frac{1}{4(1-d_{ij})}\right)\|e_i - e_j(t-T_{ij}(t))\|^2$ to the right-hand side, the upper bound becomes,

$$
\begin{aligned}
\dot{V}_1(t) \leq \sum_{i=1}^{N} \Bigg\{ & -\Big[\zeta_{F_{di}} + m_{1i}\lambda_{min}\{k_{1i}\}\Big]\|\eta_i\|^2 + \Big[\zeta_{C2i}(\zeta_{di} + \|e_{fi}\| + \|e_i\|) + 2\Big]\|\eta_i\|^2 \\
& - k_{6i}\|e_i\|^2 - k_{7i}\|e_{fi}\|^2 \\
& - \sum_{j\in\mathscr{S}_i}\delta_{ij}\Big[\lambda_{min}\{k_{3ij}\} - \left(1 + \frac{(1-d_{ij})}{4} + \frac{(1-d_{ij})}{4d_{ij}^2} + \frac{1}{4(1-d_{ij})}\right)\Big]\|e_i(t) - e_j(t-T_{ij}(t))\|^2 \\
& - \sum_{j\in\mathscr{S}_i}\delta_{ij}\Big[k_{5ij} - \frac{1}{4(1-d_{ij})}\Big]\|e_{fi}(t) - e_{fj}(t-T_{ij}(t))\|^2 \\
& + \sum_{j\in\mathscr{S}_i}\delta_{ij}(1-d_{ij})(\lambda_{max}^2\{k_{3ij}\} + \lambda_{max}^2\{k_{4ij}\})\|\eta_j(t-T_{ij}(t))\|^2 \\
& + \sum_{j\in\mathscr{S}_i}\delta_{ij}d_{ij}^2(\lambda_{max}^2\{k_{3ij}\} + \alpha^2\lambda_{max}^2\{k_{4ij}\})\|e_{fj}(t-T_{ij}(t))\|^2 \\
& + \sum_{j\in\mathscr{S}_i}\delta_{ij}d_{ij}^2(\lambda_{max}^2\{k_{3ij}\} + \lambda_{max}^2\{k_{4ij}\})\|e_j(t-T_{ij}(t))\|^2 \\
& - \Big[\frac{\rho_{1i}}{2}\|e_i\| - \|\eta_i\|\Big]^2 - \Big[\frac{\rho_{2i}}{2}\|e_{fi}\| - \|\eta_i\|\Big]^2 \\
& - \sum_{j\in\mathscr{S}_i}\delta_{ij}\Big[\frac{(\lambda_{max}\{k_{1j}\}1)\sqrt{1-d_{ij}}}{2}\|e_{fi}(t) - e_{fj}(t-T_{ij}(t))\| \\
& - \lambda_{max}\{k_{4ij}\}\sqrt{1-d_{ij}}\|\eta_j(t-T_{ij}(t))\|\Big]^2 \\
& - \sum_{j\in\mathscr{S}_i}\delta_{ij}\Big[\frac{\lambda_{max}\{k_{3ij}\}}{2}\|e_{fi}(t)\| - \|e_i(t) - e_j(t-T_{ij}(t))\|\Big]^2 \\
& - \sum_{j\in\mathscr{S}_i}\delta_{ij}\Big[\frac{\lambda_{max}\{k_{4ij}\}}{2}\|e_i(t)\| - \lambda_{max}\{k_{2i}\}\|e_i(t) - e_j(t-T_{ij}(t))\|\Big]^2 \\
& - \sum_{j\in\mathscr{S}_i}\delta_{ij}\Big[\frac{\sqrt{1-d_{ij}}}{2}\|e_i(t) - e_j(t-T_{ij}(t))\| - \lambda_{max}\{k_{3ij}\}\sqrt{1-d_{ij}}\|\eta_j(t-T_{ij}(t))\|\Big]^2 \\
& - \sum_{j\in\mathscr{S}_i}\delta_{ij}\Big[\frac{\sqrt{1-d_{ij}}}{2d_{ij}}\|e_i(t) - e_j(t-T_{ij}(t))\| - \lambda_{max}\{k_{3ij}\}d_{ij}\sqrt{1-d_{ij}}\|e_{fj}(t-T_{ij}(t))\|\Big]^2 \\
& - \sum_{j\in\mathscr{S}_i}\delta_{ij}\Big[\frac{1}{2\sqrt{1-d_{ij}}}\|e_{fi}(t) - e_{fj}(t-T_{ij}(t))\| - \lambda_{max}\{k_{4ij}\}d_{ij}\sqrt{1-d_{ij}}\alpha\|e_{fj}(t-T_{ij}(t))\|\Big]^2 \\
& - \sum_{j\in\mathscr{S}_i}\delta_{ij}\Big[\frac{1}{2\sqrt{1-d_{ij}}}\|e_i(t) - e_j(t-T_{ij}(t))\| - \lambda_{max}\{k_{3ij}\}d_{ij}\sqrt{1-d_{ij}}\|e_j(t-T_{ij}(t))\|\Big]^2 \\
& - \sum_{j\in\mathscr{S}_i}\delta_{ij}\Big[\frac{\sqrt{1-d_{ij}}}{2d_{ij}}\lambda_{max}\{k_{2j}\}\|e_{fi}(t) - e_{fj}(t-T_{ij}(t))\| \\
& \qquad\qquad - \lambda_{max}\{k_{4ij}\}d_{ij}\sqrt{1-d_{ij}}\|e_j(t-T_{ij}(t))\|\Big]^2\Bigg\}.
\end{aligned}
\tag{3.25}
$$

Since, the squared terms in brackets are always positive, the right-hand side of (3.25) can be further upper-bounded as

$$
\begin{aligned}
\dot{V}_1(t) \leq \sum_{i=1}^{N} \Bigg\{ & -\Big[\zeta_{F_{di}} + m_{1i}\lambda_{min}\{k_{1i}\}\Big]\|\eta_i\|^2 + \Big[\zeta_{C2i}(\zeta_{di} + \|e_{fi}\| + \|e_i\|) + 2\Big]\|\eta_i\|^2 \\
& - k_{6i}\|e_i\|^2 - k_{7i}\|e_{fi}\|^2 \\
& - \sum_{j\in\mathcal{S}_i} \delta_{ij}\Big[\lambda_{min}\{k_{3ij}\} - \left(1 + \frac{(1-d_{ij})}{4} + \frac{(1-d_{ij})}{4d_{ij}^2} + \frac{1}{4(1-d_{ij})}\right)\Big]\|e_i(t) - e_j(t - T_{ij}(t))\|^2 \\
& - \sum_{j\in\mathcal{S}_i} \delta_{ij}\Big[k_{5ij} - \frac{1}{4(1-d_{ij})}\Big]\|e_{fi}(t) - e_{fj}(t - T_{ij}(t))\|^2 \\
& + \sum_{j\in\mathcal{S}_i} \delta_{ij}(1-d_{ij})(\lambda_{max}^2\{k_{3ij}\} + \lambda_{max}^2\{k_{4ij}\})\|\eta_j(t - T_{ij}(t))\|^2 \\
& + \sum_{j\in\mathcal{S}_i} \delta_{ij}d_{ij}^2(\lambda_{max}^2\{k_{3ij}\} + \alpha^2\lambda_{max}^2\{k_{4ij}\})\|e_{fj}(t - T_{ij}(t))\|^2 \\
& + \sum_{j\in\mathcal{S}_i} \delta_{ij}d_{ij}^2(\lambda_{max}^2\{k_{3ij}\} + \lambda_{max}^2\{k_{4ij}\})\|e_j(t - T_{ij}(t))\|^2 \Bigg\}.
\end{aligned} \tag{3.26}
$$

The remaining part of the stability analysis proceeds with the following Lyapunov-Krasovskii functional to prove that the time-varying delay subjected terms do not effect the stability of the system

$$
\begin{aligned}
V_2(t) = & V_1(t) + \sum_{i\in\mathcal{S}}\sum_{j\in\mathcal{S}_i} \delta_{ij}z_{1ij}\int_{t-T_{ij}(t)}^{t} \eta_j^T(\omega)\eta_j(\omega)d\omega + \sum_{i\in\mathcal{S}}\sum_{j\in\mathcal{S}_i} \delta_{ij}z_{1ij}d_{ij}^2\int_{t-T_{ij}(t)}^{t} e_j^T(\omega)e_j(\omega)d\omega \\
& + \sum_{i\in\mathcal{S}}\sum_{j\in\mathcal{S}_i} \delta_{ij}z_{2ij}d_{ij}^2\int_{t-T_{ij}(t)}^{t} e_{fj}^T(\omega)e_{fj}(\omega)d\omega.
\end{aligned} \tag{3.27}
$$

The given function can be bounded similar as in (3.20). After some algebraic manipulations the upper bound for $\dot{V}_2(t)$ can be written as

$$
\begin{aligned}
\dot{V}_2(t) \leq \sum_{i\in\mathscr{S}} \Bigg\{ &- \left[\left(\zeta_{F_{di}} + m_{1i}\lambda_{min}\{k_{1i}\}\right) - \left(\zeta_{C2i}(\zeta_{di} + \|r_{fi}\| + \|e_i\|) + 2 + \sum_{i\in\mathscr{S}_l} \delta_{li} z_{1li} \right) \right] \|\eta_i(t)\|^2 \\
&- \left[k_{6i} - \sum_{i\in\mathscr{S}_l} \delta_{li} d_{li}^2 z_{1li} \right] \|e_i(t)\|^2 \\
&- \left[k_{7i} - \sum_{i\in\mathscr{S}_l} \delta_{li} d_{li}^2 z_{2li} \right] \|e_{fi}(t)\|^2 \\
&- \sum_{j\in\mathscr{S}_i} \delta_{ij} \left[\lambda_{min}\{k_{3ij}\} - \left(1 + \frac{1-d_{ij}}{4} + \frac{(1-d_{ij})}{4d_{ij}^2} + \frac{1}{4(1-d_{ij})} \right) \right] \|e_i(t) - e_j(t - T_{ij}(t))\|^2 \\
&- \sum_{j\in\mathscr{S}_i} \delta_{ij} \left[k_{5ij} - \frac{1}{4(1-d_{ij})} \right] \|e_{fi}(t) - e_{fj}(t - T_{ij}(t))\|^2 \Bigg\}.
\end{aligned} \tag{3.28}
$$

As long as the gain conditions given in Theorem (3.1) hold, $\dot{V}_2(t)$ in (3.28) is negative semi-definite

$$\dot{V}_2(t) \leq -\kappa\|y(t)\|^2 \tag{3.29}$$

with $\kappa \in \mathbb{R}^+$ and $y(t) = \begin{bmatrix} y_1^T(t) & y_2^T(t) & .... & y_N^T(t) \end{bmatrix}^T$. $V_2(t)$ is a decreasing function with a maximum value of $V_2(0)$. Then, it can be said that $y(t), \tilde{\theta}(t), \tilde{b}(t) \in \mathscr{L}_\infty$. Using (3.4) and (3.6), with the fact that $e(t), \eta(t), e_f(t) \in \mathscr{L}_\infty$, it is clear that $\dot{e_f}(t), \dot{e}(t) \in \mathscr{L}_\infty$ as well as $p(t), \dot{p}(t) \in \mathscr{L}_\infty$. Also, $q(t) \in \mathscr{L}_\infty$ since $q_d(t)$ is bounded. Since $\tilde{\theta}(t), \tilde{b}(t) \in \mathscr{L}_\infty$ and θ, b are constant, $\hat{\theta}(t)$ and $\hat{b}(t)$ are bounded and converge to constant values. By utilizing all these bounded signals, it can be concluded that $\tau(t) \in \mathscr{L}_\infty$, owing $Y_d(t)$ is bounded function of $q_d(t), \dot{q}_d(t), \ddot{q}_d(t)$.

Integrating both sides of (3.29), it is clear that $y(t) \in \mathscr{L}_2$ and employing Barbalat's Lemma [40], the analysis can be finalized that all error signals in $y(t)$ converge to zero semi-globally asymptotically as $t \to \infty$, since $y(t) \in \mathscr{L}_2 \cap \mathscr{L}_\infty$ and the gain k_1 can be selected arbitrarily large to cover any set of initial conditions.

Also, from (3.29), it is clear that

$$\lim_{t\to\infty} e_i(t) - e_j(t - T_{ij}(t)) = 0 \tag{3.30}$$

and can be said that

$$\lim_{t\to\infty} e_i(t) - e_j(t - T_{ij}(t)) = q_{di}(t) - q_i(t) - q_{dj}(t - T_{ij}(t)) + q_j(t - T_{ij}(t)) = 0. \tag{3.31}$$

After adding and subtracting $q_j(t)$ and $q_{dj}(t)$ to the right-hand side of the equation, it is obtained

$$\begin{aligned}\lim_{t\to\infty} e_i(t)-e_j(t-T_{ij}(t)) =& q_j(t)-q_i(t)-q_j(t)+q_{dj}(t)-q_{dj}(t)+q_{di}(t)\\ &+q_j(t-T_{ij}(t))-q_{dj}(t-T_{ij}(t))\\ =& q_j(t)-q_i(t)+e_j(t)-q_{dj}(t)+q_{di}(t)-e_j(t-T_{ij}(t))\\ =& 0\end{aligned} \tag{3.32}$$

and as stated in Theorem (3.1),

$$\lim_{t\to\infty} q_i(t)-q_j(t)=q_{di}(t)-q_{dj}(t) \tag{3.33}$$

if agents have different desired trajectories, or

$$\lim_{t\to\infty} q_i(t)-q_j(t)=0 \tag{3.34}$$

in case of same q_d, since $\lim_{t\to\infty} e_j(t), e_j(t-T_{ij}(t))=0$.

■

3.6 Simulation Results

The simulation study is set up to assess the feasibility of the proposed linear filter in (3.2)-(3.3) and the control structure (3.12), in $MATLAB^{TM}/Simulink^{TM}$, consisting of 5 two-link robot manipulators, with the following dynamics

$$\begin{aligned}&\begin{bmatrix} p_1+2p_3cos(q_{i_2}) & p_2+p_3cos(q_{i_2}) \\ p_2+p_3cos(q_{i_2}) & p_2\end{bmatrix}\begin{bmatrix}\ddot{q}_{i_1}\\ \ddot{q}_{i_2}\end{bmatrix}\\ &+\begin{bmatrix} -p_3sin(q_{i_2})\dot{q}_{i_2} & -p_3sin(q_{i_2})(\dot{q}_{i_1}+\dot{q}_{i_2}) \\ p_3sin(q_{i_2})\dot{q}_{i_1} & 0\end{bmatrix}\begin{bmatrix}\dot{q}_{i_1}\\ \dot{q}_{i_2}\end{bmatrix}\\ &+\begin{bmatrix} f_{d1} & 0\\ 0 & f_{d2}\end{bmatrix}\begin{bmatrix}\dot{q}_{i_1}\\ \dot{q}_{i_2}\end{bmatrix}=\begin{bmatrix}\tau_{i_1}\\ \tau_{i_2}\end{bmatrix}\end{aligned} \tag{3.35}$$

where p_1, p_2, p_3 and f_{d1}, f_{d2} stand for the mass parameters and friction coefficients, respectively, with the numerical values listed in Table 3.1 [37]. Communication topology between robot manipulators is illustrated in Figure 3.1.

The unknown parameter vector θ is in the form of

$$\theta = \begin{bmatrix} p_1 & p_2 & p_3 & f_{d1} & f_{d2} \end{bmatrix}^T \tag{3.36}$$

and all the parameter and disturbance estimates are initialized to zero, $\hat{\theta}(0), \hat{b}(0) = 0$. The desired trajectory of all robot manipulators is defined as

$$q_d(t) = \begin{bmatrix} 22.92sin(1.5t)(1-exp(-0.3t^3)) \\ -11.45 + 22.92sin(1.5t)(1-exp(-0.3t^3)) \end{bmatrix} [deg] \tag{3.37}$$

and the disturbance signal applied to the second link of the Robot 4 between $t = 25 - 26s$ is given in Figure 3.2.

Table 3.1 Actual Robot Parameters

Parameters	Robot 1	Robot 2	Robot 3	Robot 4	Robot 5
p_{i1} $[kg.m^2]$	2.355	3.473	3.105	2.734	3.207
p_{i2} $[kg.m^2]$	0.2095	0.193	0.3012	0.412	0.212
p_{i3} $[kg.m^2]$	0.195	0.242	0.241	0.322	0.293
f_{di1} $[Nm.s]$	5.3	4.2	4.9	4.73	4.89
f_{di2} $[Nm.s]$	1.1	1.5	1.24	1.62	1.23

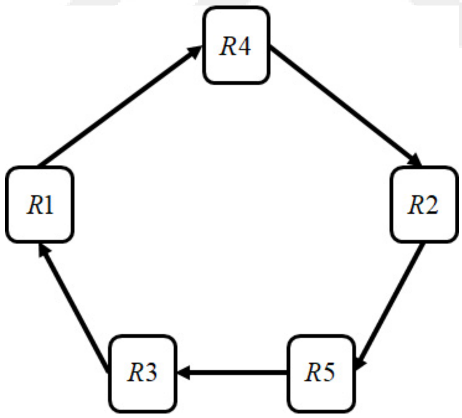

Figure 3.1 Communication topology

Initial states of joint positions are assumed arbitrarily as

$$q_1(0) = \begin{bmatrix} 30 & 30 \end{bmatrix}^T [deg] \qquad q_2(0) = \begin{bmatrix} 10 & 10 \end{bmatrix}^T [deg]$$
$$q_3(0) = \begin{bmatrix} 40 & 40 \end{bmatrix}^T [deg] \qquad q_4(0) = \begin{bmatrix} 20 & 20 \end{bmatrix}^T [deg]$$
$$q_5(0) = \begin{bmatrix} 50 & 0 \end{bmatrix}^T [deg]$$

and $\dot{q}_i(0) = 0$. The control and adaptation gains are set to the following values

$$k_{1i} = diag\left\{\begin{array}{cc} 6 & 15 \end{array}\right\} \qquad k_{2i} = diag\left\{\begin{array}{cc} 6 & 6 \end{array}\right\}$$
$$k_{3ij} = diag\left\{\begin{array}{cc} 60 & 100 \end{array}\right\} \qquad k_{4ij} = diag\left\{\begin{array}{cc} 3 & 1 \end{array}\right\}$$
$$\gamma_i = diag\left\{\begin{array}{cc} 10 & 5 \end{array}\right\} \qquad \alpha = 0.01$$

$$\Gamma_{1i} = diag\left\{\begin{array}{ccccc} 80 & 10 & 10 & 100 & 100 \end{array}\right\}$$
$$\Gamma_{2i} = diag\left\{\begin{array}{cc} 3 & 8 \end{array}\right\}.$$

Lastly, time-varying delay values on the communication topology are taken as

$$\begin{aligned} T_{13}(t) &= 0.1 + 0.06sin(t) \\ T_{41}(t) &= 0.12 + 0.05sin(0.5t) \\ T_{24}(t) &= 0.15 + 0.14sin(0.3t) \\ T_{52}(t) &= 0.08 + 0.02sin(0.5t) \\ T_{35}(t) &= 0.3 + 0.2sin(0.4t). \end{aligned} \tag{3.38}$$

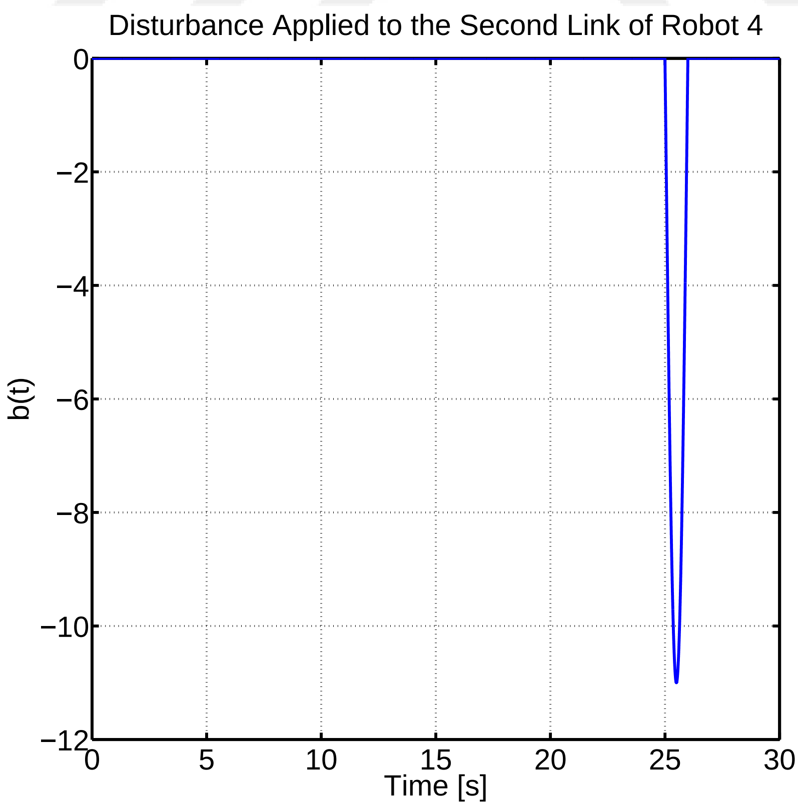

Figure 3.2 Disturbance signal subject 2^{nd} link of robot 4

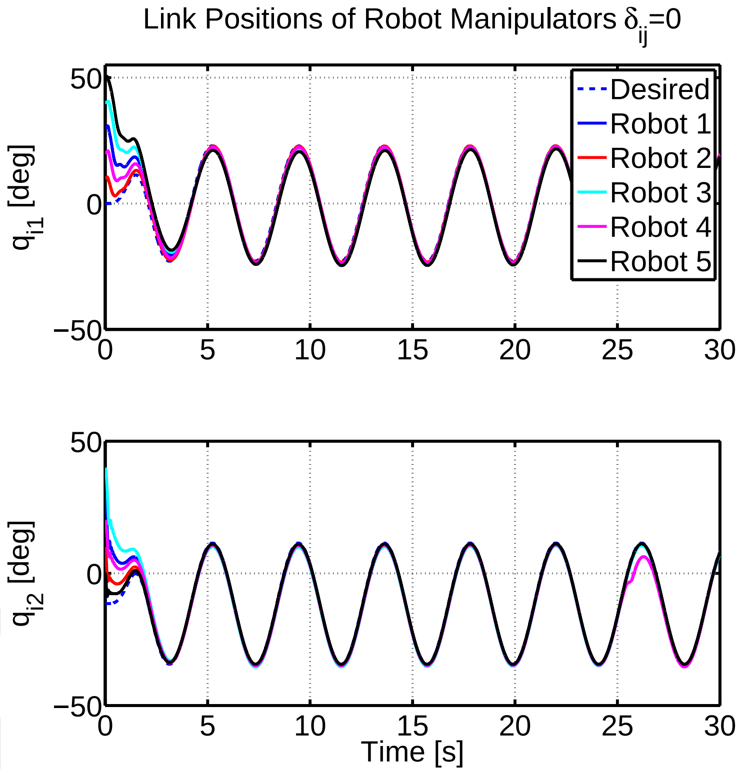

Figure 3.3 Link positions without synchronization $\delta_{ij} = 0$

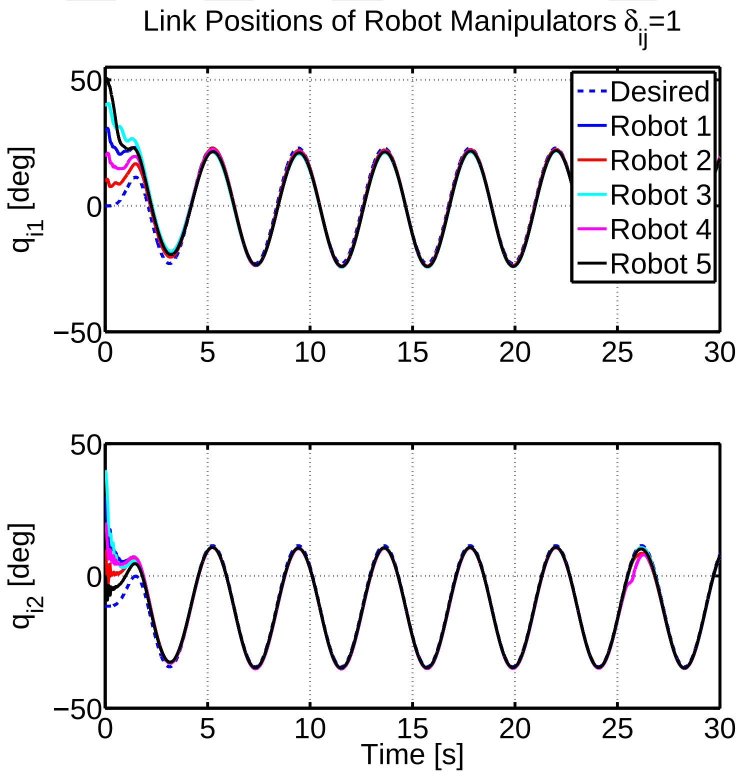

Figure 3.4 Link positions with synchronization $\delta_{ij} = 1$

In Figures 3.3 and 3.4, link positions without and with synchronization can be seen, respectively. Without synchronization ($i.e.\delta_{ij} = 0$), robot manipulators reach to the desired trajectory from different points. On the other side, when synchronization is activated ($i.e.\delta_{ij} = 1$), manipulators meet, then converge to the given desired trajectory, simultaneously and time-varying communication delays do not effect convergence of manipulators. Also, from Figures 3.5 and 3.6 position errors converge to zero in both cases with the help of the disturbance estimator, but as an advantage of synchronization, disturbance signal effect the relevant manipulator less, when there is a synchronization between manipulators. As given in Figures 3.8 and 3.9 estimated parametric values and disturbance values converge to constant values. Applied control signals are depicted in Figure 3.10.

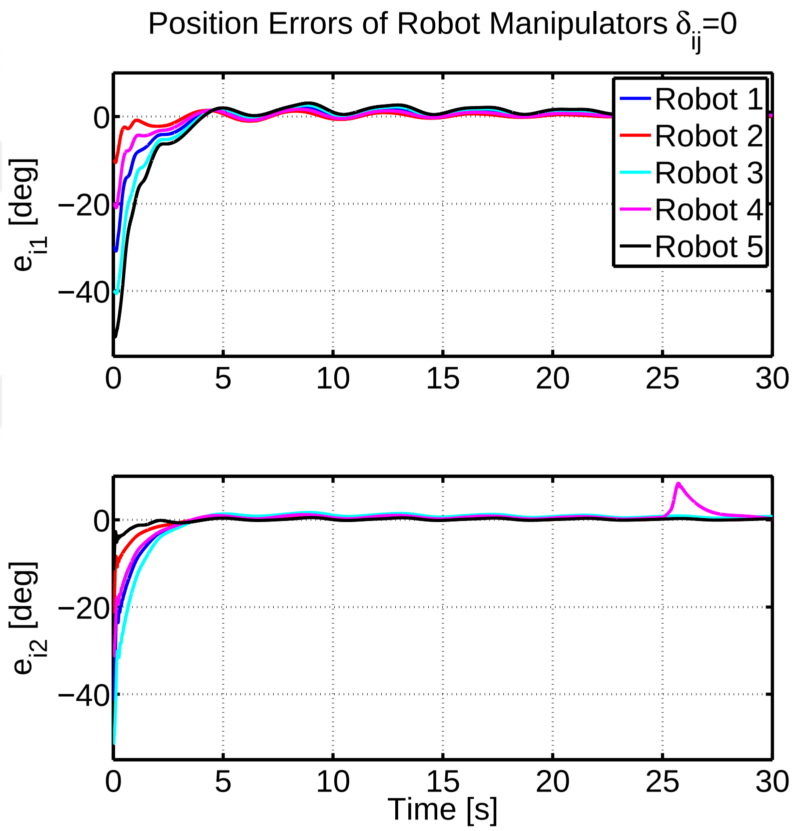

Figure 3.5 Position errors without synchronization $\delta_{ij} = 0$

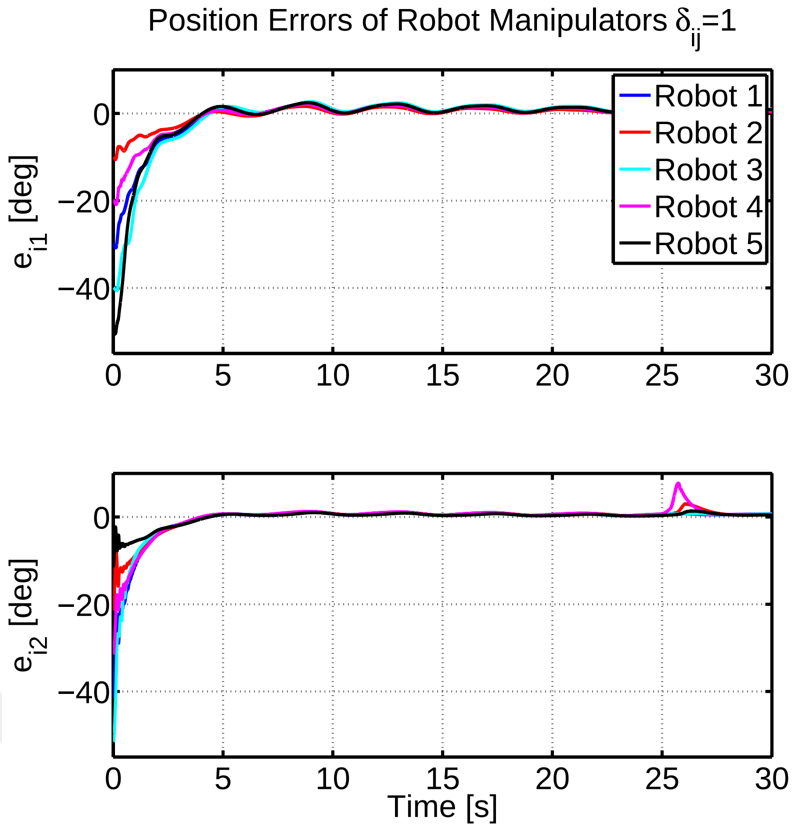

Figure 3.6 Position errors with synchronization $\delta_{ij} = 1$

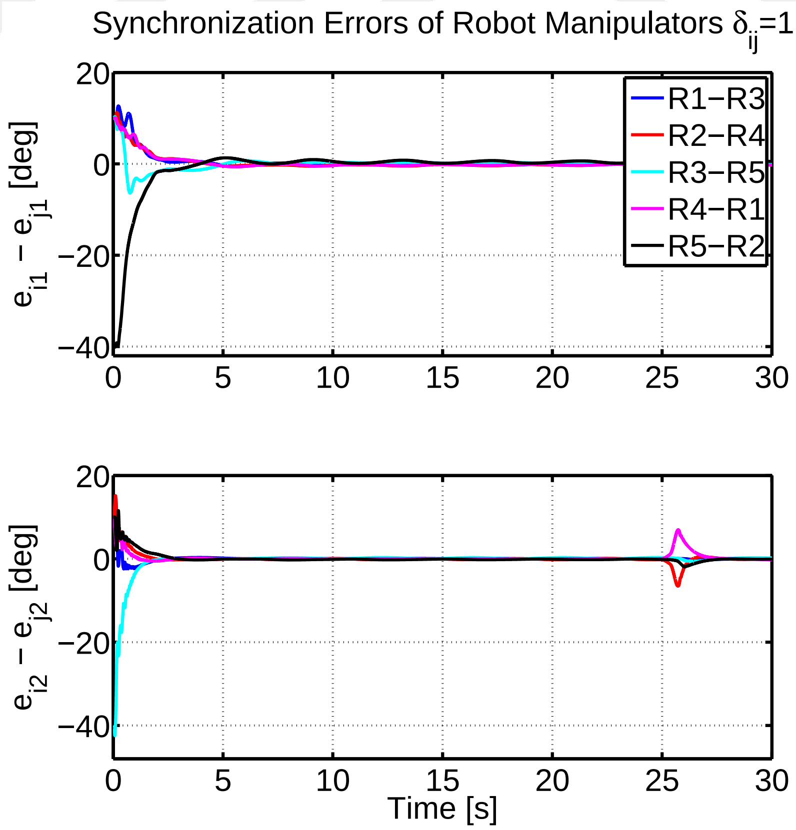

Figure 3.7 Position synchronization errors with synchronization $\delta_{ij} = 1$

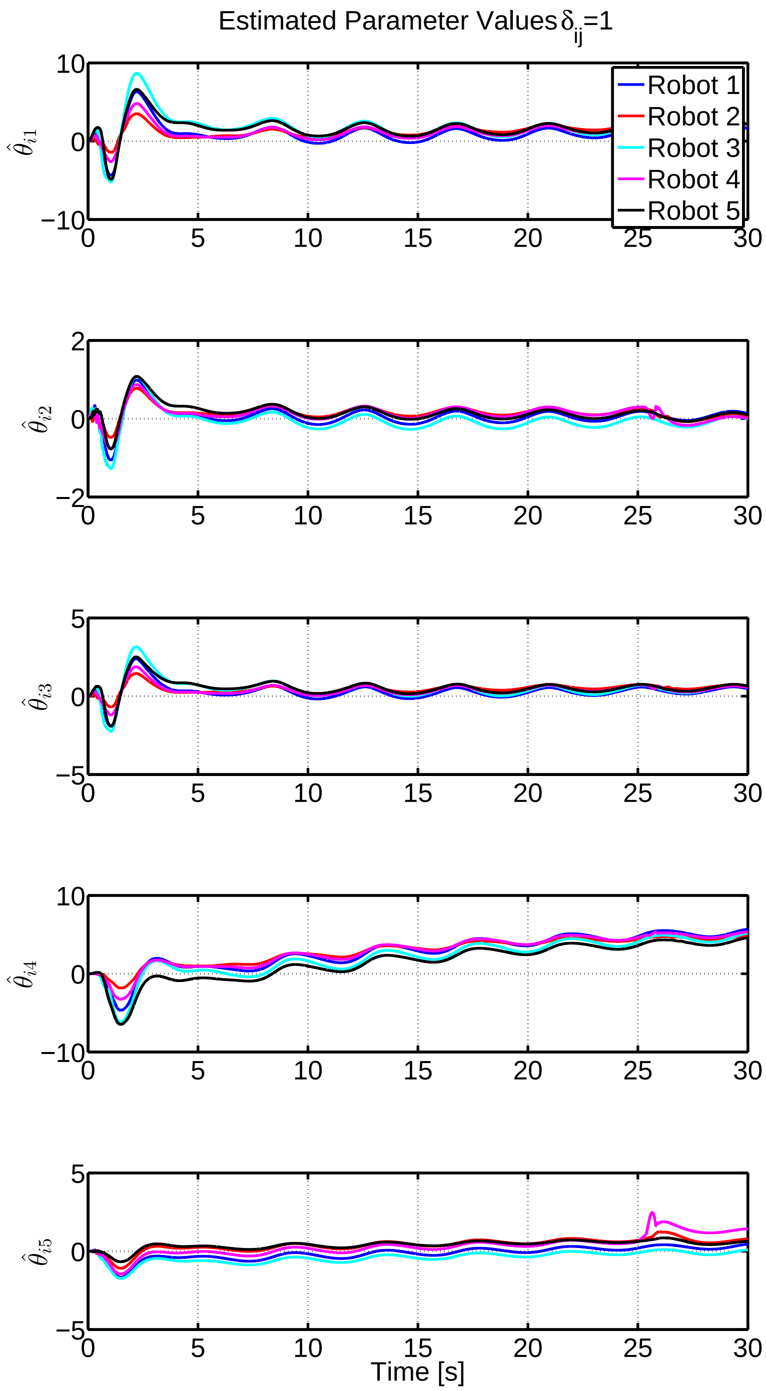

Figure 3.8 Parameter estimation values with synchronization $\delta_{ij} = 1$

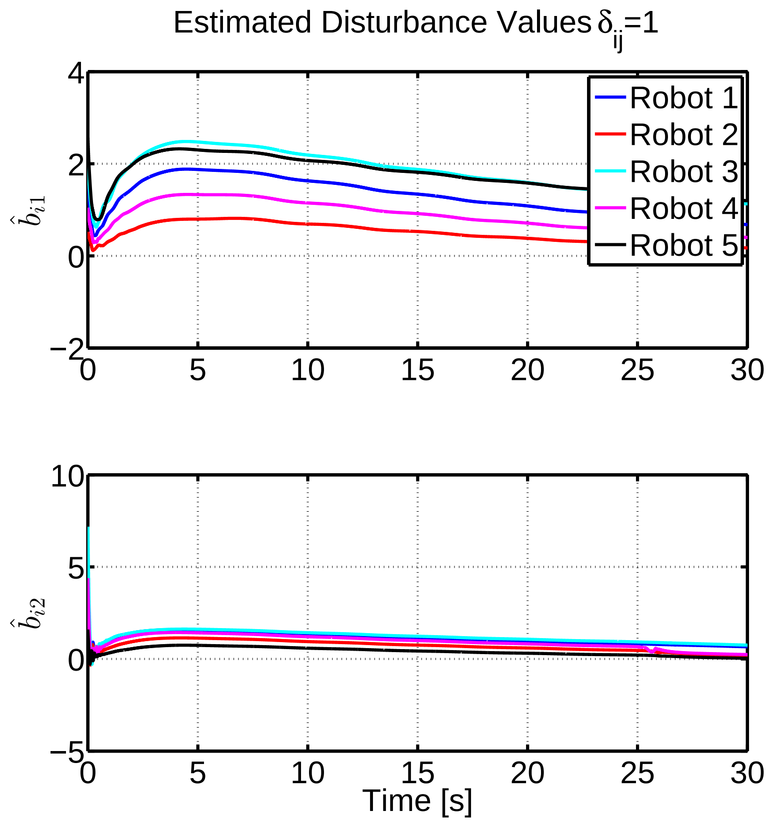

Figure 3.9 Disturbance estimation values with synchronization $\delta_{ij} = 1$

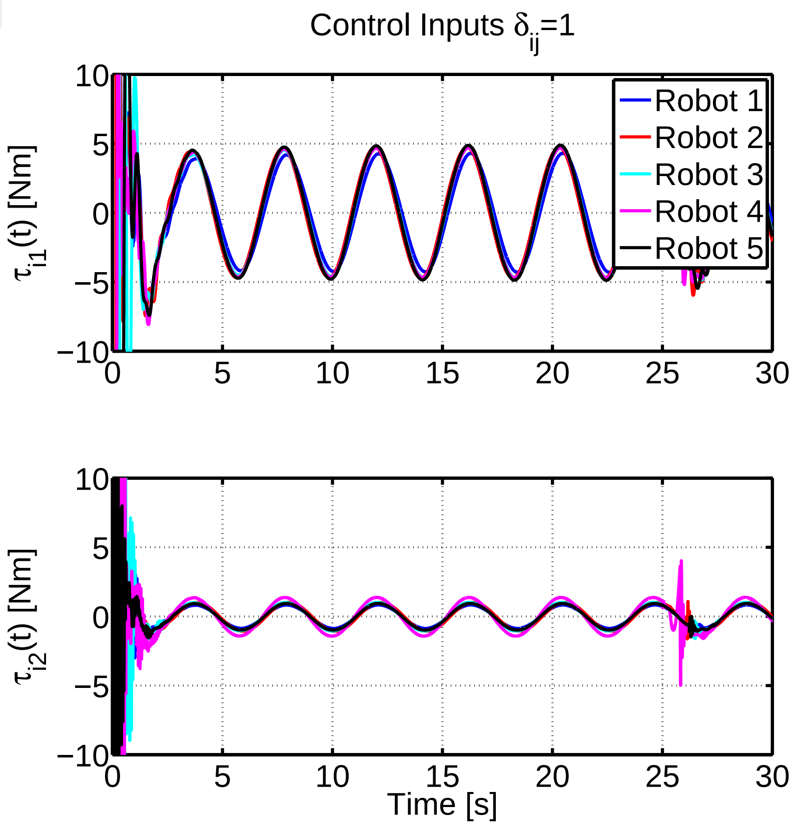

Figure 3.10 Control input signals with synchronization $\delta_{ij} = 1$

3.7 Experimental Results

The experimental study is performed on the system given in Section 2.2. To show the applicability of proposed linear filter in (3.2)-(3.3) and the control structure (3.12), first two links of robot manipulators are used with the dynamics as follows

$$\begin{bmatrix} m_{i_{11}} & 0 \\ 0 & m_{i_{22}} \end{bmatrix}\begin{bmatrix} \ddot{q}_{i_1} \\ \ddot{q}_{i_2} \end{bmatrix}+\begin{bmatrix} -c_{i_1}\dot{q}_{i_2} & -c_{i_1}\dot{q}_{i_1} \\ c_{i_1}\dot{q}_{i_1} & 0 \end{bmatrix}\begin{bmatrix} \dot{q}_{i_1} \\ \dot{q}_{i_2} \end{bmatrix}+\begin{bmatrix} 0 \\ p_{i_4}cos(q_{i_2}) \end{bmatrix}=\begin{bmatrix} \tau_{i_1} \\ \tau_{i_2} \end{bmatrix} \tag{3.39}$$

where

$$\begin{aligned} m_{i_{11}} =& p_{i_1}cos(q_{i_2})+p_{i_2} \\ m_{i_{22}} =& p_{i_3} \\ c_{i_1} =& p_{i_1}sin(q_{i_2})cos(q_{i_2}) \end{aligned} \tag{3.40}$$

and the control input of 3^{rd} links are set to zero. The control and adaptation gains are adjusted to the following values

$$\begin{aligned} k_{1i} &= diag\left\{ 3 \quad 3 \right\} & k_{2i} &= diag\left\{ 12 \quad 10 \right\} \\ k_{3ij} &= diag\left\{ 3 \quad 5 \right\} & k_{4ij} &= diag\left\{ 0.1 \quad 0.1 \right\} \\ \gamma_i &= diag\left\{ 0.5 \quad 0.8 \right\} & \alpha &= 100 \end{aligned}$$

$$\begin{aligned} \Gamma_{1i} &= diag\left\{ 70 \quad 1 \quad 1 \quad 1 \right\} \\ \Gamma_{2i} &= diag\left\{ 0.5 \quad 3 \right\} \end{aligned}$$

and all the parameter and disturbance estimates are initialized to zero, $\hat{\theta}(0), \hat{b}(0) = 0$. The desired trajectory of all robot manipulators is defined as

$$q_d(t) = \begin{bmatrix} 14.32sin(0.4t)(1-exp(-0.3t^3)) \\ 14.32+8.59sin(0.4t)(1-exp(-0.3t^3)) \end{bmatrix}[deg] \tag{3.41}$$

and the disturbance signal applied to the second link of Robot 2 between $t = 15-17s$ is given in Figure 3.12.

Since, the natural time-delay values caused by wireless modem are small, to show the effectiveness of the proposed control mechanism, following time-delay values are added on Simulink

$$\begin{aligned} T_{1,2} &= 0.1 + 0.05sin(0.2t) \\ T_{2,3} &= 0.08 + 0.02sin(0.5t) \\ T_{3,1} &= 0.095 + 0.03sin(0.25t) \end{aligned} \tag{3.42}$$

for the communication topology as in Figure 3.11.

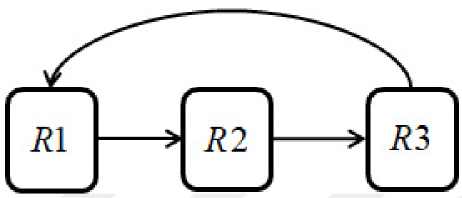

Figure 3.11 Communication topology

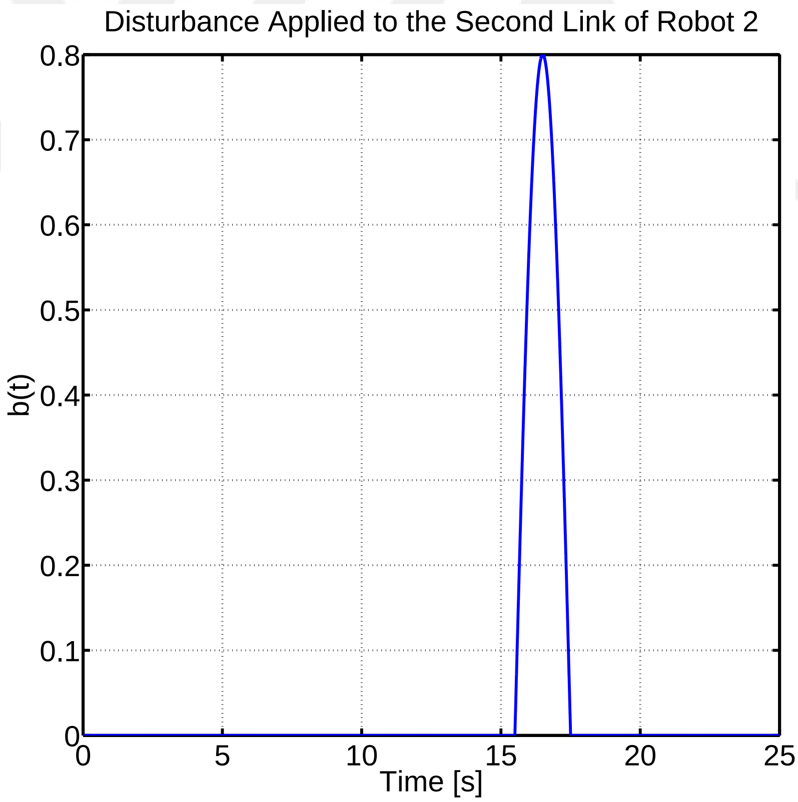

Figure 3.12 Disturbance signal subject 2^{nd} link of robot 2

In Figures 3.13 and 3.14, link positions without and with synchronization are presented, respectively. Especially from the q_{i2} values of manipulators, it can be seen that synchronization terms ($i.e.\delta_{ij} = 1$) create a significant difference and guarantee simultaneous convergence of manipulators to the desired trajectory under the effect

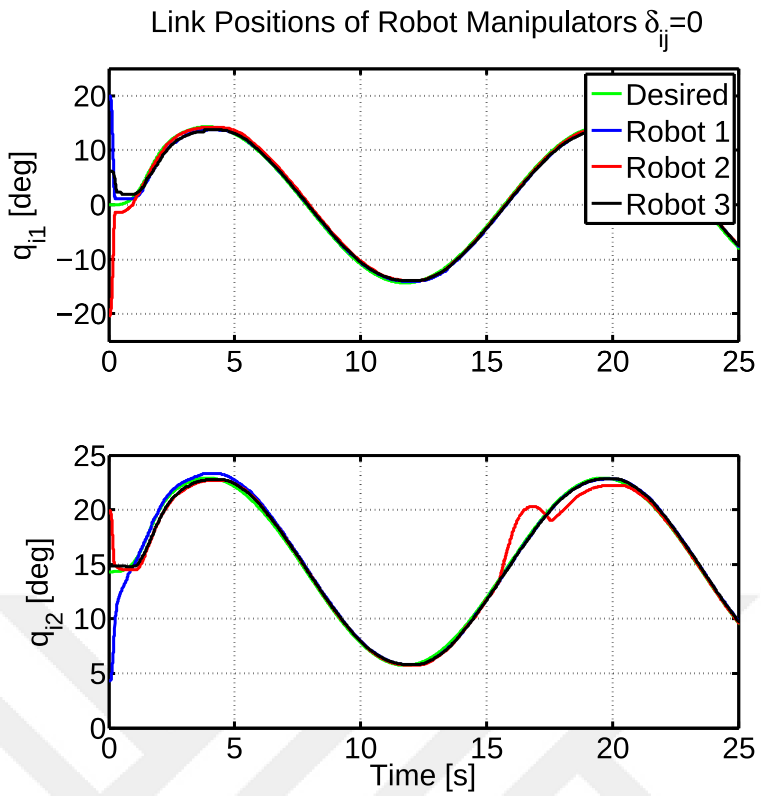

Figure 3.13 Link positions without synchronization $\delta_{ij} = 0$

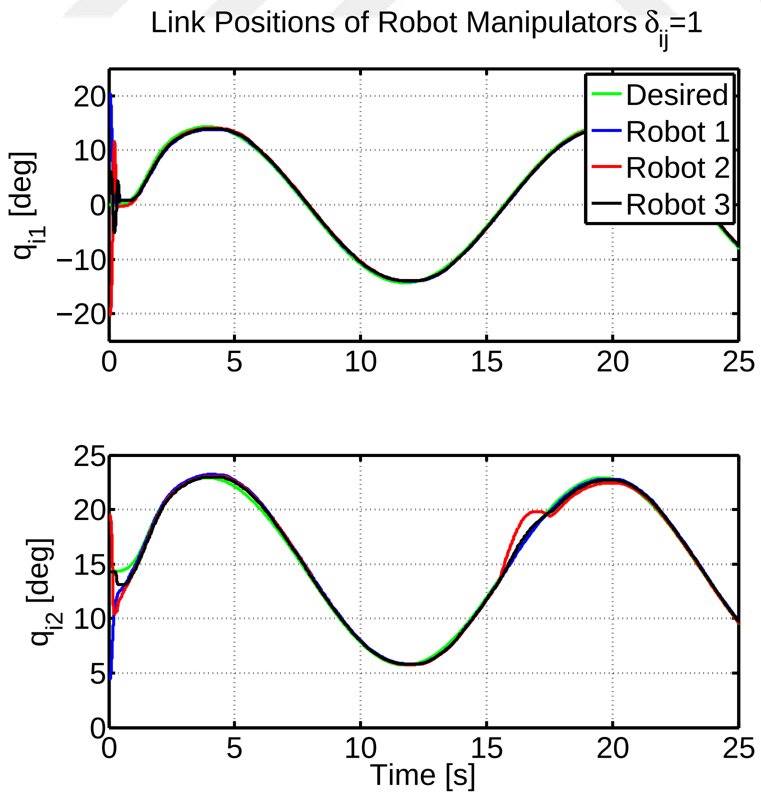

Figure 3.14 Link positions with synchronization $\delta_{ij} = 1$

of time-varying communication delays. Also, from the comparison of Figures 3.15 and 3.16, it is clear that with the effect of synchronization, manipulators converge to the desired trajectory with the same position errors and as depicted in Figure 3.17, synchronization errors converge to zero before the position errors of manipulators.

Besides, as observed in simulation study, position errors converge to zero in both cases with the help of the disturbance estimator, but as an advantage of synchronization, added disturbance signal effect the relevant manipulator less and the position error of Robot 2 converge to zero faster than the case when $\delta_{ij} = 0$. As given in Figures 3.18 and 3.19 estimated parametric values and disturbance values converge to constant values. Finally, applied control signals for all manipulators are introduced in Figure 3.20.

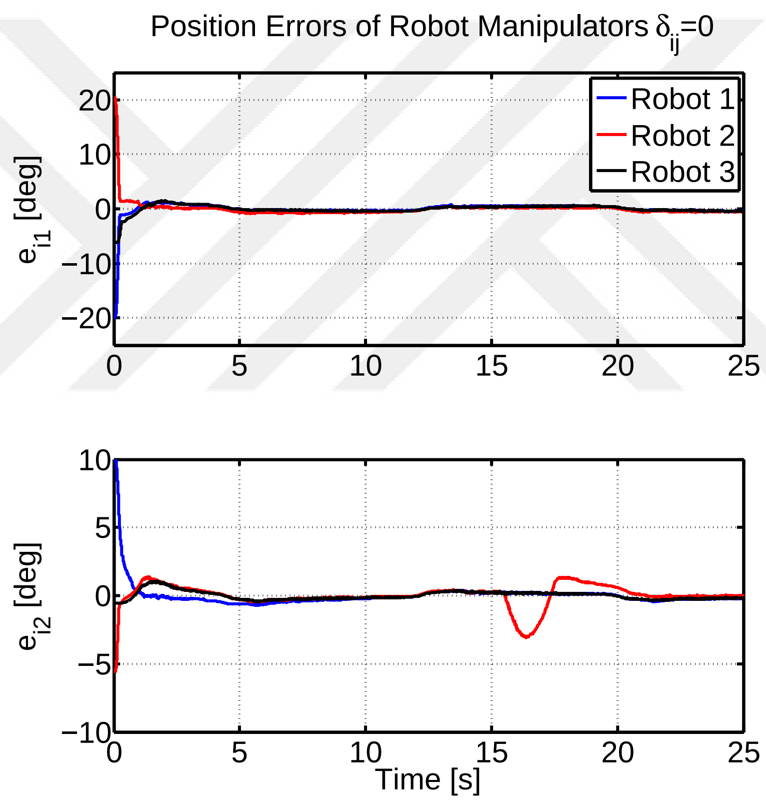

Figure 3.15 Position errors without synchronization $\delta_{ij} = 0$

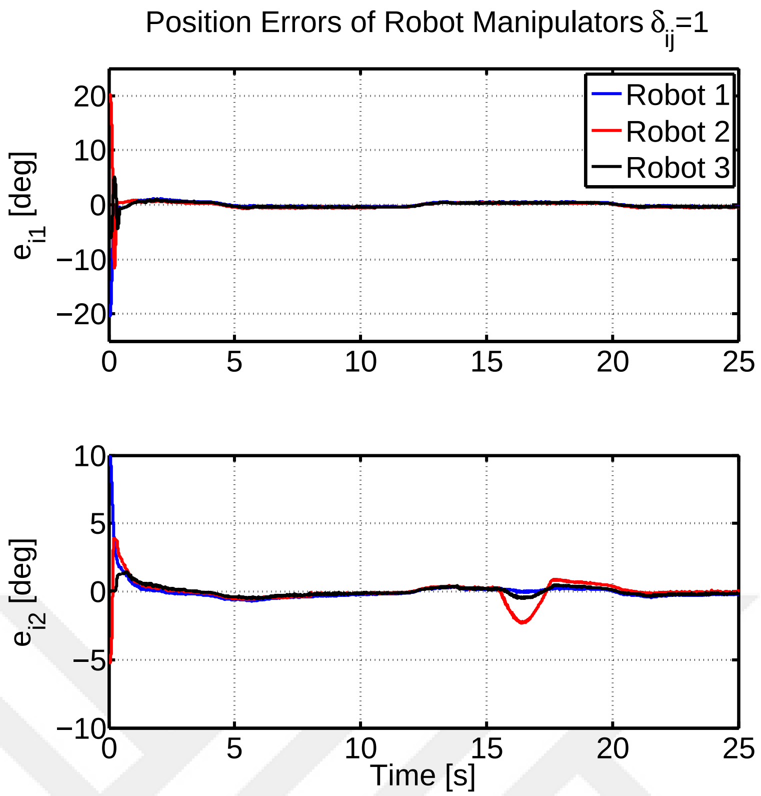

Figure 3.16 Position errors with synchronization $\delta_{ij} = 1$

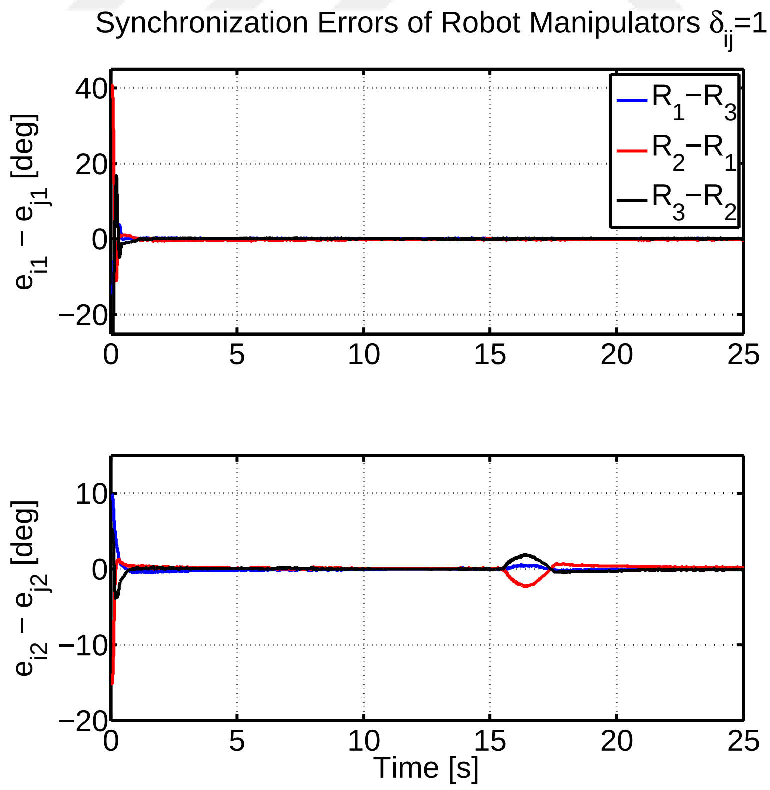

Figure 3.17 Position synchronization errors with synchronization $\delta_{ij} = 1$

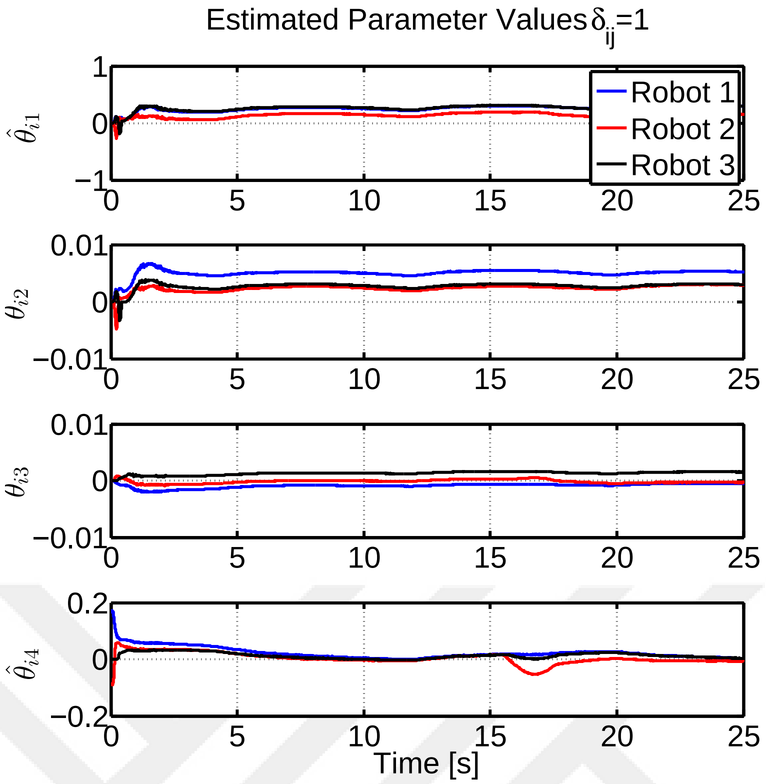

Figure 3.18 Parameter estimation values with synchronization $\delta_{ij} = 1$

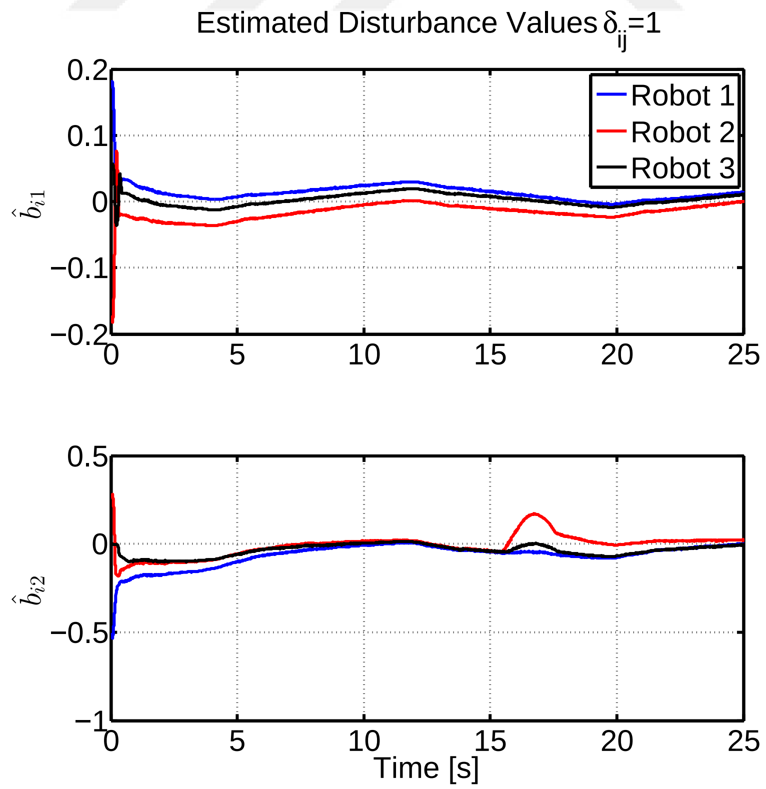

Figure 3.19 Disturbance estimation values with synchronization $\delta_{ij} = 1$

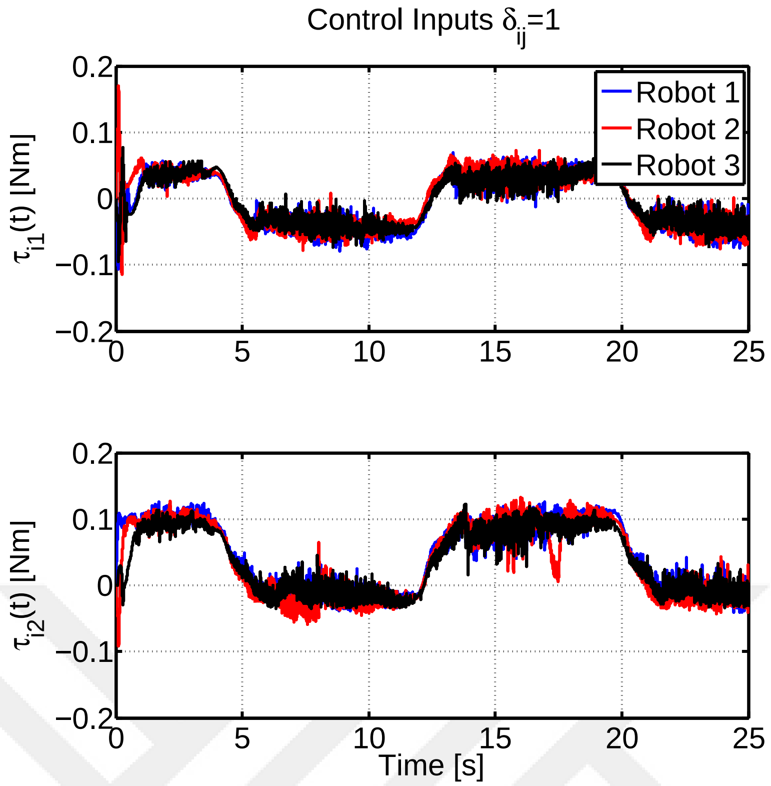

Figure 3.20 Control input signals with synchronization $\delta_{ij} = 1$

4
Robust Output Feedback Synchronization

The section below presents a solution for position synchronization problem of Euler-Lagrange formulated systems with an output-feedback robust control structure. After the problem definition, suggested model-free filter and controller structures are introduced, in detail. By employing a Lyapunov-based convergence analysis using Lyapunov-Krasovskii functionals, it is concluded that all errors, including synchronization errors, converge to an adjustable hyperball and stay bounded, under the effects of parametric uncertainty, external disturbances and variable communication delay. Lastly, simulation and experimental results of proposed filter based robust controller are presented.

4.1 Problem Definition

In this part of the thesis, it is aimed to provide an output-feedback robust controller for the problem defined in Chapter 3. Unlikely the presented former filter based controller, in this chapter model free structures for both filter and controller are proposed. The basic performance criteria is similar to the one given in Section 3.1 as below

$$e_i(t) = q_{di} - q_i \tag{4.1}$$

where $q_{di}(t)$ represents the desired trajectory and it is assumed that it is a bounded function of time as well as its first three time derivatives.

4.2 Filter Design

Since it is assumed that the velocity variables are not measurable, the following linear filter structure with the output $e_{fi} \in \mathbb{R}^n$ is designed

$$e_{fi} = p_i - (k_{1i} + 1)e_i. \tag{4.2}$$

The variable $p_i(t) \in \mathbb{R}^n$ is an auxiliary variable with the dynamic equation

$$\dot{p}_i = -(k_{1i}+1+\alpha)p_i + ((k_{1i}+1)^2 + \alpha(k_{1i}+1) - (k_{1i}+1) + k_{2i})e_i - r_{fi}. \tag{4.3}$$

In the given equation, $k_{1i}, k_{2i} \in \mathbb{R}^{nxn}$, $\alpha \in \mathbb{R}^1$ are positive constant gains and α is same for all agents. $r_{fi}(t) \in \mathbb{R}^n$ is an auxiliary variable with the dynamic

$$\dot{r}_{fi} = -k_{fi} r_{fi} + e_{fi} \tag{4.4}$$

where $k_{fi} \in \mathbb{R}^{nxn}$ is the positive constant gain. Proposed design for the linear filter, basically derived from the works of [48] and [34], is redesigned according to the subsequent stability analysis and is similar to a high-order compensator, with the position error $e_i(t)$ as the input and the surrogate signal $e_{fi}(t)$, instead of the actual velocity error, as the output. The given filter definition requires just the position error information like in Section 3.2.

To obtain the dynamics of $e_{fi}(t)$, time derivative of (4.2) is taken and (4.3) and (4.4) are substituted

$$\dot{e}_{fi} = -\alpha e_{fi} - (k_{1i}+1)\eta_i + k_{2i}e_i - r_{fi}. \tag{4.5}$$

The auxiliary signal $\eta_i(t) \in \mathbb{R}^n$ has the following expression

$$\eta_i = e_{fi} + e_i + \dot{e}_i. \tag{4.6}$$

By using (4.6), derivative of position error and velocity variable can be formulated as below

$$\dot{e}_i = \eta_i - e_{fi} - e_i \tag{4.7}$$

$$\dot{q}_i = \dot{q}_{di} - \eta_i + e_{fi} + e_i. \tag{4.8}$$

4.3 Error System Dynamics

After pre-multiplying time derivative of (4.6) with $M_i(q_i)$ and substituting (4.5), (4.7) the open loop dynamics are generated as

$$M_i\dot{\eta}_i = M_i\ddot{q}_{di} - \tau_i - b_i + C_i(q_i,\dot{q}_i)\dot{q}_i + F_{di}\dot{q}_i + G_i(q_i) - M_i k_{1i}\eta_i - M_i((\alpha+1)e_{fi} + r_{fi}) + M_i(k_{2i}-1)e_i + N_{di} - N_{di} \tag{4.9}$$

where

$$N_{di} = M_i(q_{di})\ddot{q}_{di} + C_i(q_{di},\dot{q}_{di})\dot{q}_{di} + F_{di}\dot{q}_{di} + G_i(q_{di}). \tag{4.10}$$

Using the *Property 3* in Section 2.3.1, (4.8) and performing some algebraic manipulations, (4.9) can be rewritten as

$$M_i\dot{\eta}_i = \tilde{N}_i - C_i(q_i,\dot{q}_i)\eta_i - F_{di}\eta_i - \tau_i - b_i - M_i k_{1i}\eta_i + N_{di} - C_i(q_i,\dot{q}_{di} + e_{fi} + e_i)\eta_i. \tag{4.11}$$

The auxiliary signal $\tilde{N}_i$ can be bounded with the norm of measurable signals as

$$\|\tilde{N}_i\| \leq \rho_{1i}(\|e_i\|,\|e_{fi}\|)\|e_i\| + \rho_{2i}(\|e_i\|,\|e_{fi}\|)\|e_{fi}\| + \rho_{3i}\|r_{fi}\|. \tag{4.12}$$

Details on (4.12), is presented in Appendix A.2.

4.4 The Proposed Control Scheme

In this section, to ensure the position tracking and synchronization of agents in the system, a model-free robust controller is presented. Based on the subsequent stability analysis, the controller is designed as

$$\tau_i = -\gamma_i(k_{1i}+1)e_{fi} + \gamma_i k_{2i}e_i + \beta_i tanh(e_i + k_{fi}r_{fi}) - \hat{b}_i + \sum_{j\in\mathscr{S}_i}\delta_{ij}k_{3ij}(e_i(t) - e_j(t - T_{ij}(t))) - (k_{1i}+1)\sum_{j\in\mathscr{S}_i}\delta_{ij}k_{4ij}(e_{fi}(t) - e_{fj}(t - T_{ij}(t))) \tag{4.13}$$

with the positive and diagonal control gain matrices $\gamma_i, k_{3ij}, k_{4ij} \in \mathbb{R}^{nxn}$, the estimated external disturbances $\hat{b}_i \in \mathbb{R}^n$, with the update function

$$\hat{b}_i = -\Gamma_i \left(e_i(t) + \int_0^t (e_{fi}(\omega) + e_i(\omega))d\omega \right) \tag{4.14}$$

where $\Gamma_i \in \mathbb{R}^{pxp}$ is the positive definite, constant and diagonal adaptation gain matrix. With the help of η_i defined in (4.6), dynamic of $\hat{b}_i$ can be defined as

$$\dot{\hat{b}}_i = -\Gamma_i \eta_i. \tag{4.15}$$

The proposed control structure given in (4.13) has two general parts similar to the control structure in Section 3.4, except the model-free tracking control side. Unlikely in (3.12), the term $\beta_i tanh(e_i + k_{fi} r_{fi})$ is used to compensate the effects of nonlinear terms in the dynamics [49]. The synchronization side has the same properties with (3.12).

With the substitution of the control law (4.13) into (4.11), the closed loop dynamics for the filtered tracking error-like signal $\eta_i(t)$ can be obtained as

$$\begin{aligned} M_i \dot{\eta}_i =& \gamma_i (k_{1i} + 1) e_{fi} - \gamma_i k_{2i} e_i - \beta_i tanh(e_i + k_{fi} r_{fi}) + \tilde{b}_i + \tilde{N}_i + N_{di} \\ & - \sum_{j \in \mathscr{S}_i} \delta_{ij} k_{3ij} (e_i(t) - e_j(t - T_{ij}(t))) + (k_{1i} + 1) \sum_{j \in \mathscr{S}_i} \delta_{ij} k_{4ij} (e_{fi}(t) - e_{fj}(t - T_{ij}(t))) \\ & - C_i(q_i, \dot{q}_i)\eta_i - F_{di}\eta_i - M_i k_{1i} \eta_i - C_i(q_i, \dot{q}_{di} + e_{fi} + e_i)\eta_i \end{aligned} \tag{4.16}$$

where $\tilde{b}_i \in \mathbb{R}^n$ represents the difference between estimated and real values of external disturbances, i.e. $\tilde{b}_i = \hat{b}_i - b_i$.

4.5 Stability Analysis

Prior to the stability analysis, the following Lemma is stated, to guarantee the boundedness of Lyapunov candidate function.

Lemma 4.1. *[50] Let the auxiliary function $\nu_i(t)$ be represented as*

$$\nu_i(t) \triangleq \sigma_{bi} - \varphi_i \tag{4.17}$$

where

$$\varphi_i \triangleq \int_0^t \eta_i^T(\tau)(N_{di}(\tau) - \beta_i tanh(\mu_i(\tau)))d\tau \tag{4.18}$$

and

$$\sigma_{bi} \triangleq \sum_{c=0}^{n} \beta_{ic}(ln(cosh(\mu_{ic}(0))) + 1) - \mu_i^T(0)N_{di}(0) \tag{4.19}$$

with the following transformations

$$\eta_i = \dot{\mu}_i + \mu_i \tag{4.20}$$

$$\mu_i = e_i + k_{fi} r_{fi}. \tag{4.21}$$

The function $\nu_i(t)$ *is lower bounded in the sense that*

$$\nu_i(t) \geq 0, \qquad \forall \|\mu_i(t)\| \geq d(\epsilon_i) \tag{4.22}$$

as long as constant gain β_i *satisfies the following condition*

$$\beta_{ic} > \frac{1}{\epsilon_i}\left[\|N_{dic}\|_\infty + \|\dot{N}_{dic}\|_\infty\right] \tag{4.23}$$

where subscript c express the c^{th} *element of a vector or a diagonal matrix* $(c = 1,..,n)$*, the operator* $\|\cdot\|_\infty$ *stands for the supremum of a time-varying signal and* ϵ_i *is a positive design parameter, which determines the radius of the hyperball* $d(\epsilon_i)$*. In other words, for* $\mu_i(t)$ *defined as the outside of a hyperball around the origin and sufficiently large selected* β_i*,*

$$\sigma_{bi} \geq \int_0^t \eta_i^T(\tau)(N_{di}(\tau) - \beta_i tanh(\mu_i(\tau)))d\tau. \tag{4.24}$$

Proof. Consider (4.18) is integrated and (4.21) is substituted as

$$\begin{aligned} \varphi_i(t) = \int_0^t \Big\{ \left[\mu_i^T(\tau)(N_{di}(\tau) - \beta_i tanh(\mu_i(\tau)))\right] + \frac{d\mu_i^T(\tau)}{d\tau} N_{di}(\tau) \\ - \beta_i \frac{d\mu_i^T(\tau)}{d\tau} tanh(\mu_i(\tau)) \Big\} d\tau. \end{aligned} \tag{4.25}$$

After the integration of second and third terms, (4.25) yields to

$$\begin{aligned}\varphi_i(t) = &\int_0^t \mu_i^T(\tau)\left(N_{di}(\tau) - \frac{dN_{di}(\tau)}{d\tau} - \beta_i tanh(\mu_i(\tau))\right)d\tau \\ &+\left[\mu_i^T(t)N_{di}(t) - \sum_{c=1}^{n}\beta_{ic}\left(ln(cosh(\mu_{ic}(t))) + 1\right)\right] \\ &+\left[\sum_{c=1}^{n}\beta_{ic}\left(ln(cosh(\mu_{ic}(0))) + 1\right) - \mu_i^T(0)N_{di}(0)\right]\end{aligned} \tag{4.26}$$

and can be upper-bounded as

$$\begin{aligned}\varphi_i(t) \leq &\int_0^t \sum_{c=1}^{n}|\mu_{ic}(\tau)|\left[\|N_{dic}(\tau)\|_\infty + \left\|\frac{dN_{dic}(\tau)}{d\tau}\right\|_\infty - \beta_{ic}|tanh(\mu_{ic}(t))|\right]d\tau \\ &+\left[\|\mu_i(t)\|\|N_{di}(t)\| - \sum_{c=1}^{n}\beta_{ic}\left(ln(cosh(\mu_{ic}(t))) + 1\right)\right] \\ &+\left[\sum_{c=1}^{n}\beta_{ic}\left(ln(cosh(\mu_{ic}(0))) + 1\right) - \mu_i^T(0)N_{di}(0)\right]\end{aligned} \tag{4.27}$$

with the fact that $\mu_i(t)tanh(\mu_i(t)) \geq 0$. It is clear that when $\|\mu_i(t)\| \geq d(\epsilon_i)$ and β_i is selected satisfying (4.23), first line of (4.27) takes negative values. Also, the second line of (4.27) is

$$\frac{1}{\lambda}\left(\sum_{c=0}^{n} ln(cosh(\mu_{ic}(t))) + 1\right) > \|\mu_i(t)\|, \qquad \forall\lambda \in (0,1) \tag{4.28}$$

as long as $\epsilon_i < \|tanh(\mu_i(t))\|$. Finally, with the given definition of σ_{bi} in (4.19), it can be proven that the inequality represented in (4.24) holds, when $\epsilon_i < \|tanh(\mu_i(t))\|$. Alternatively, it can be said, given auxiliary function $\nu_i(t)$ is positive if $\|\mu_i(t)\|$ is outside the hyperball $d(\epsilon_i)$, whose radius can be specified by using ϵ_i. ■

After completing the proof of Lemma 4.1 the following Theorem is presented.

Theorem 4.2. *The filter structure of* (4.2)-(4.4) *along with the output feedback robust control law* (4.13) *and the estimation rule in* (4.14) *guarantee semi-global asymptotic convergence of all errors, including synchronization errors, of the system with N agents, to a hyperball with an adjustable radius as long as the positive gains satisfy following conditions*

$$\alpha = \frac{k_{5ij}}{\lambda_{min}\{k_{4ij}\}} + \frac{\lambda_{max}^2\{k_{1j}+1\}(1-d_{ij})}{4\lambda_{min}\{k_{4ij}\}} + \frac{\lambda_{max}^2\{k_{2i}\}}{\lambda_{min}\{k_{4ij}\}} + \frac{\lambda_{max}^2\{k_{2j}\}(1-d_{ij})}{4\lambda_{min}\{k_{4ij}\}d_{ij}^2} + \frac{\lambda_{max}^2\{k_{4ij}\}(1-d_{ij})}{4\lambda_{min}\{k_{4ij}\}}$$

$$\lambda_{min}\{k_1 i\} + \zeta_{F_{di}} > \zeta_{C_{2i}}\left(\zeta_{di} + \|e_{fi}(0)\| + \|e_i(0)\|\right) + 3 + \sum_{i\in\mathcal{S}_l} \delta_{li} z_{1li}$$

$$\gamma_i = \frac{k_{6i}}{\alpha} + \frac{\lambda_{max}^2\{k_{3ij}\}}{4\alpha} + \frac{\rho_{2i}^2}{4\alpha}$$

$$k_{2i} = \frac{k_{8i}}{\gamma_i} + \frac{\rho_{1i}^2}{4\gamma_i} + \frac{\lambda_{max}^2\{k_{4ij}\}}{4\gamma_i}$$

$$k_{fi} = \frac{k_{7i}}{\gamma_i} + \frac{\lambda_{max}^2\{k_{4ij}\}}{4\gamma_i} + \frac{\rho_{3i}^2}{4\gamma_i}$$

$$\lambda_{min}\{k_{3ij}\} > 1 + \frac{1-d_{ij}}{4} + \frac{(1-d_{ij})}{4d_{ij}^2} + \frac{1}{4(1-d_{ij})}$$

$$k_{5ij} > 1 + \frac{1}{4(1-d_{ij})}$$

$$k_{6i} > \sum_{i\in\mathcal{S}_l} \delta_{li} z_{2li} d_{li}^2$$

$$k_{7i} > \sum_{i\in\mathcal{S}_l} \delta_{li} I_{nxn}$$

$$k_{8i} > \sum_{i\in\mathcal{S}_l} \delta_{li} z_{1li} d_{li}^2$$

where

$$z_{1ij} = \lambda_{max}^2\{k_{3ij}\} + \lambda_{max}^2\{k_{4ij}\}, \quad z_{2ij} = \lambda_{max}^2\{k_{3ij}\} + \alpha^2\lambda_{max}^2\{k_{4ij}\}$$

and the subindice l symbolizes other agents in the system, that receive information from agent i.

Proof. A non-negative function $V_1(t)$, which is the summation of functions $V_{1i}(t)$, can be defined for whole system as

$$
\begin{aligned}
V_1(t) =& \sum_{i\in\mathscr{S}} V_{1i}(t) \\
=& \frac{1}{2}\sum_{i\in\mathscr{S}} \Big\{ \eta_i^T M_i(q_i)\eta_i + e_i^T k_{2i}\gamma_i e_i + r_{fi}^T\gamma_i r_{fi} + e_{fi}^T\gamma_i e_{fi} + \nu_i(t) + \tilde{b}_i^T\Gamma_i^{-1}\tilde{b}_i \\
&+ \sum_{j\in\mathscr{S}_i} \delta_{ij}(e_i(t)-e_j(t-T_{ij}(t)))^T k_{3ij}(e_i(t)-e_j(t-T_{ij}(t))) \\
&+ \sum_{j\in\mathscr{S}_i} \delta_{ij}(e_{fi}(t)-e_{fj}(t-T_{ij}(t)))^T k_{4ij}(e_{fi}(t)-e_{fj}(t-T_{ij}(t))) \Big\}
\end{aligned}
\tag{4.29}
$$

which can be bounded as

$$
\lambda_1\|y(t)\|^2 \le \lambda_1\|h(t)\|^2 \le V_1(t) \le \lambda_2\|h(t)\|^2, \qquad \forall\|h(t)\| \ge \|y(t)\| \ge \|\mu(t)\| \ge d(\epsilon)
\tag{4.30}
$$

where

$$
h(t) = \begin{bmatrix} y^T(t) & \tilde{b}^T(t) & \sqrt{\nu} \end{bmatrix}^T
\tag{4.31}
$$

$$
y_i(t) = \begin{bmatrix} \eta_i(t)^T & r_{fi}(t)^T & e_{fi}(t)^T & e_i(t)^T & s_{ij}(t)^T \end{bmatrix}^T
$$

$$
s_{ij}(t) = \begin{bmatrix} \delta_{ij}(e_i(t)-e_j(t-T_{ij}(t)))^T & \delta_{ij}(e_{fi}(t)-e_{fj}(t-T_{ij}(t)))^T \end{bmatrix}^T
$$

and

$$
\begin{aligned}
\lambda_{1i} =& \frac{1}{2} min\Big\{m_{1i}, \lambda_{min}\{\gamma_i\}, \lambda_{min}\{k_{2i}\}, \lambda_{min}\{k_{3ij}\}, \lambda_{min}\{k_{4ij}\}, \lambda_{min}\{\Gamma_i^{-1}\}\Big\} \\
\lambda_{2i} =& \frac{1}{2} max\Big\{m_{2i}, \lambda_{max}\{\gamma_i\}, \lambda_{max}\{k_{2i}\}, \lambda_{max}\{k_{3ij}\}, \lambda_{max}\{k_{4ij}\}, \lambda_{max}\{\Gamma_i^{-1}\}\Big\}.
\end{aligned}
\tag{4.32}
$$

Differentiating (4.29) with respect to time and substituting (4.5), (4.7), (4.15), (4.16)

$$
\begin{aligned}
\dot{V}_1(t) = \sum_{i=1}^{N} \Big\{ & \eta_i^T \Big[\tilde{b}_i - C_i(q_i,\dot{q}_i)\eta_i - F_{di}(q_i)\eta_i - M_i(q_i)k_{1i}\eta_i - C_i(q_i,\dot{q}_{di} + e_{fi} + e_i)\eta_i \\
& + N_{di} + \tilde{N}_i + \gamma_i(k_{1i}+1)e_{fi} \\
& - \gamma_i k_{2i} e_i - \beta_i tanh(e_i + k_{fi} r_{fi}) - \sum_{j\in\mathscr{S}_i} k_{3ij}(e_i(t) - e_j(t - T_{ij}(t))) \\
& + (k_{1i}+1)\sum_{j\in\mathscr{S}_i} k_{4ij}(e_{fi}(t) - e_{fj}(t - T_{ij}(t)))\Big] \\
& + \frac{1}{2}\eta_i^T \dot{M}_i(q_i)\eta_i - \tilde{b}_i^T \Gamma_i^{-1}\Gamma_i\eta_i + e_i^T k_{2i}\gamma_i\Big[\eta_i - e_{fi} - e_i\Big] + r_{fi}^T\gamma_i\Big[-k_{fi}r_{fi} + e_{fi}\Big] \\
& + e_{fi}^T\gamma_i\Big[-(k_{1i}+1)\eta_i - \alpha e_{fi} + k_{2i}e_i - r_{fi}\Big] - \eta_i^T\Big[N_{di} - \beta_i tanh(e_i + k_{fi}r_{fi})\Big] \\
& + \sum_{j\in\mathscr{S}_i} \delta_{ij}(e_i(t) - e_j(t - T_{ij}(t)))^T k_{3ij}\Big[\eta_i(t) - e_{fi}(t) - e_i(t) - (1-d_{ij})\eta_j(t - T_{ij}(t)) \\
& + (1-d_{ij})e_{fj}(t - T_{ij}(t)) + (1-d_{ij})e_j(t - T_{ij}(t))\Big] \\
& + \sum_{j\in\mathscr{S}_i} \delta_{ij}(e_{fi}(t) - e_{fj}(t - T_{ij}(t)))^T k_{4ij}\Big[-(k_{1i}+1)\eta_i(t) - \alpha e_{fi}(t) + k_{2i}e_i(t) - r_{fi}(t) \\
& + (1-d_{ij})(k_{1j}+1)\eta_j(t - T_{ij})) \\
& + \alpha(1-d_{ij})e_{fj}(t - T_{ij}(t)) - k_{2j}(1-d_{ij})e_j(t - T_{ij}(t)) + (1-d_{ij})r_{fj}(t - T_{ij}(t))\Big]\Big\}.
\end{aligned}
\tag{4.33}
$$

By applying the upper-bound in (4.12) and making some algebraic manipulations, the following expression is obtained

$$
\begin{aligned}
\dot{V}_1(t) = \sum_{i=1}^{N} \Bigg\{ & -\Big[\zeta_{F_{di}} + m_{1i}\lambda_{min}\{k_{1i}\}\Big]\|\eta_i\|^2 + \Big[\zeta_{C2i}(\zeta_{di} + \|e_{fi}\| + \|e_i\|)\Big]\|\eta_i\|^2 \\
& + \rho_{1i}\|\eta_i\|\|e_i\| + \rho_{2i}\|\eta_i\|\|e_{fi}\| + \rho_{3i}\|\eta_i\|\|r_{fi}\| - \gamma_i k_{2i}\|e_i\|^2 - \gamma_i k_{fi}\|r_{fi}\|^2 - \gamma_i \alpha_i \|e_{fi}\|^2 \\
& - \sum_{j\in\mathscr{S}_i} \delta_{ij}\lambda_{min}\{k_{3ij}\}\|e_i(t) - e_j(t - T_{ij}(t))\|^2 - \sum_{j\in\mathscr{S}_i} \delta_{ij}\lambda_{min}\{k_{4ij}\}\alpha\|e_{fi}(t) - e_{fj}(t - T_{ij}(t))\|^2 \\
& + \sum_{j\in\mathscr{S}_i} \delta_{ij}\lambda_{max}\{k_{3ij}\}\|e_i(t) - e_j(t - T_{ij}(t))\|\|r_{fi}(t)\| \\
& + \sum_{j\in\mathscr{S}_i} \delta_{ij}(1 - d_{ij})\lambda_{max}\{k_{3ij}\}\|e_i(t) - e_j(t - T_{ij}(t))\|\|\eta_j(t - T_{ij}(t))\| \\
& + \sum_{j\in\mathscr{S}_i} \delta_{ij}(1 - d_{ij})\lambda_{max}\{k_{3ij}\}\|e_i(t) - e_j(t - T_{ij}(t))\|\|e_{fj}(t - T_{ij}(t))\| \\
& + \sum_{j\in\mathscr{S}_i} \delta_{ij} d_{ij}\lambda_{max}\{k_{3ij}\}\|e_i(t) - e_j(t - T_{ij}(t))\|\|e_j(t - T_{ij}(t))\| \\
& + \sum_{j\in\mathscr{S}_i} \delta_{ij}\lambda_{max}\{k_{4ij}\}\lambda_{max}\{k_{2i}\}\|e_{fi}(t) - e_{fj}(t - T_{ij}(t))\|\|e_i(t)\| \\
& + \sum_{j\in\mathscr{S}_i} \delta_{ij}\lambda_{max}\{k_{4ij}\}\|e_{fi}(t) - e_{fj}(t - T_{ij}(t))\|\|r_{fi}(t)\| \\
& + \sum_{j\in\mathscr{S}_i} \delta_{ij}(1 - d_{ij})\lambda_{max}\{k_{4ij}\}\lambda_{max}\{k_{1j} + 1\}\|e_{fi}(t) - e_{fj}(t - T_{ij}(t))\|\|\eta_j(t - T_{ij}(t))\| \\
& + \sum_{j\in\mathscr{S}_i} \delta_{ij}\alpha d_{ij}\lambda_{max}\{k_{4ij}\}\|e_{fi}(t) - e_{fj}(t - T_{ij}(t))\|\|e_{fj}(t - T_{ij}(t))\| \\
& + \sum_{j\in\mathscr{S}_i} \delta_{ij}(1 - d_{ij})\lambda_{max}\{k_{4ij}\}\lambda_{max}\{k_{2j}\}\|e_{fi}(t) - e_{fj}(t - T_{ij}(t))\|\|e_j(t - T_{ij}(t))\| \\
& + \sum_{j\in\mathscr{S}_i} \delta_{ij}(1 - d_{ij})\lambda_{max}\{k_{4ij}\}\|e_{fi}(t) - e_{fj}(t - T_{ij}(t))\|\|r_{fj}(t - T_{ij}(t))\| \Bigg\}.
\end{aligned}
\tag{4.34}
$$

After a similar square completing process given in the Proof of Theorem 3.1, upper-bound of $\dot{V}_1(t)$ can be given as

$$
\begin{aligned}
\dot{V}_1(t) \leq \sum_{i=1}^{N} \Bigg\{ & -\Big[\zeta_{F_{di}} + m_{1i}\lambda_{min}\{k_{1i}\} - \zeta_{C2i}(\zeta_{di} + \|e_{fi}\| + \|e_i\|) - 3\Big]\|\eta_i\|^2 \\
& - k_{8i}\|e_i\|^2 - k_{7i}\|r_{fi}\|^2 - k_{6i}\|e_{fi}\|^2 \\
& - \sum_{j\in\mathscr{S}_i} \delta_{ij}\left[\lambda_{min}\{k_{3ij}\} - \left(1 + \frac{1-d_{ij}}{4} + \frac{1-d_{ij}}{4d_{ij}^2} + \frac{1}{4(1-d_{ij})}\right)\right]\|e_i(t) - e_j(t - T_{ij}(t))\|^2 \\
& - \sum_{j\in\mathscr{S}_i} \delta_{ij}\left[k_{5ij} - \left(1 + \frac{1}{4(1-d_{ij})}\right)\right]\|e_{fi}(t) - e_{fj}(t - T_{ij}(t))\|^2 \\
& + \sum_{j\in\mathscr{S}_i} \delta_{ij}(1-d_{ij})z_{1ij}\|\eta_j(t - T_{ij})\|^2 + \sum_{j\in\mathscr{S}_i} \delta_{ij}d_{ij}^2(1-d_{ij})z_{1ij}\|e_j(t - T_{ij})\|^2 \\
& + \sum_{j\in\mathscr{S}_i} \delta_{ij}d_{ij}^2(1-d_{ij})z_{2ij}\|e_{fj}(t - T_{ij})\|^2 + \sum_{j\in\mathscr{S}_i} \delta_{ij}(1-d_{ij})\|r_{fj}(t - T_{ij}(t))\| \Bigg\}.
\end{aligned}
\tag{4.35}
$$

For the time-varying delayed signals, a Lyapunov-Krasovskii functional can be defined as

$$
\begin{aligned}
V_2(t) = & V_1(t) + \sum_{i\in\mathscr{S}}\sum_{j\in\mathscr{S}_i} \delta_{ij} z_{1ij} \int_{t-T_{ij}(t)}^{t} \eta_j^T(\omega)\eta_j(\omega)d\omega + \sum_{i\in\mathscr{S}}\sum_{j\in\mathscr{S}_i} \delta_{ij} z_{1ij} d_{ij}^2 \int_{t-T_{ij}(t)}^{t} e_j^T(\omega)e_j(\omega)d\omega \\
& + \sum_{i\in\mathscr{S}}\sum_{j\in\mathscr{S}_i} \delta_{ij} z_{2ij} d_{ij}^2 \int_{t-T_{ij}(t)}^{t} e_{fj}^T(\omega)e_{fj}(\omega)d\omega + \sum_{i\in\mathscr{S}}\sum_{j\in\mathscr{S}_i} \delta_{ij} \int_{t-T_{ij}(t)}^{t} r_{fj}^T(\omega)r_{fj}(\omega)d\omega
\end{aligned}
\tag{4.36}
$$

that can be bounded similar as in (4.30). Then, $\dot{V}_2(t)$ can be obtained as

$$\dot{V}_2(t) \leq \sum_{i\in\mathscr{S}} \Bigg\{ -\left[\left(\zeta_{F_{di}} + m_{1i}\lambda_{min}\{k_{1i}\}\right) - \left(\zeta_{C2i}(\zeta_{di} + \|e_{fi}\| + \|e_i\|) + 3 + \sum_{i\in\mathscr{S}_l} \delta_{li} z_{1li} \right) \right] \|\eta_i(t)\|^2$$
$$- \left[k_{8i} - \sum_{i\in\mathscr{S}_l} \delta_{li} d_{li}^2 z_{1li} \right] \|e_i(t)\|^2 - \left[k_{7i} - \sum_{i\in\mathscr{S}_l} \delta_{li} I_{nxn} \right] \|r_{fi}\|^2$$
$$- \left[k_{6i} - \sum_{i\in\mathscr{S}_l} \delta_{li} d_{li}^2 z_{2li} \right] \|e_{fi}(t)\|^2$$
$$- \sum_{j\in\mathscr{S}_i} \delta_{ij} \left[\lambda_{min}\{k_{3ij}\} - \left(1 + \frac{1-d_{ij}}{4} + \frac{(1-d_{ij})}{4d_{ij}^2} + \frac{1}{4(1-d_{ij})} \right) \right] \|e_i(t) - e_j(t - T_{ij}(t))\|^2$$
$$- \sum_{j\in\mathscr{S}_i} \delta_{ij} \left[k_{5ij} - \left(1 + \frac{1}{4(1-d_{ij})} \right) \right] \|e_{fi}(t) - e_{fj}(t - T_{ij}(t))\|^2 \Bigg\}. \tag{4.37}$$

As long as the gain conditions given in Theorem (4.2) hold, it is concluded that

$$\dot{V}_2(t) \leq -\kappa \|y(t)\|^2, \qquad \forall \|h(t)\| \geq \|y(t)\| \geq \|\mu(t)\| \geq d(\epsilon) \tag{4.38}$$

with $\kappa \in \mathbb{R}^+$ and $y(t) = \left[y_1^T(t) \;\; y_2^T(t) \;\; .... \;\; y_N^T(t) \right]^T$. $V_2(t)$ is a decreasing function with a maximum value of $V_2(0)$. Then, it can be said that $y(t), \tilde{b}(t), \nu(t) \in \mathscr{L}_\infty$. Using (4.4), (4.5) and (4.7), with the fact that $e(t), \eta(t), e_f(t), r_f(t) \in \mathscr{L}_\infty$, it is clear that $\dot{e}_f(t), \dot{r}_f(t), \dot{e}(t) \in \mathscr{L}_\infty$ as well as $p(t), \dot{p}(t) \in \mathscr{L}_\infty$. Also, $q(t) \in \mathscr{L}_\infty$ since $q_d(t)$ is bounded. Since $\tilde{b}(t) \in \mathscr{L}_\infty$ and b is constant, $\hat{b}(t)$ is bounded and converges to constant values. By utilizing all these bounded signals, it can be concluded that $\tau(t) \in \mathscr{L}_\infty$.

The analysis can be finalized that all error signals in $y(t)$ converge to a hyperball $d(\epsilon)$ as defined in Lemma 4.1, with sufficiently large selected β_i, given in (4.23), as $t \to \infty$.

■

4.6 Simulation Results

The simulation study is established to illustrate the performance of the proposed linear filter in (4.2)-(4.4) and the control structure (4.13), in $MATLAB^{TM}/Simulink^{TM}$, consisting of 5 two-link robot manipulators, with the dynamics and parameters given in (3.35) and Table 3.1, respectively. The desired trajectory given to manipulators has the function as in (3.37). The initial states of manipulators are assumed arbitrarily as

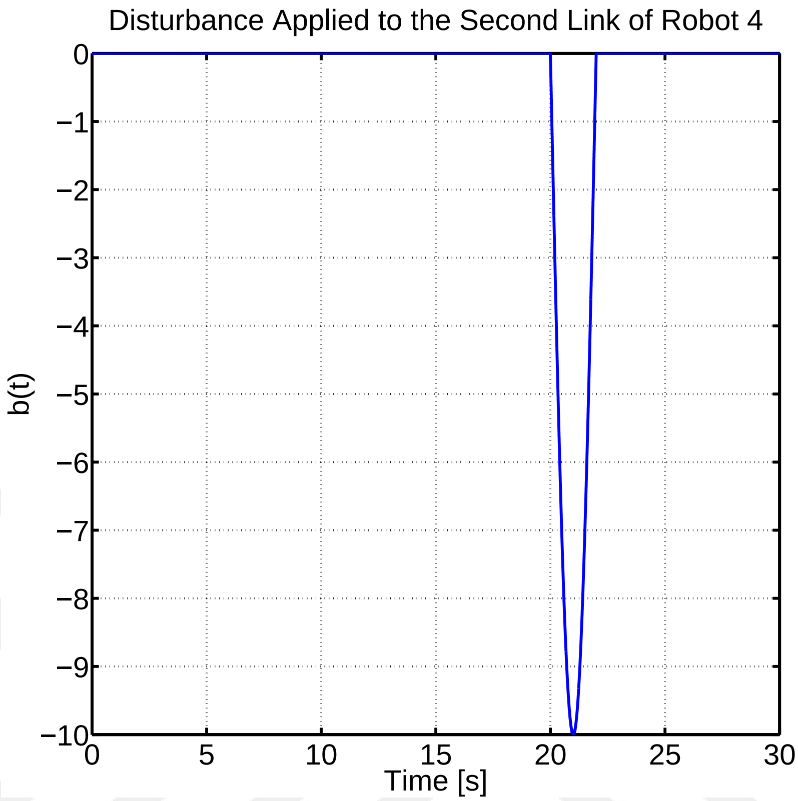

Figure 4.1 Disturbance signal subject link 2 of robot 4

$$q_1(0) = \begin{bmatrix} 5 & 30 \end{bmatrix}^T [deg] \qquad q_2(0) = \begin{bmatrix} 30 & 10 \end{bmatrix}^T [deg]$$

$$q_3(0) = \begin{bmatrix} 20 & 40 \end{bmatrix}^T [deg] \qquad q_4(0) = \begin{bmatrix} 40 & 20 \end{bmatrix}^T [deg]$$

$$q_5(0) = \begin{bmatrix} 15 & 0 \end{bmatrix}^T [deg]$$

and $\dot{q}_i(0) = 0$.

The control and disturbance adaptation gains are set to the following values

$$k_{1i} = diag\left\{ 12 \quad 12 \right\} \qquad k_{2i} = diag\left\{ 5 \quad 5 \right\}$$

$$k_{fi} = diag\left\{ 50 \quad 50 \right\} \qquad k_{3ij} = diag\left\{ 400 \quad 300 \right\}$$

$$k_{4ij} = diag\left\{ 3 \quad 1 \right\} \qquad \gamma_i = diag\left\{ 30 \quad 30 \right\}$$

$$\beta_i = diag\left\{ 50 \quad 50 \right\} \qquad \Gamma_i = diag\left\{ 0.5 \quad 0.5 \right\}$$

with $\alpha = 0.01$.

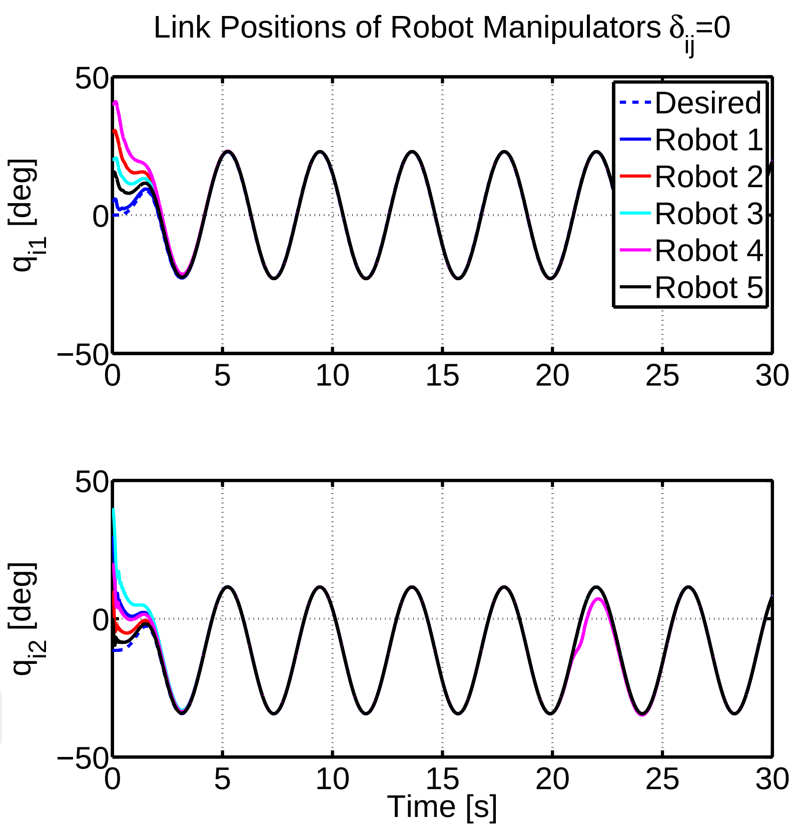

Figure 4.2 Link positions without synchronization $\delta_{ij} = 0$

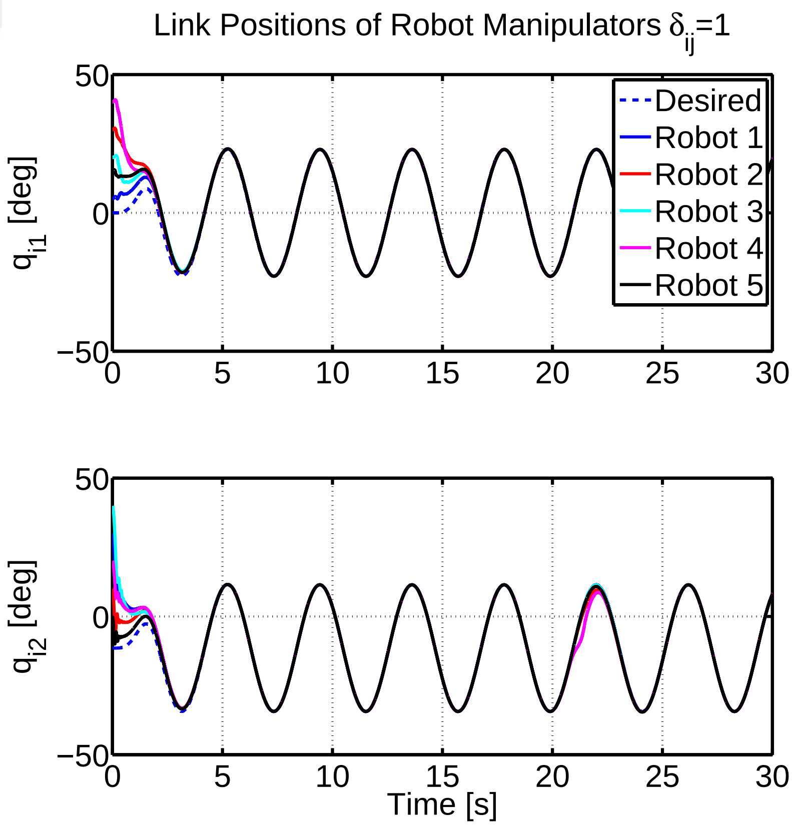

Figure 4.3 Link positions with synchronization $\delta_{ij} = 1$

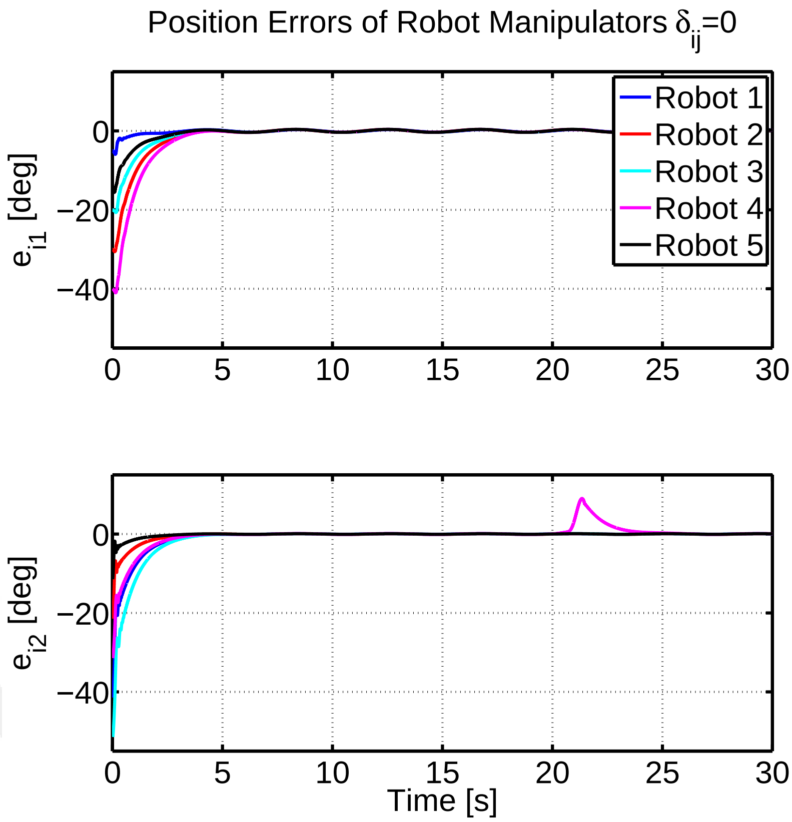

Figure 4.4 Position errors without synchronization $\delta_{ij} = 0$

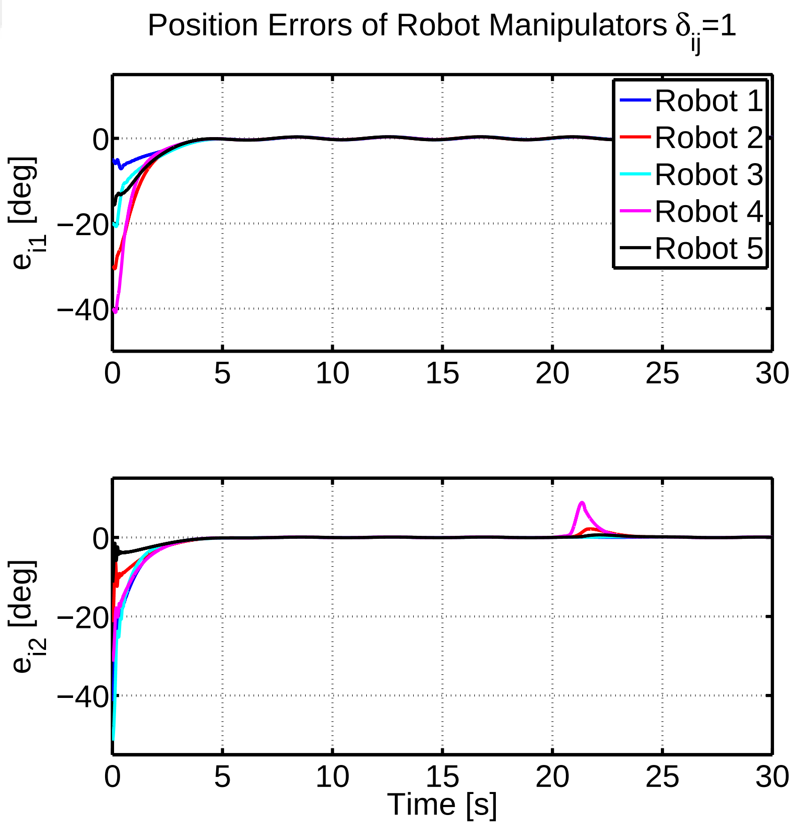

Figure 4.5 Position errors with synchronization $\delta_{ij} = 1$

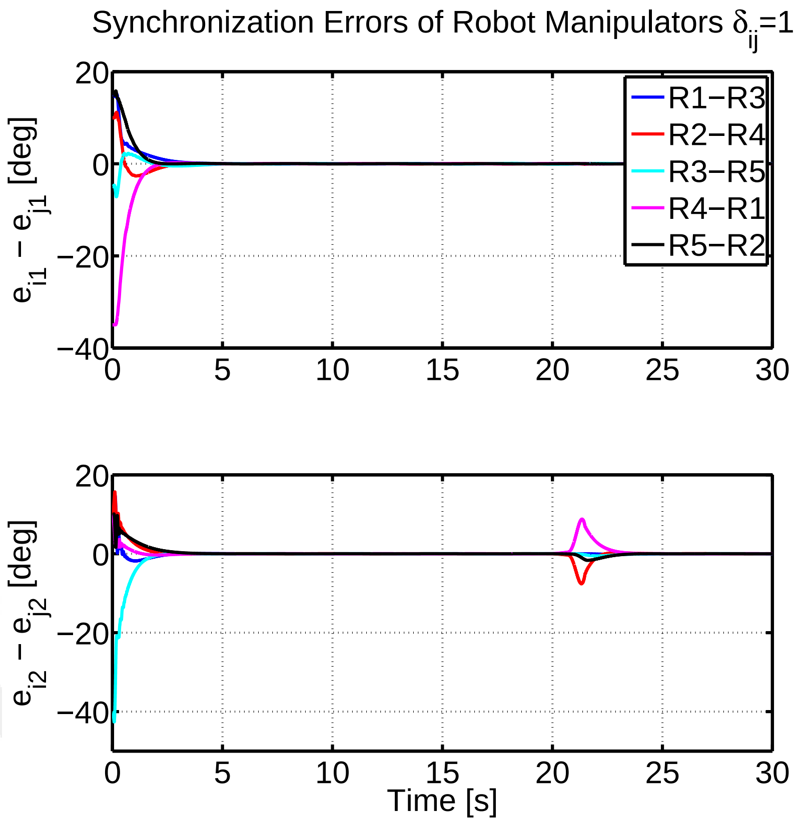

Figure 4.6 Position synchronization errors with synchronization $\delta_{ij} = 1$

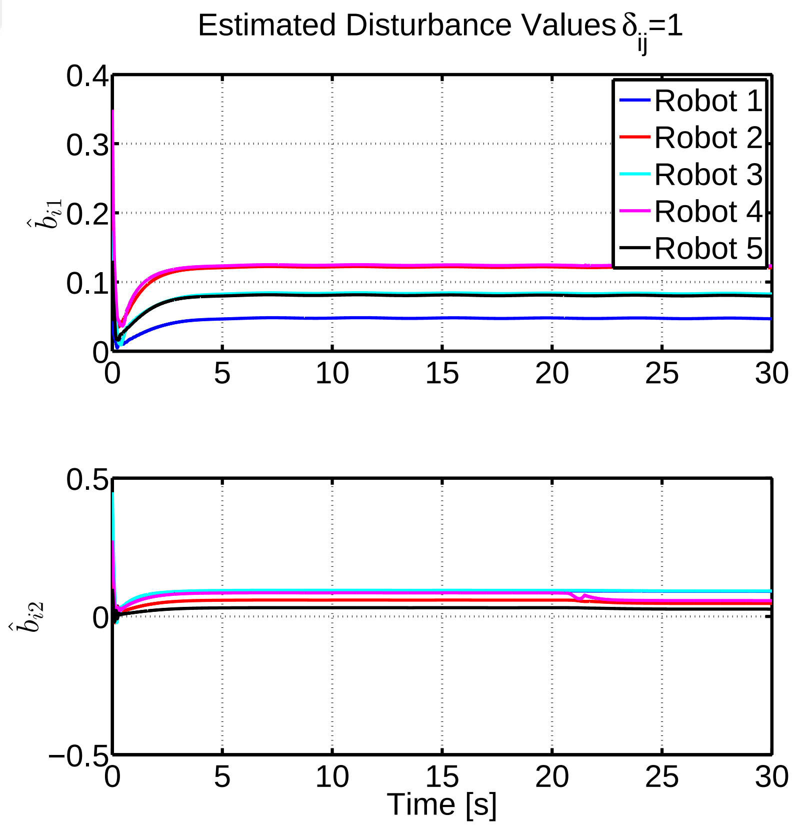

Figure 4.7 Disturbance estimation values with synchronization $\delta_{ij} = 1$

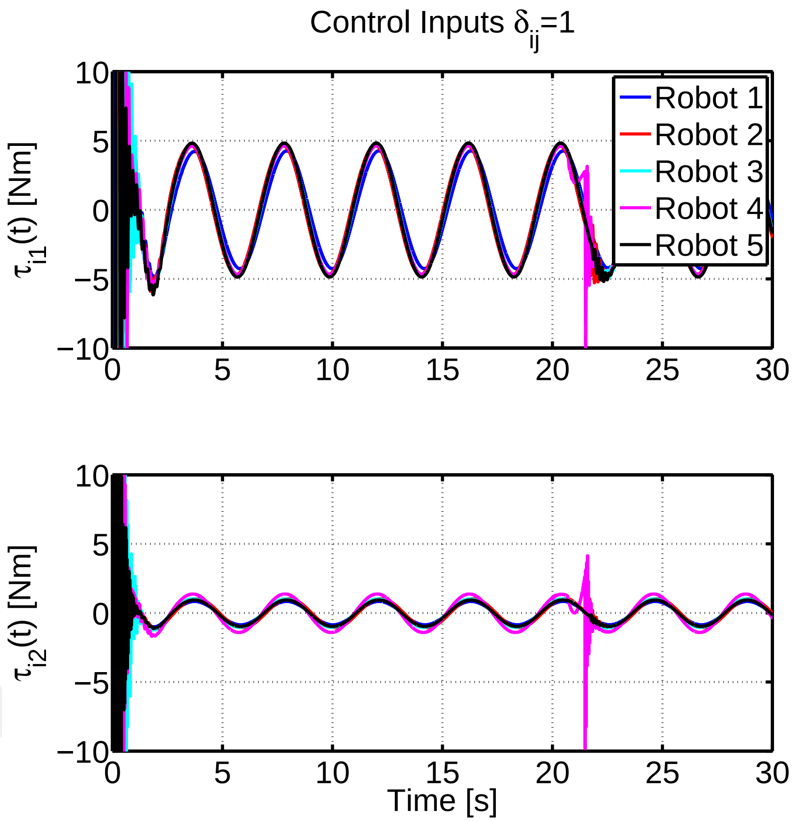

Figure 4.8 Control input signals with synchronization $\delta_{ij} = 1$

It is assumed that the manipulators have the communication topology as in Figure 3.1 with time-varying delay values in (3.38) and the disturbance signal applied to the second link of Robot 4 between $t = 20 - 22s$ is given in Figure 4.1.

The results obtained from the simulation study are presented in Figures 4.2 - 4.8. From Figures 4.2 and 4.4, it is clear that manipulators converge to the desired trajectory in different times, especially Robot 1 reaches to the desired trajectory before the others. The results, as shown in Figures 4.3 and 4.5, indicate that with the effect of synchronization terms, manipulators meet and converge to the desired trajectory, simultaneously. With the help of disturbance estimation, in both cases, Robot 4 turns to desired trajectory after the impact of disturbance signal, but it can be seen by comparing Figures of Link positions and Position Errors, disturbance signal effects Robot 4 less, when $\delta_{ij} = 1$. Estimated disturbance values are presented in Figure 4.7 and applied control signals are depicted in 4.8.

4.7 Experimental Results

The proposed linear filter in (4.2)-(4.4) and the control structure (4.13) is implemented on the experimental setup given in Section 2.2, for the end-effector control and synchronization of robot manipulators. For the task-space synchronization of non-redundant robot manipulators, mathematical model of a robot manipulator can be represented with

$$M_i(x_i)\ddot{x}_i + C_i(x_i,\dot{x}_i)\dot{x}_i + G_i(x_i) = F_i + b_i$$

where $x_i(t) \in \mathbb{R}^n$ is the vector of end-effector coordinates with its time-derivatives $\dot{x}_i(t)$, $\ddot{x}_i(t)$ and

$$\begin{aligned}
M_i(x_i) &= J_i(q_i)^{-T} M_i(q_i) J_i(q_i)^{-1} \\
C_i(x_i,\dot{x}_i) &= J_i(q_i)^{-T} C_i(q_i,\dot{q}_i) J_i(q_i)^{-1} - J_i(q_i)^{-T} M_i(q_i) J_i(q_i)^{-1} \dot{J}_i(q_i) J_i(q_i)^{-1} \\
G_i(x_i) &= J_i(q_i)^{-T} G_i(q_i) \\
F_i &= J_i(q_i)^{-T} \tau_i \\
b_i &= J_i(q_i)^{-T} b_i^*.
\end{aligned}$$

with the Jacobian matrix $J_i(q_i)$ introduced in Section 2.1.4. Then, the linear filter and controller structures given in (4.2)-(4.4) and (4.13) can be used, assuming that the position error

$$e_i(t) = x_{di}(t) - x_i(t).$$

The desired trajectory given to manipulators has the function as in (4.39)

$$x_{di}(t) = \begin{bmatrix} 40cos(0.1\pi t) \\ -20 - 30sin(0.2\pi t) \\ -20 \end{bmatrix}^T [mm] \tag{4.39}$$

and the disturbance signal applied to the second link of Robot 2 between $t = 20 - 22s$ is given in Figure 4.9.

The control and disturbance adaptation gains are set to the following values

$$k_{1i} = diag\left\{ \begin{array}{ccc} 4 & 4 & 4 \end{array} \right\} \qquad k_{2i} = diag\left\{ \begin{array}{ccc} 7 & 6 & 6 \end{array} \right\}$$
$$k_{fi} = diag\left\{ \begin{array}{ccc} 500 & 500 & 500 \end{array} \right\} \qquad k_{3ij} = diag\left\{ \begin{array}{ccc} 190 & 190 & 190 \end{array} \right\}$$
$$k_{4ij} = diag\left\{ \begin{array}{ccc} 0.5 & 0.5 & 0.1 \end{array} \right\} \qquad \gamma_i = diag\left\{ \begin{array}{ccc} 20 & 20 & 20 \end{array} \right\}$$
$$\beta_i = diag\left\{ \begin{array}{ccc} 100 & 100 & 100 \end{array} \right\} \qquad \Gamma_i = diag\left\{ \begin{array}{ccc} 100 & 100 & 100 \end{array} \right\}$$

with $\alpha = 100$.

Additional to the natural time-delay values caused by wireless modem, variable time-delay functions given in (3.42) are implemented to the system on Simulink, for the communication topology as in Figure 3.11

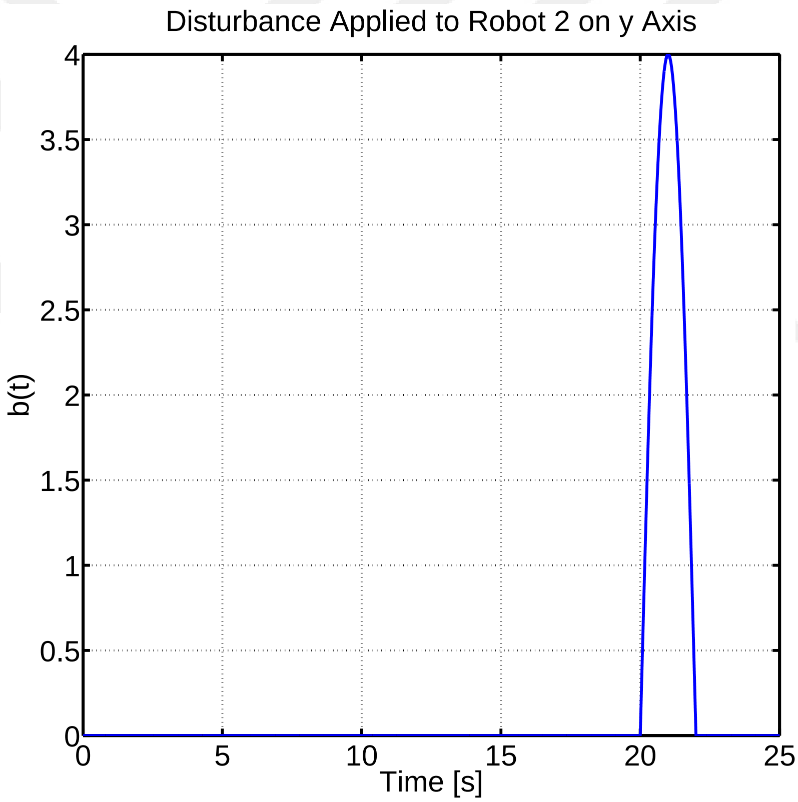

Figure 4.9 Disturbance signal subject robot 2 on y axis

The results are presented in Figures 4.10-4.15. In the absence of synchronization as can be seen from Figure 4.10, end-effectors of manipulators converge to the desired trajectory from different points, while Figure 4.11, 4.12 and 4.13 prove that with the help of the synchronization terms end-effectors of manipulators meet before their tracking errors stay close to zero, without need of model knowledge in controller. Comparing Figures 4.10 and 4.11, synchronization reduces the effects of disturbance signal and help Robot 2 to converge to the desired trajectory in less time.

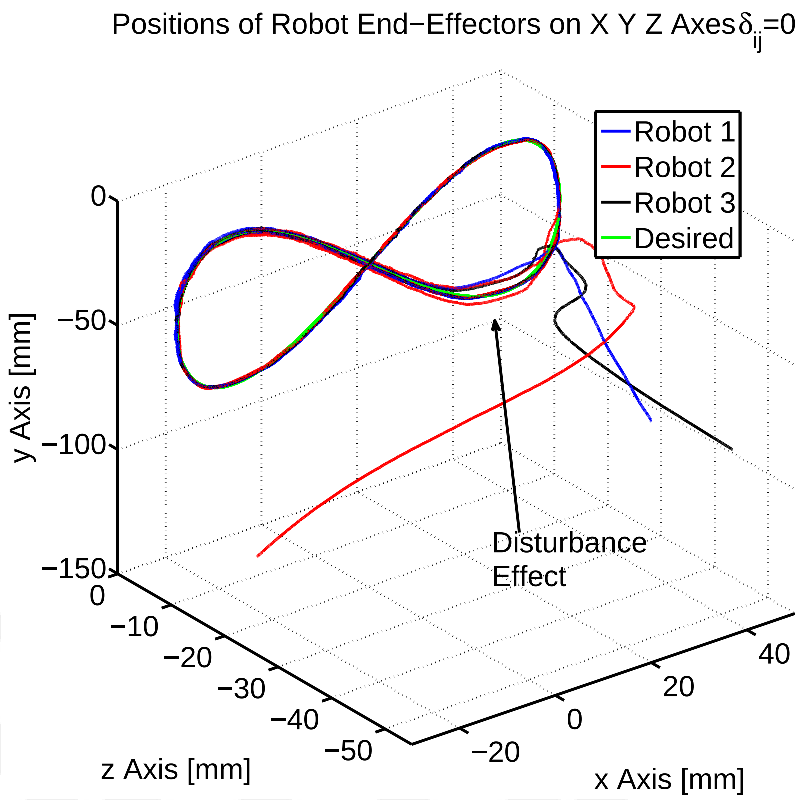

Figure 4.10 End-effector trajectories without synchronization $\delta_{ij} = 0$

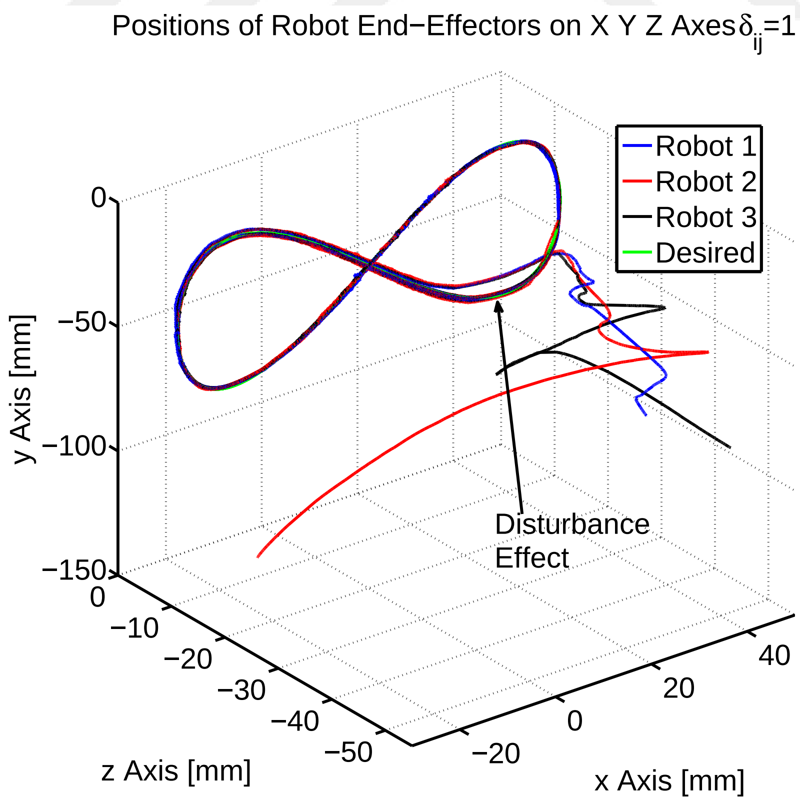

Figure 4.11 End-effector trajectories without synchronization $\delta_{ij} = 1$

Estimated disturbance values $\hat{b}_i$ converge to constant, as shown in Figure 4.14. Finally, Figure 4.15 reveals that control input signals remain in applicable bounds during the operation.

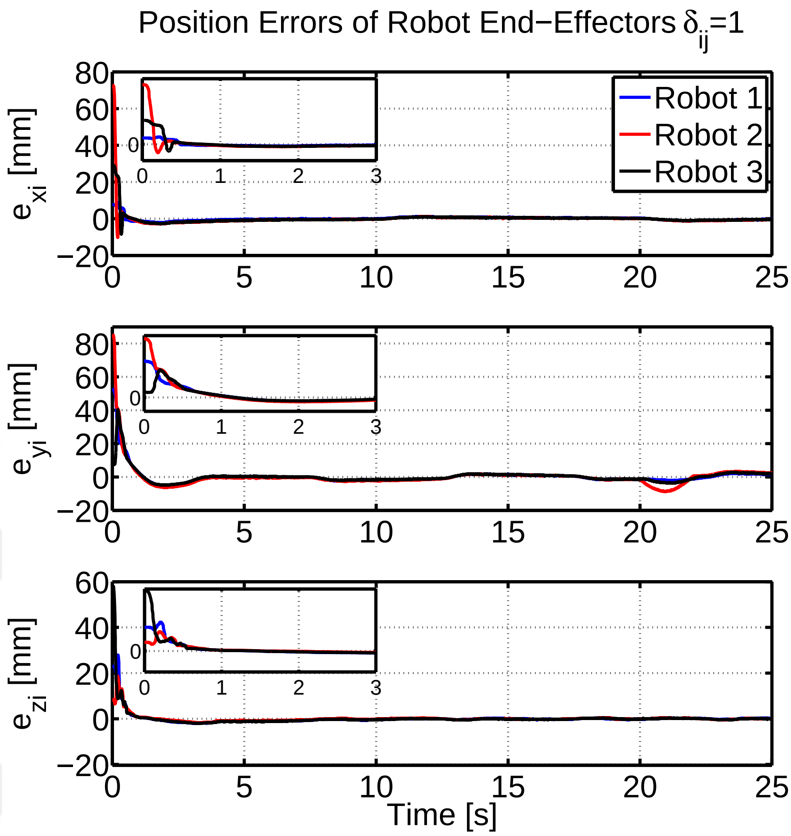

Figure 4.12 Position errors with synchronization $\delta_{ij} = 1$

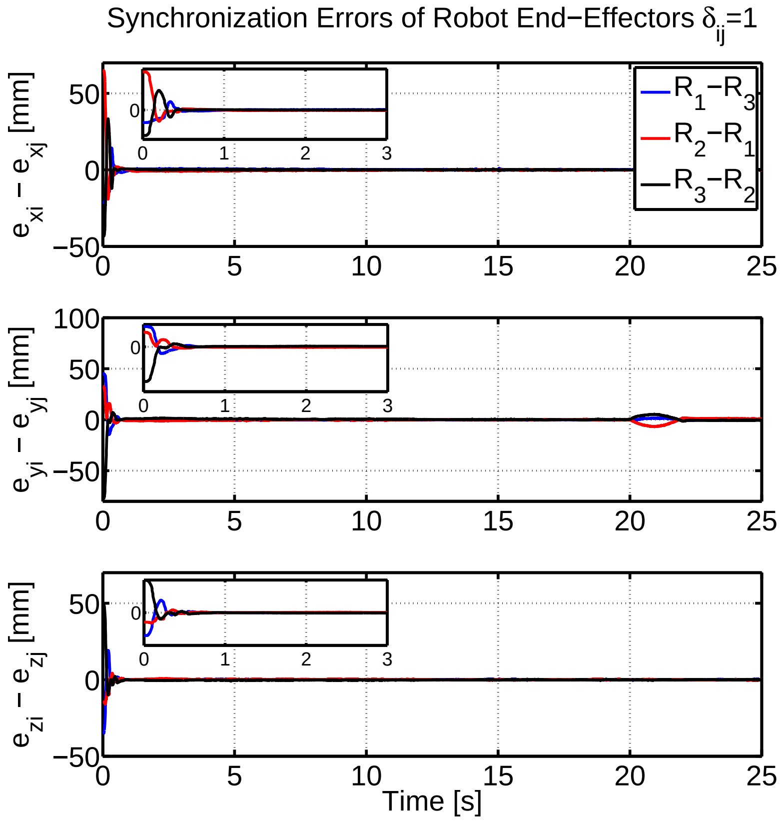

Figure 4.13 Position synchronization errors with synchronization $\delta_{ij} = 1$

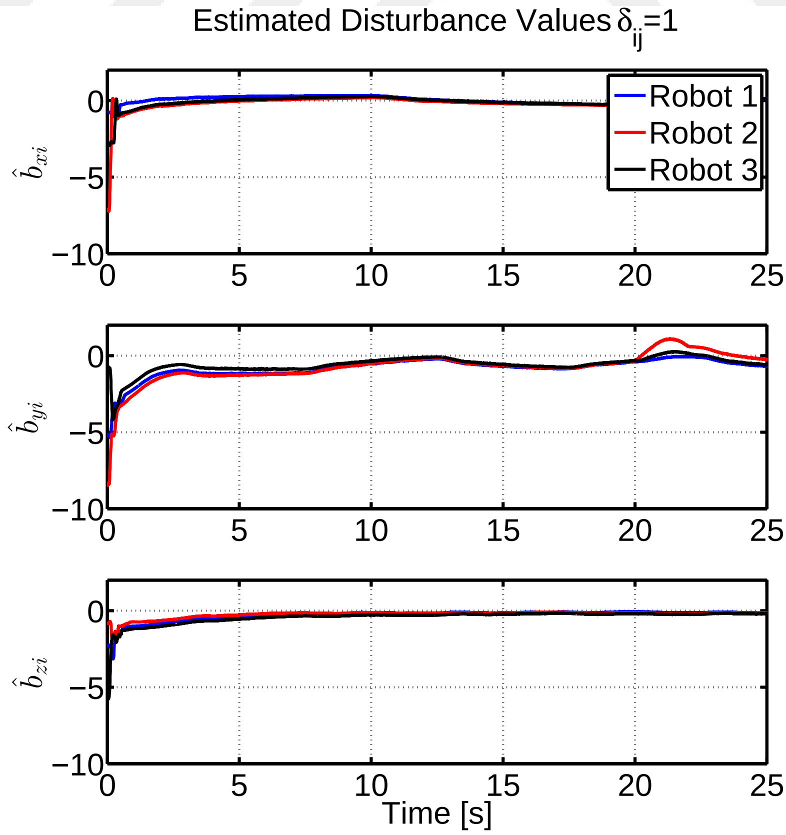

Figure 4.14 Disturbance estimation values with synchronization $\delta_{ij} = 1$

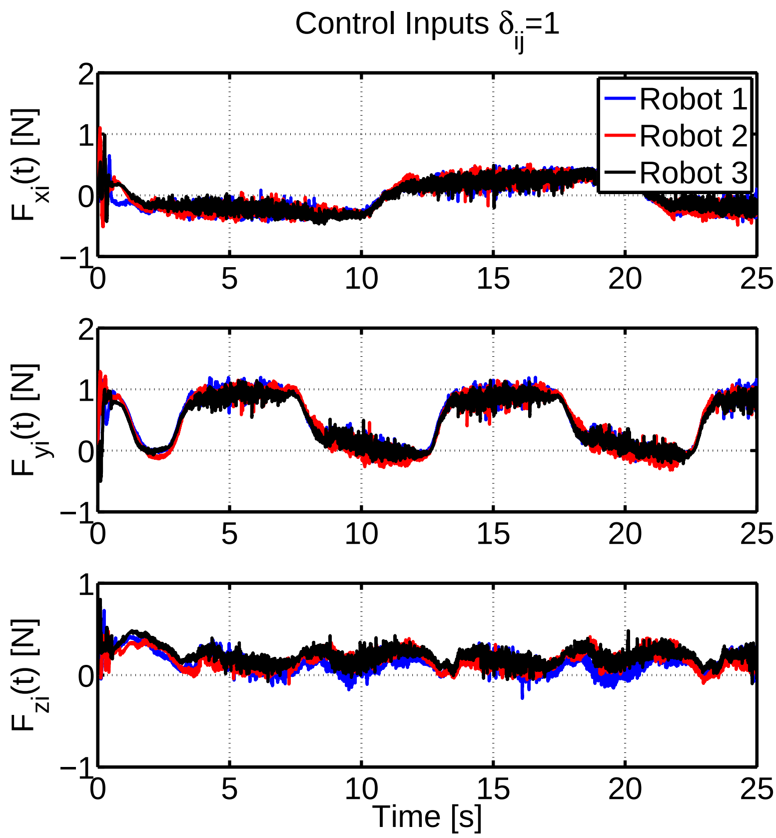

Figure 4.15 Control input signals with synchronization $\delta_{ij} = 1$

5 Robust Output Feedback Synchronization of Kinematically Redundant Robot Manipulators in Task Space

In this section, design and implementation of output-feedback robust controller for synchronization of kinematically redundant robot manipulators in task space is described. Following the stability analysis, the simulation study results on a system with 3 three-link robot manipulators are presented.

5.1 Problem Definition

In this study, the problem is handled as position synchronization for the end-effectors of multiple kinematically redundant robot manipulators. In many robot applications, desired trajectories are usually formed according to the end-effector positions on task/operation space, in agreement with the task to be achieved. This makes the general joint-based control structures impractical, since the solution of inverse kinematics to convert the desired task-space trajectory into the desired joint-space trajectory is required [51].

Kinematically redundant manipulators provide advantage in terms of dexterity and versatility, since they have more degrees of freedom than the required to execute the given task [52, 53]. In other words, the dimension of link position variables n is greater than the dimension of operation space m. However, this special structure requires control schemes, that also include effects of redundancy [52].

As the performance criteria, position tracking error $e_i(t) \in \mathbb{R}^m$ ($i \in \mathscr{S} \triangleq \{1, .., N\}$), for each manipulator with the dynamical model given in (2.3), is defined as

$$e_i = x_{di} - x_i \tag{5.1}$$

where $x_i(t) \in \mathbb{R}^m$ stands for actual position of end-effectors, as defined in (2.9), and

$x_{di}(t) \in \mathbb{R}^m$ symbolizes the desired trajectory applied to the robot manipulators.

5.2 Filter Design

Since it is assumed that neither the end-effector nor the joint velocities are measurable, a linear-filter with the output $e_{fi} \in \mathbb{R}^m$ is defined as

$$e_{fi} = p_i - (k_{1i} + 1)e_i \tag{5.2}$$

where $p_i(t) \in \mathbb{R}^n$ is an auxiliary variable with the dynamic equation

$$\dot{p}_i = -(k_{1i} + 1 + \alpha)p_i + ((k_{1i} + 1)^2 + \alpha(k_{1i} + 1) - (k_{1i} + 1) + k_{2i})e_i - r_{fi}. \tag{5.3}$$

In the given equation, $k_{1i}, k_{2i} \in \mathbb{R}^{nxn}$ are positive definite, diagonal gain matrices, $\alpha \in \mathbb{R}$ is positive scalar constant gain and α is same for all agents. $r_{fi}(t)$ is an auxiliary variable with the expression

$$\dot{r}_{fi} = -k_{fi}r_{fi} + e_{fi} \tag{5.4}$$

where $k_{fi} \in \mathbb{R}^{nxn}$ is the positive definite, diagonal constant gain matrix. Dynamics of (5.2) can be presented as,

$$\dot{e}_{fi} = -\alpha e_{fi} - (k_{1i} + 1)J_i(q_i)\eta_i + k_{2i}e_i - r_{fi} \tag{5.5}$$

with the Jacobian matrix $J_i(q_i) \in \mathbb{R}^{mxn}$ and $\eta_i(t) \in \mathbb{R}^n$ is an auxiliary signal defined as follows

$$\eta_i = J_i^+(q_i)(e_{fi} + e_i + \dot{x}_{di}) + (I_n - J_i^+(q_i)J_i(q_i))g_i - \dot{q}_i \tag{5.6}$$

where (2.10) is utilized for $\dot{x}_i$. The pseudo-inverse $J_i^+(q_i)$ has the properties given in Subsection 2.1.4.

Since the considered robot manipulators are redundant, $J_i(q_i) \in \mathbb{R}^{nxm}$ with $n > m$, which means that the dimension of null-space of Jacobian matrix $\mathcal{N}(J_i(q_i))$ is at least $n - m$. This shows that any joint-space velocity $\dot{q}_i$ in $\mathcal{N}(J_i(q_i))$ does not contribute to the task-space velocity. If the controller does not include these unobservable joint velocities in $\mathcal{N}(J_i(q_i))$, the system may become unstable [44]. For this purpose vector function $g(.) \in \mathbb{R}^n$, given in (5.6), is used as the sub-task function, which can be thought as the desired null-space joint velocity with the projection $(I_n - J_i^+(q_i)J_i(q_i))$. The function $g_i(q_i)$ can be chosen according to pre-defined sub-task, e.g. singularity avoidance, joint limitation, manipulability, obstacle avoidance, etc. With the sub-task error definition

$$e_N = (I_n - J_i^+(q_i)J_i(q_i))(g_i - \dot{q}_i) \tag{5.7}$$

it is easy to show that

$$e_N = (I_n - J_i^+(q_i)J_i(q_i))\eta_i \tag{5.8}$$

which means e_N can be regulated as long as η_i is regulated [44, 53]. From this point, for the ease of presentation following notation is used

$$\vartheta_i = J_i^+(q_i)(e_{fi} + e_i + \dot{x}_{di}) + (I_n - J_i^+(q_i)J_i(q_i))g_i. \tag{5.9}$$

Based on the structure of (5.6), the velocity error and joint velocity can be defined as

$$\dot{e}_i = J_i(q_i)\eta_i - e_{fi} - e_i \tag{5.10}$$

$$\dot{q}_i = \vartheta_i - \eta_i, \tag{5.11}$$

respectively.

5.3 Error System Dynamics

To derive the error dynamics, time derivative of (5.6) is taken, both sides are multiplied by $M_i(q_i)$, (5.5), $\dot{e}_i$ and $\ddot{q}_i$ from E-L model given in (2.3) are substituted

$$\begin{aligned} M_i\dot{\eta}_i =& C_i(q_i,\dot{q}_i)\dot{q}_i + F_{di}\dot{q}_i + G_i(q_i) - \tau_i + W_i(q_i)\dot{q}_i \\ &+ M_i(q_i)J_i^+(q_i)\Big(-(\alpha+1)e_{fi} - k_{1i}J_i(q_i)\eta_i + (k_{2i}-1)e_i - r_{fi} + \ddot{x}_{di}\Big). \end{aligned} \tag{5.12}$$

The auxiliary term $W_i(q_i) \in \mathbb{R}^{nxn}$ has the linearly parameterizable expression as follows

$$\begin{aligned} W_i(q_i)\dot{q}_i =& M_i(q_i)\Big(\dot{J}_i^+(q_i)(e_{fi} + e_i + \dot{x}_{di}) + (-\dot{J}_i^+(q_i)J_i(q_i) - J_i^+(q_i)\dot{J}_i(q_i))g_i \\ &+ (I_n - J_i^+(q_i)J_i(q_i))\dot{g}_i\Big). \end{aligned} \tag{5.13}$$

With minor algebraic manipulations and using *Property 3* in Section 2.1.3 with (5.11), the open-loop error dynamics can be reformulated as

$$\begin{aligned} M_i(q_i)\dot{\eta}_i =& -M_i(q_i)J_i^+(q_i)k_{1i}J_i(q_i)\eta_i - C_i(q_i,\dot{q}_i)\eta_i - F_{di}\eta_i - W_i(q_i)\eta_i \\ &- C_i(q_i,\eta_i)\vartheta_i - \tau_i + Y_i\theta_i \end{aligned} \tag{5.14}$$

where $Y_i\theta_i \in \mathbb{R}^n$ is a linear parametrization of

$$\begin{aligned} Y_i\theta_i =& C_i(q_i,\vartheta_i)\vartheta_i + F_{di}\vartheta_i + G_i(q_i) + W_i(q_i)\vartheta_i \\ &+ M_i(q_i)J_i^+(q_i)\Big(-(\alpha+1)e_{fi} + (k_{2i}-1)e_i - r_{fi} + \ddot{x}_{di}\Big) \end{aligned} \tag{5.15}$$

denoting $Y_i(x_{di},\dot{x}_{di},\ddot{x}_{di},x_i,q_i,e_i,e_{fi},r_{fi},g_i) \in \mathbb{R}^{nxr}$ the regression matrix and $\theta_i \in \mathbb{R}^r$ system parameters, e.g. mass, intertia, friction coefficients.

5.4 The Proposed Control Scheme

Based on the subsequent stability analysis, we design the controller as follows

$$\begin{aligned} \tau_i =& Y_i\hat{\theta}_i + J_i^T(q_i)\Big(-\gamma_i(k_{1i}+1)e_{fi} + \gamma_i k_{2i}e_i + \Gamma_i\|Y_i\|^2(e_{fi}+e_i) \\ &+ \sum_{j\in\mathscr{S}_i}\delta_{ij}k_{3ij}(e_i(t) - e_j(t-T_{ij}(t))) - (k_{1i}+1)\sum_{j\in\mathscr{S}_i}\delta_{ij}k_{4ij}(e_{fi}(t) - e_{fj}(t-T_{ij}(t)))\Big). \end{aligned} \tag{5.16}$$

Given $\Gamma_i,\gamma_i,k_{2i},k_{3ij},k_{4ij} \in \mathbb{R}^{mxm}$ are the positive definite and diagonal control gain matrices. In (5.16), $\hat{\theta}_i$ symbolizes the constant best-guess values of system parameters. First three terms in parentheses are for tracking problem of each robot manipulator, with the nonlinear damping term $\|Y_i\|^2(e_{fi}+e_i)$. Last two terms are included to ensure the position and velocity synchronization between agents, respectively, and have the same structure with the controllers given in Sections 3.4 and 4.4.

After substituting the control law (5.16) into (5.14), the closed loop dynamics for the filtered tracking error-like signal $\eta_i(t)$ can be obtained as

$$\begin{aligned} M_i(q_i)\dot{\eta}_i =& -M_i(q_i)J_i^+(q_i)k_{1i}J_i(q_i)\eta_i - C_i(q_i,\dot{q}_i)\eta_i - F_{di}\eta_i - W_i(q_i)\eta_i - C_i(q_i,\eta_i)\vartheta_i + Y_i\tilde{\theta}_i \\ &- J_i^T(q_i)\Big(-\gamma_i(k_{1i}+1)e_{fi} + \gamma_i k_{2i}e_i + \Gamma_i\|Y_i\|^2(e_{fi}+e_i) \\ &+ \sum_{j\in\mathscr{S}_i}\delta_{ij}k_{3ij}(e_i(t) - e_j(t-T_{ij}(t))) - (k_{1i}+1)\sum_{j\in\mathscr{S}_i}\delta_{ij}k_{4ij}(e_{fi}(t) - e_{fj}(t-T_{ij}(t)))\Big) \end{aligned} \tag{5.17}$$

with $\tilde{\theta}_i = \theta_i - \hat{\theta}_i$.

5.5 Stability Analysis

Theorem 5.1. *For a system with N robot manipulators, each has the dynamic structure in* (2.3)*, the filter formulation in* (5.2), (5.3), (5.4) *and the output feedback control law given in* (5.16)*, guarantee uniform ultimate boundedness of tracking and synchroniza-*

tion errors in the sense that

$$\|y(t)\| \leq \sqrt{\frac{\lambda_2}{\lambda_1}\|y(0)\|^2 exp(-Kt/\lambda_2) + \frac{\lambda_2}{2\Gamma\kappa\lambda_1}\|\tilde{\theta}\|^2(1-exp(-Kt/\lambda_2))}$$

where

$$y_i(t) = \begin{bmatrix} \eta_i(t)^T & r_{fi}(t)^T & e_{fi}(t)^T & e_i(t)^T & s_{ij}(t)^T \end{bmatrix}^T$$

and

$$s_{ij}(t) = \begin{bmatrix} \delta_{ij}(e_i(t) - e_j(t - T_{ij}(t)))^T & \delta_{ij}(e_{fi}(t) - e_{fj}(t - T_{ij}(t)))^T \end{bmatrix}^T$$

with

$$\begin{aligned} \lambda_{1i} &= \frac{1}{2} min\Big\{m_{1i}, \lambda_{min}\{\gamma_i\}, \lambda_{min}\{k_{2i}\}, \lambda_{min}\{k_{3ij}\}, \lambda_{min}\{k_{4ij}\}\Big\} \\ \lambda_{2i} &= \frac{1}{2} max\Big\{m_{2i}, \lambda_{max}\{\gamma_i\}, \lambda_{max}\{k_{2i}\}, \lambda_{max}\{k_{3ij}\}, \lambda_{max}\{k_{4ij}\}\Big\}. \end{aligned} \tag{5.18}$$

All closed-loop signals remain bounded, as long as the positive gains satisfy following conditions

$$\alpha = \frac{k_{5ij}}{\lambda_{min}\{k_{4ij}\}} + \frac{\lambda^2_{max}\{k_{1j}+1\}(1-d_{ij})}{4\lambda_{min}\{k_{4ij}\}} + \frac{\lambda^2_{max}\{k_{2i}\}}{\lambda_{min}\{k_{4ij}\}} + \frac{\lambda^2_{max}\{k_{2j}\}(1-d_{ij})}{4\lambda_{min}\{k_{4ij}\}d^2_{ij}} + \frac{\lambda^2_{max}\{k_{4ij}\}(1-d_{ij})}{4\lambda_{min}\{k_{4ij}\}}$$

$$\lambda_{min}\{k_{1i}\} > \zeta_{C_{2i}}\|\vartheta_i(0)\| + \Gamma_i(\|Y_i(0)\|^2 + \|Y_i(0)\|^4) + \sum_{i\in\mathscr{S}_l}\delta_{li}z_{1li}$$

$$\gamma_i = \frac{k_{6i}}{\alpha} + \frac{\lambda^2_{max}\{k_{3ij}\}}{4\alpha} + \frac{\Gamma_i}{4\alpha}$$

$$k_{2i} = \frac{k_{8i}}{\gamma_i} + \frac{\lambda^2_{max}\{k_{4ij}\}}{4\gamma_i} + \frac{\Gamma_i}{4\gamma_i}$$

$$k_{fi} = \frac{k_{7i}}{\gamma_i} + \frac{\lambda^2_{max}\{k_{4ij}\}}{4\gamma_i}$$

$$\lambda_{min}\{k_{3ij}\} > 1 + \frac{1-d_{ij}}{4} + \frac{(1-d_{ij})}{4d^2_{ij}} + \frac{1}{4(1-d_{ij})}$$

$$k_{5ij} > 1 + \frac{1}{4(1-d_{ij})}$$

$$k_{6i} > \sum_{i\in\mathscr{S}_l}\delta_{li}z_{3li}d^2_{li}$$

$$k_{7i} > \sum_{i\in\mathscr{S}_l}\delta_{li}I_{nxn}$$

$$k_{8i} > \sum_{i \in \mathscr{S}_l} \delta_{li} z_{2li} d_{li}^2$$

where $z_{1ij} = j_{2j}^2(\lambda_{max}^2\{k_{3ij}\} + \lambda_{max}^2\{k_{4ij}\})$, $z_{2ij} = \lambda_{max}^2\{k_{3ij}\} + \lambda_{max}^2\{k_{4ij}\}$, $z_{3ij} = \lambda_{max}^2\{k_{3ij}\} + \alpha^2\lambda_{max}^2\{k_{4ij}\}$ *with the upper bound of* $\|J_j(q_j)\| \geq j_{2j}$ *and the subindice* l *symbolizes other agents in the system, that receive information from agent* i.

Proof. Let $V_1(t) = \sum_{i \in \mathscr{S}} V_{1i}(t)$ express the following non-negative function

$$\begin{aligned} V_1(t) &= \sum_{i \in \mathscr{S}} V_{1i}(t) \\ &= \frac{1}{2} \sum_{i \in \mathscr{S}} \Big\{ \eta_i^T M_i \eta_i + e_i^T \gamma_i k_{2i} e_i + r_{fi}^T \gamma_i r_{fi} + e_{fi}^T \gamma_i e_{fi} \\ &+ \sum_{j \in \mathscr{S}_i} \delta_{ij} (e_i(t) - e_j(t - T_{ij}(t)))^T k_{3ij} (e_i(t) - e_j(t - T_{ij}(t))) \\ &+ \sum_{j \in \mathscr{S}_i} \delta_{ij} (e_{fi}(t) - e_{fj}(t - T_{ij}(t)))^T k_{4ij} (e_{fi}(t) - e_{fj}(t - T_{ij}(t))) \Big\} \end{aligned} \tag{5.19}$$

that can be upper and lower bounded as

$$\lambda_1 \|y(t)\|^2 \leq V_1(t) \leq \lambda_2 \|y(t)\|^2 \tag{5.20}$$

with λ_1 and λ_2 given in (5.18). Differentiating (5.19) with respect to time and substituting (5.4), (5.5), (5.10), (5.17) with some algebraic manipulations and similar square completing process as in the Proof of Theorem 3.1, an upper-bound for the time derivative of (5.19) as

$$\begin{aligned} \dot{V}_1(t) \leq \sum_{i=1}^{N} \Big\{ &-\Big[m_{1i} j_{1i} j_{1i}^{+} \lambda_{min}\{k_{1i}\}\Big]\|\eta_i\|^2 + \Big[\|\vartheta_i(t)\| + \Gamma_i(\|Y_i\|^2 + \|Y_i\|^4)\Big]\|\eta_i\|^2 \\ &+ \frac{1}{4\Gamma_i}\|\tilde{\theta}_i\|^2 - k_{6i}\|e_{fi}\|^2 - k_{7i}\|r_{fi}\|^2 - k_{8i}\|e_i\|^2 \\ &- \sum_{j \in \mathscr{S}_i} \delta_{ij}\Big[\lambda_{min}\{k_{3ij}\} - \Big(1 + \frac{(1-d_{ij})}{4} + \frac{(1-d_{ij})}{4d_{ij}^2} \\ &\qquad + \frac{1}{4(1-d_{ij})}\Big)\Big]\|e_i(t) - e_j(t - T_{ij}(t))\|^2 \\ &- \sum_{j \in \mathscr{S}_i} \delta_{ij}\Big[k_{5ij} - (1 + \frac{1}{4(1-d_{ij})})\Big]\|e_{fi}(t) - e_{fj}(t - T_{ij}(t))\|^2 \\ &+ \sum_{j \in \mathscr{S}_i} \delta_{ij}(1-d_{ij}) z_{1ij}\|\eta_j(t - T_{ij}(t))\|^2 + \sum_{j \in \mathscr{S}_i} \delta_{ij} d_{ij}^2 (1-d_{ij}) z_{2ij}\|e_j(t - T_{ij}(t))\|^2 \\ &+ \sum_{j \in \mathscr{S}_i} \delta_{ij}(1-d_{ij})\|r_{fj}(t - T_{ij}(t))\|^2 + \sum_{j \in \mathscr{S}_i} \delta_{ij} d_{ij}^2 (1-d_{ij}) z_{3ij}\|e_{fj}(t - T_{ij}(t))\|^2 \Big\} \end{aligned} \tag{5.21}$$

where j_{1i} and j_{1i}^{+} are lower bounds of $\|J_i(q_i)\|$ and $\|J_i^{+}(q_i)\|$, respectively. To analyze the stability of last four terms indicating time-delay, the following Lyapunov-Krasovskii functional is defined as

$$\begin{aligned} V_2(t) = \sum_{i\in\mathcal{S}} \Big\{ V_{1i}(t) + \sum_{j\in\mathcal{S}_i} \delta_{ij} z_{1ij} \int_{t-T_{ij}(t)}^{t} \eta_j^T(\omega)\eta_j(\omega)d\omega + \sum_{j\in\mathcal{S}_i} \delta_{ij} z_{2ij} d_{ij}^2 \int_{t-T_{ij}(t)}^{t} e_j^T(\omega)e_j(\omega)d\omega \\ + \sum_{j\in\mathcal{S}_i} \delta_{ij} z_{3ij} d_{ij}^2 \int_{t-T_{ij}(t)}^{t} e_{fj}^T(\omega)e_{fj}(\omega)d\omega + \sum_{j\in\mathcal{S}_i} \delta_{ij} \int_{t-T_{ij}(t)}^{t} r_{fj}^T(\omega)r_{fj}(\omega)d\omega \Big\} \end{aligned} \tag{5.22}$$

that can be bounded similar as V_1 and the upper bound for $\dot{V}_2(t)$ can be written as

$$\begin{aligned} \dot{V}_2(t) \leq \sum_{i=1}^{N} \Big\{ & -\Big[m_{1i} j_{1i} j_{1i}^{+} \lambda_{min}\{k_{1i}\}\Big]\|\eta_i\|^2 + \Big[\|\vartheta_i(t)\| + \Gamma_i(\|Y_i\|^2 + \|Y_i\|^4) + \sum_{i\in\mathcal{S}_l} \delta_{li} z_{1li}\Big]\|\eta_i\|^2 \\ & + \frac{1}{4\Gamma_i}\|\tilde{\theta}_i\|^2 - \Big[k_{6i} - \sum_{i\in\mathcal{S}_l} \delta_{li} z_{3li} d_{li}^2\Big]\|e_{fi}\|^2 - \Big[k_{7i} - \sum_{i\in\mathcal{S}_l} \delta_{li} I_{nxn}\Big]\|r_{fi}\|^2 \\ & - \Big[k_{8i} - \sum_{i\in\mathcal{S}_l} \delta_{li} z_{2li} d_{li}^2\Big]\|e_i\|^2 \\ & - \sum_{j\in\mathcal{S}_i} \delta_{ij}\Big[\lambda_{min}\{k_{3ij}\} - \Big(1 + \frac{(1-d_{ij})}{4} + \frac{(1-d_{ij})}{4d_{ij}^2} \\ & \qquad + \frac{1}{4(1-d_{ij})}\Big)\Big]\|e_i(t) - e_j(t - T_{ij}(t))\|^2 \\ & - \sum_{j\in\mathcal{S}_i} \delta_{ij}\Big[k_{5ij} - (1 + \frac{1}{4(1-d_{ij})})\Big]\|e_{fi}(t) - e_{fj}(t - T_{ij}(t))\|^2 \Big\}. \end{aligned} \tag{5.23}$$

For the general system, (5.23) can be reformed as

$$\dot{V}_2(t) \leq -\kappa\|y(t)\|^2 + \frac{1}{4\Gamma}\|\tilde{\theta}\|^2 \tag{5.24}$$

and the solution of the differential inequality can be expressed as [54]

$$\|y(t)\| \leq \sqrt{\frac{\lambda_2}{\lambda_1}\|y(0)\|^2 exp(-Kt/\lambda_2) + \frac{\lambda_2}{2\Gamma\kappa\lambda_1}\|\tilde{\theta}\|^2(1 - exp(-Kt/\lambda_2))}. \tag{5.25}$$

In conclusion, from (5.25), it is possible to show that $y(t)$ is bounded as given in Theorem 5.1 (i.e. $\eta(t), r_f(t), e(t), e_f(t), s_{ij}(t)$). Under the assumption that desired trajectory x_{di} and its derivatives, sub-task function $g(t)$ and $\dot{g}(t)$ are all bounded, by employing standard signal chasing arguments, it can be said that all signals remain bounded.

Also, due to the boundedness of $J_i(q_i)$ and $J_i^{+}(q_i)$, sub-task error $e_N(t)$ in (5.8) will be bounded in the following sense

$$\|e_N(t)\| \leq \psi\sqrt{\frac{\lambda_2}{\lambda_1}\|y(0)\|^2 exp(-Kt/\lambda_2) + \frac{\lambda_2}{2\Gamma\kappa\lambda_1}\|\tilde{\theta}\|^2(1 - exp(-Kt/\lambda_2))} \quad (5.26)$$

where $\psi = \|I_n - J^+(q)J(q)\|_\infty$.

■

5.6 Simulation Results

The simulation study is established to determine the feasibility of the proposed linear filter in (5.2)-(5.4) and the control structure (5.16), in $MATLAB^{TM}/Simulink^{TM}$, with 3 three-link robot manipulators, have the dynamics as follows

$$\begin{bmatrix} \beta_1 + 2p_1c_2 + 2p_2c_{23} + 2p_3c_3 & \beta_2 + p_1c_2 + p_2c_{23} + 2p_3c_3 & \beta_3 + p_2c_{23} + p_3c_3 \\ \beta_2 + p_1c_2 + p_2c_{23} + 2p_3c_3 & \beta_2 + 2p_3c_3 & \beta_3 + p_3c_3 \\ \beta_3 + p_2c_{23} + p_3c_3 & \beta_3 + p_3c_3 & \beta_3 \end{bmatrix} \begin{bmatrix} \ddot{q}_1 \\ \ddot{q}_2 \\ \ddot{q}_3 \end{bmatrix} + \begin{bmatrix} C_{11} & C_{12} & C_{13} \\ C_{21} & C_{22} & C_{23} \\ C_{31} & C_{32} & C_{33} \end{bmatrix} \begin{bmatrix} \dot{q}_1 \\ \dot{q}_2 \\ \dot{q}_3 \end{bmatrix} + \begin{bmatrix} f_{d1} & 0 & 0 \\ 0 & f_{d2} & 0 \\ 0 & 0 & f_{d3} \end{bmatrix} \begin{bmatrix} \dot{q}_1 \\ \dot{q}_2 \\ \dot{q}_3 \end{bmatrix} = \begin{bmatrix} \tau_1 \\ \tau_2 \\ \tau_3 \end{bmatrix}$$

with

$$\begin{aligned}
C_{11} &= -(p_1s_2 + p_2s_{23})\dot{q}_2 - (p_2s_{23} + p_3s_3)\dot{q}_3 \\
C_{12} &= -(p_1s_2 + p_2s_{23})(\dot{q}_1 + \dot{q}_2) - (p_2s_{23} + p_3s_3)\dot{q}_3 \\
C_{13} &= -(p_2s_{23} + p_3s_3)(\dot{q}_1 + \dot{q}_2 + \dot{q}_3) \\
C_{21} &= (p_1s_2 + p_2s_{23})\dot{q}_1 - p_3s_3\dot{q}_3 \\
C_{22} &= -p_3s_3\dot{q}_3 \\
C_{23} &= -p_3s_3(\dot{q}_1 + \dot{q}_2 + \dot{q}_3) \\
C_{31} &= (p_2s_{23} + p_3s_3)\dot{q}_1 + p_3s_3\dot{q}_2 \\
C_{32} &= p_3s_3(\dot{q}_1 + \dot{q}_2) \\
C_{33} &= 0.
\end{aligned}$$

Table 5.1 Actual Robot Parameters

Parameters	Robot 1	Robot 2	Robot 3
p_{i1} $[kg.m^2]$	0.4752	0.32	0.5666
p_{i2} $[kg.m^2]$	0.12	0.0819	0.1594
p_{i3} $[kg.m^2]$	0.108	0.0725	0.1442
β_{i1} $[kg.m^2]$	1.2684	0.8528	1.4993
β_{i2} $[kg.m^2]$	0.3884	0.2587	0.485
β_{i3} $[kg.m^2]$	0.045	0.0304	0.0626
f_{di1} $[Nm.s]$	5.3	4.6	4.8
f_{di2} $[Nm.s]$	2.4	1.9	1.6
f_{di3} $[Nm.s]$	1.1	0.8	1.2
l_{i1} $[m]$	0.2	0.3	0.25
l_{i2} $[m]$	0.25	0.3	0.35
l_{i3} $[m]$	0.25	0.3	0.25

Manipulator parameters given in Table 5.1. It is assumed that link lengths are known and the other parameter values are estimated to be 20%, 30% and 15% for Robot 1,2 and 3 incorrectly, respectively. Time-delay values with communication topology as in Figure 3.11 are taken as

$$\begin{aligned} T_{1,2}(t) =& 0.1+0.06sin(t) \\ T_{2,3}(t) =& 0.12+0.05sin(0.5t) \\ T_{3,1}(t) =& 0.15+0.14sin(0.3t). \end{aligned} \tag{5.27}$$

The desired trajectory of robot manipulators is defined as

$$x_{di}(t) = \begin{bmatrix} 0.6+0.1cos(t) \\ 0.9-0.1sin(t) \end{bmatrix}^T [m]. \tag{5.28}$$

The subtask function $g(t)$ is selected for all robots as [53]

$$g(t) = -2(q_3 - q_2 + 0.5q_1)[1 \quad -1 \quad 1]^T \tag{5.29}$$

to obtain the optimum link configuration that is given by $(q_3 - 0.5q_2) = 0.5(q_2 - q_1)$.

Finally, control and filter gains are adjusted as

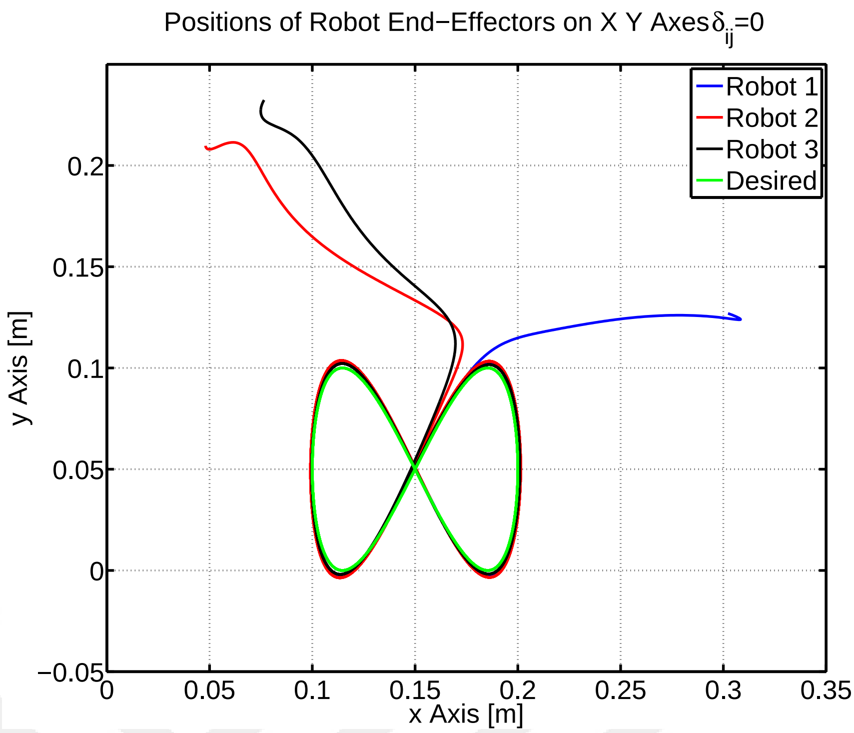

Figure 5.1 End-effector trajectories without synchronization $\delta_{ij} = 0$

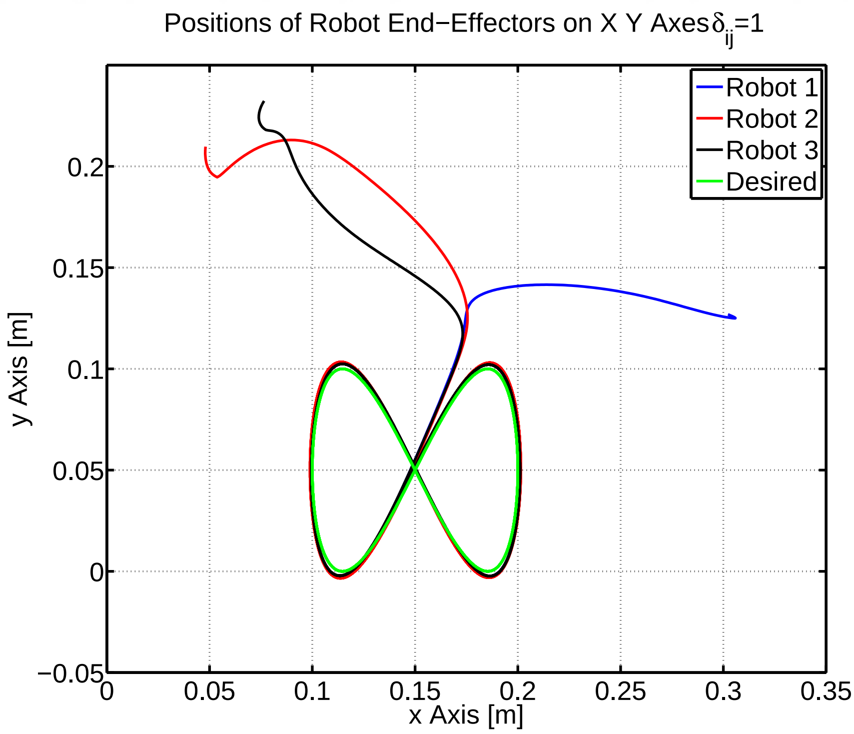

Figure 5.2 End-effector trajectories with synchronization $\delta_{ij} = 1$

$$k_{1i} = diag\left\{ \begin{array}{cc} 0.5 & 0.5 \end{array} \right\} \qquad k_{2i} = diag\left\{ \begin{array}{cc} 2 & 2 \end{array} \right\}$$
$$k_{fi} = diag\left\{ \begin{array}{cc} 50 & 50 \end{array} \right\} \qquad k_{3ij} = diag\left\{ \begin{array}{cc} 35 & 35 \end{array} \right\}$$
$$k_{4ij} = diag\left\{ \begin{array}{cc} 60 & 60 \end{array} \right\} \qquad \gamma_i = diag\left\{ \begin{array}{cc} 3 & 3 \end{array} \right\}$$
$$\Gamma_i = diag\left\{ \begin{array}{cc} 0.01 & 0.01 \end{array} \right\} \qquad \alpha = 15.$$

Comparing Figures 5.1 and 5.2, as well as Figures 5.3 and 5.4, it is clear that under the effect of synchronization, end-effectors of robot manipulators meet before they track to the given desired trajectory. It can be seen from Figure 5.4 that tracking errors of each robot and from the Figure 5.5 synchronization error between them stay in a bound around zero as stated in Theorem 5.1. Applied control signals are presented in Figure 5.6. Also, the clear effect of sub-task function $g(t)$ can be seen by comparing Figures 5.7 and 5.8, where $g(t) = 0$ and $g(t)$ is taken as given in (5.29), respectively. The function given in (5.29) ensures the optimum link configuration of each robot manipulator during synchronization and tracking.

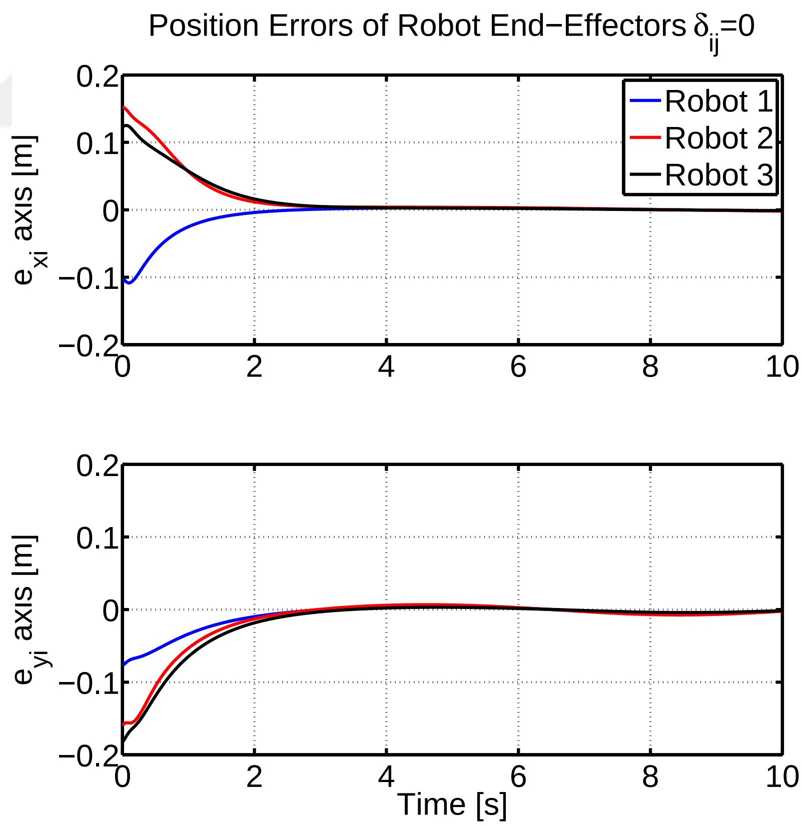

Figure 5.3 Position errors without synchronization $\delta_{ij} = 0$

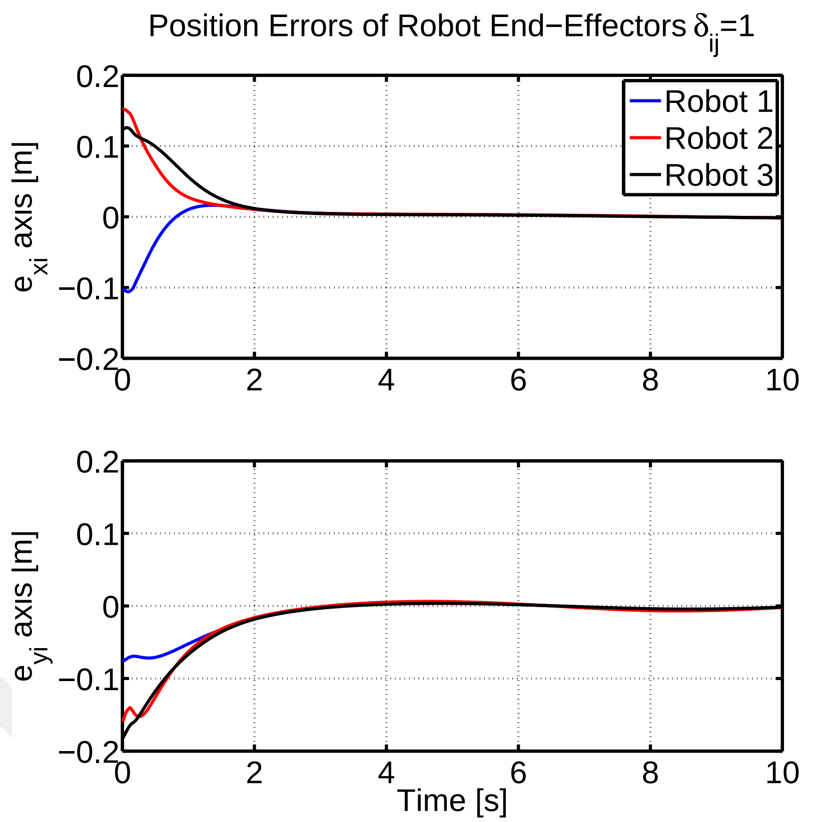

Figure 5.4 Position errors with synchronization $\delta_{ij} = 1$

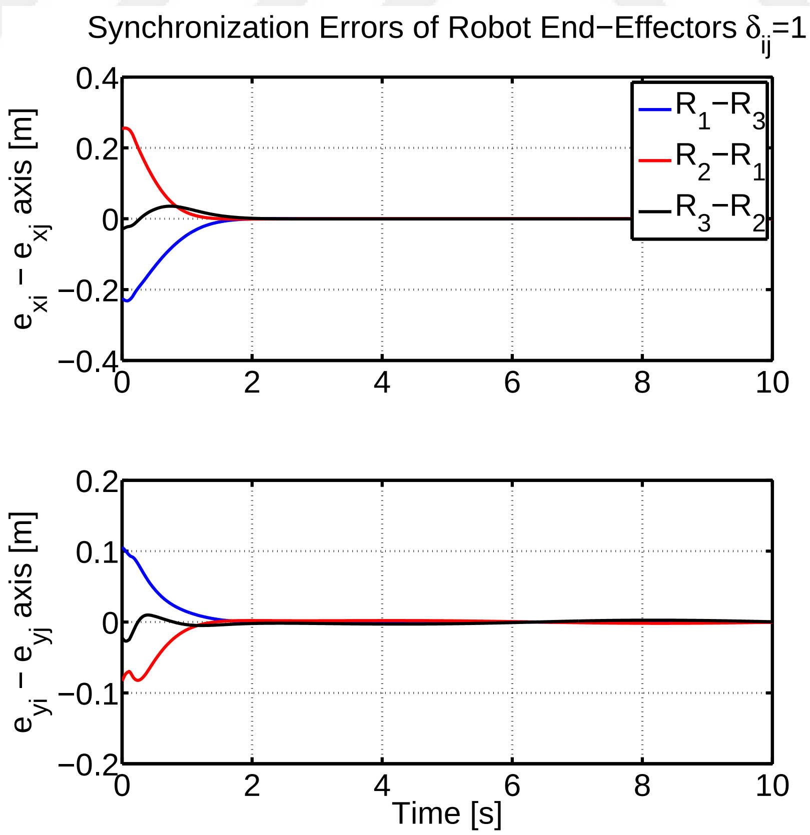

Figure 5.5 Position synchronization errors with synchronization $\delta_{ij} = 1$

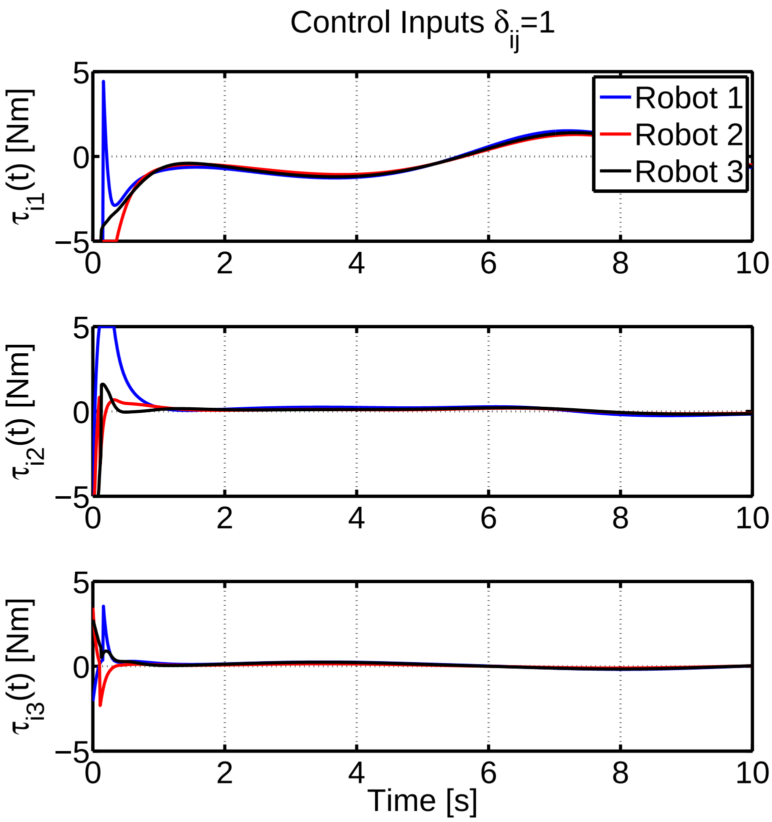

Figure 5.6 Control input signals with synchronization $\delta_{ij} = 1$

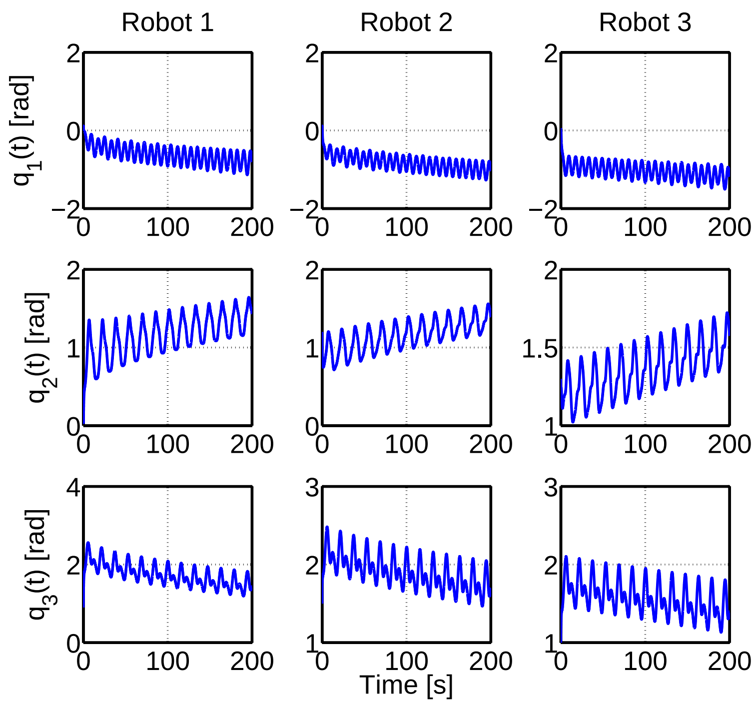

Figure 5.7 Joint positions without sub-task function $\delta_{ij} = 1$

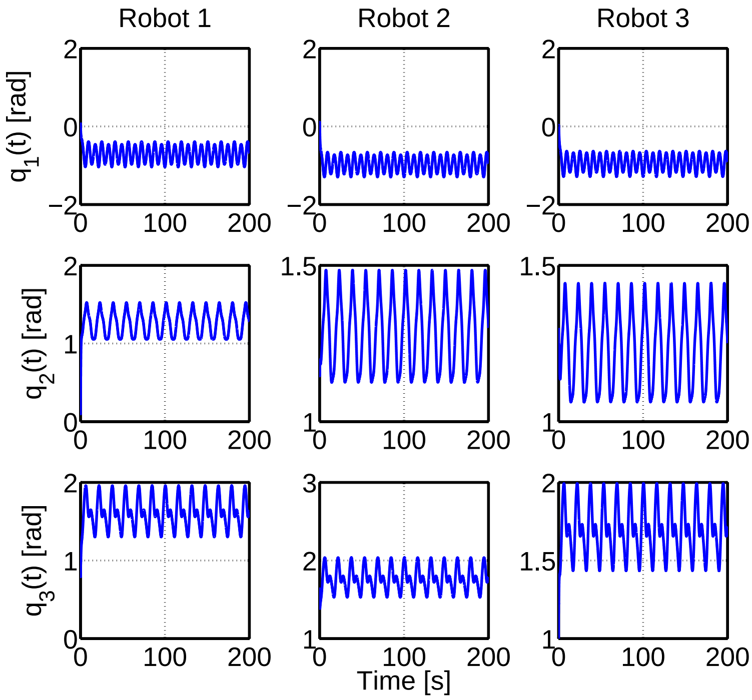

Figure 5.8 Joint positions with sub-task function $\delta_{ij} = 1$

6
Results And Discussion

In this dissertation, distributed tracking synchronization of Euler-Lagrange systems was considered. The problem was handled as a combination of tracking and synchronization problems and three different output-feedback control structures were proposed. In all cases, the output signal of suggested dynamic model-free linear-filter was used, instead of actual velocity error. So, the velocity measurement for synchronization was not needed.

The output-feedback adaptive controller, suggested in Section 3, ensured tracking synchronization in a multi-agent system, under the effects of parametric uncertainty and external disturbance. On the other hand, in Section 4, it was assumed that the entire dynamic model of agents in the system, could not be obtained. For this reason, an output-feedback robust control law was presented. The designed controller provided synchronization without velocity measurement and dynamic model knowledge.

For both control systems, simulation and experimental studies were introduced at the end of each Section. The results have shown that both controllers were applicable for electromechanical systems, that can be formulated by Euler-Lagrange equations and successful in providing tracking synchronization, over a directed communication topology with variable time-delay and under the effect of external disturbance.

Lastly, in Section 5, tracking synchronization of kinematically redundant robot manipulators in task-space was subjected. Specifically, the main idea was to design an output-feedback controller for a multi-agent system with extra degree of freedom and guarantee agents' tracking synchronization, under the effect of dynamic uncertainty. By the performed stability analysis and presented simulation results, it was shown that the tracking and synchronization errors remain bounded around zero, with the help of proposed output-feedback robust controller.

Future works may proceed along the following avenues.

- Output feedback mechanisms are preferred to reduce the effects of measurement noise. However, these control structures usually lead to a semi-global (asymptotic) stability result. As an open problem, it needs to be extended to global (asymptotic) stability result.

- For the synchronization problems considered in this dissertation, exact delay values have not been determined. Having information about delay values may possibly improve the performance of control system. Therefore, one may suggest an upper bound estimation procedure.

- Communication losses may deteriorate synchronization performance or even cause instability. A robust approach with respect to communication losses between agents can be addressed in terms of switching communication topologies. Alternatively, one may suggest an event-based control algorithm to reduce the information exchange over the communication network in the system.

A
Bounds

A.1 Bound of χ_i in Section 3.3

In this section, the upper bound of $\chi_i(e_i(t), e_{fi}(t)) \in \mathbb{R}^n$, in (3.10), is presented. From (3.9), $\chi_i(t)$ can be defined as

$$\begin{aligned}\chi_i =& M_i(q_i)\ddot{q}_{di} + C_i(q_i, \dot{q}_{di} + e_{fi} + e_i)(\dot{q}_{di} + e_{fi} + e_i) + F_{di}(\dot{q}_{di} + e_{fi} + e_i) \\ &+ G_i(q_i) - M_i(q_i)(-(\alpha+1)e_{fi} + (k_{2i} - 1)e_i) - Y_{di}\theta_i\end{aligned} \tag{A.1}$$

By exploiting $Y_{di}\theta_i$, (A.1) can be reformulated as

$$\begin{aligned}\chi_i =& [M_i(q_i) - M_i(q_{di})]\ddot{q}_{di} + [C_i(q_i, \dot{q}_i) - C_i(q_{di}, \dot{q}_{di})]\dot{q}_{di} + [G_i(q_i) - G_i(q_{di})] \\ &+ C_i(q_i, \dot{q}_{di})(e_{fi} + e_i) + C_i(q_i, e_{fi} + e_i)(\dot{q}_{di} + e_{fi} + e_i) + F_{di}(e_{fi} + e_i) \\ &- M_i(q_i)(-(\alpha+1)e_{fi} + (k_{2i} - 1)e_i)\end{aligned} \tag{A.2}$$

After introducing the upper bounds for the terms in square brackets as

$$\begin{aligned}\|[M_i(q_i) - M_i(q_{di})]\| &\leq m_{2i}\|e_i\| \\ \|[C_i(q_i, \dot{q}_{di}) - C_i(q_{di}, \dot{q}_{di})]\| &\leq \zeta_{C_{2i}}\zeta_{di}\|e_i\| \\ \|[G_i(q_i) - G_i(q_{di})]\| &\leq \zeta_{G_{2i}}\|e_i\|.\end{aligned} \tag{A.3}$$

The upper-bound for $\chi_i(t)$, with the help of bounds given in *Properties 1,3,4* given in Section 2.1.3, can be obtained as follows

$$\|\chi_i\| \leq \rho_{1i}(\|e_i\|, \|e_{fi}\|)\|e_i\| + \rho_{2i}(\|e_i\|, \|e_{fi}\|)\|e_{fi}\| \tag{A.4}$$

with

$$\begin{aligned}\rho_{1i}(\|e_i\|, \|e_{fi}\|) =& m_{2i}\|\ddot{q}_{di}\| + \zeta_{C_{2i}}\zeta_{di}^2 + \zeta_{G_{2i}} + 2\zeta_{C_{2i}}\zeta_{di} + \zeta_{C_{2i}}\left(\|e_{fi}\| + \|e_i\|\right) \\ &+ m_{2i}\lambda_{max}\{k_{2i}\} + \zeta_{F_{di}} \\ \rho_{2i}(\|e_i\|, \|e_{fi}\|) =& 2\zeta_{C_{2i}}\zeta_{di} + \zeta_{C_{2i}}\left(\|e_i\| + \|e_{fi}\|\right) + m_{2i}\alpha + \zeta_{F_{di}}.\end{aligned} \tag{A.5}$$

A.2 Bound of $\tilde{N}_i$ in Section 4.3

The equation of of $\tilde{N}_i(e_i(t), e_{fi}(t), r_{fi}(t)) \in \mathbb{R}^n$, can be given by using (4.9) and (4.10) as

$$\begin{aligned}\tilde{N}_i =& M_i(q_i)\ddot{q}_{di} - M_i(q_{di})\ddot{q}_{di} + C_i(q_i, \dot{q}_{di})\dot{q}_{di} - C_i(q_{di}, \dot{q}_{di})\dot{q}_{di} + G_i(q_i) - G_i(q_{di}) \\ &+ C_i(q_i, \dot{q}_{di})(e_{fi} + e_i) + C_i(q_i, e_{fi} + e_i)(\dot{q}_{di} + e_{fi} + e_i) \\ &+ F_{di}(e_{fi} + e_i) - M_i(q_i)((\alpha + 1)e_{fi} + r_{fi}) + M_i(q_i)(k_{2i} - 1)e_i.\end{aligned} \tag{A.6}$$

With the bounds presented in (A.3), upper-bound for $\tilde{N}_i$ can be obtained as

$$\|\tilde{N}_i\| \leq \rho_{1i}(\|e_i\|, \|e_{fi}\|)\|e_i\| + \rho_{2i}(\|e_i\|, \|e_{fi}\|)\|e_{fi}\| + \rho_{3i}\|r_{fi}\| \tag{A.7}$$

where

$$\begin{aligned}\rho_{1i}(\|e_i\|, \|e_{fi}\|) =& m_{2i}(\|\ddot{q}_{di}\| + \lambda_{max}\{k_{2i}\}) + \zeta_{C2i}(\zeta_{di}^2 + 2\zeta_{di} + \|e_{fi}\| + \|e_i\|) + \zeta_{G2i} + \zeta_{F_{di}} \\ \rho_{2i}(\|e_i\|, \|e_{fi}\|) =& m_{2i}(\alpha + 1) + \zeta_{C2i}(2\zeta_{di} + \|e_{fi}\| + \|e_i\|) + \zeta_{F_{di}} \\ \rho_{3i} =& m_{2i}.\end{aligned}$$

References

[1] I. Blekhman, P. Landa, and M. Rosenblum, "Synchronization and chaotization in interacting dynamical systems," *Applied Mechanics Reviews*, vol. 48, pp. 733–752, 1995.

[2] W. Ren and E. Atkins, "Distributed multi-vehicle coordinated control via local information exchange," *International Journal of Robust and Nonlinear Control*, vol. 17, no. 10-11, pp. 1002–1033, 2007.

[3] I. A. Ihle, J. Jouffoy, and T. Fossen, *Group Coordination and Cooperative Control*, K. Pettersen, J. Gravdahl, and H. Nijmeijer, Eds., ser. Lecture Notes in Control and Information Science. Berlin, Germany: Springer-Verlag, 2006.

[4] N. Chopra, M. Spong, and R. Lozano, "Synchronization of bilateral teleoperators with time-delay," *Automatica*, vol. 44, no. 8, pp. 2142–2148, 2008.

[5] E. Cicek, J. Dasdemir, and E. Zergeroglu, "Coordinated synchronization of multiple robot manipulators with dynamical uncertainty," *Transactions of the Institute of Measurement and Control*, vol. 37, no. 5, pp. 672–683, 2015.

[6] D. J. W. Belleter and K. Y. Pettersen, "Underactuated leader-follower synchronisation for multi-agent systems with rejection of unknown disturbances," in *Proc. American Control Conference (ACC)*, Chicago, IL, USA, Jul. 2015, pp. 3094–3100.

[7] Y. Song and Y. Wang, *Cooperative Control of Nonlinear Networked Systems: Infinite-time and Finite-time Design Methods*, A. Isidori, J. H. van Schuppen, E. D. Sontag, and M. Kristic, Eds., ser. Communications and Control Engineering. Switzerland: Springer, 2019.

[8] E. Nuno, R. Ortega, L. Basanez, and D. Hill, "Synchronization of networks of nonidentical euler-lagrange systems with uncertain parameters and communication delays," *IEEE Trans. Autom. Control*, vol. 56, no. 4, pp. 935–941, 2011.

[9] J. R. Klotz, S. Obuz, Z. Kan, and W. E. Dixon, "Synchronization of uncertain euler-lagrange systems with unknown time-varying communication delays," in *Proc. of the 2015 American Control Conference*, Chicago, IL, USA, Jul. 2015, pp. 683–688.

[10] J. R. Klotz, Z. Kan, J. Shea, E. L. Pasiliao, and W. E. Dixon, "Asymptotic synchronization of a leader-follower network of uncertain euler-lagrange systems," *IEEE Transactions on Control of Network Systems*, vol. 2, no. 2, pp. 174–182, 2015.

[11] S. Avila-Becerril, G. Espinosa-Pérez, E. Panteley, and R. Ortega, "Consensus control of flexible-joint robots," *International Journal of Control*, vol. 88, no. 6, pp. 1201–1208, 2015.

[12] S. J. Chung and J. J. E. Slotine, "Cooperative robot control and concurrent synchronization of lagrangian systems," *IEEE Trans. Robot.*, vol. 25, no. 3, pp. 686–700, 2009.

[13] E. Nuno, R. Ortega, and L. Basanez, "Adaptive control for the synchronization of multiple robot manipulators with coupling time-delays," in *Proc. of the 2010 IEEE/RSJ International Conference on Intelligent Robots and Systems*, Taipei, Taiwan, Oct. 2010, pp. 3308–3313.

[14] G. Chen and F. L. Lewis, "Distributed adaptive tracking control for synchronization of unknown networked lagrangian systems," *IEEE Transactions on Systems, Man and Cybernetics*, vol. 41, no. 3, pp. 805–816, 2011.

[15] Z. Dongya, L. Shaoyuan, and Z. Quanmin, "Adaptive jacobian synchronized tracking control for multiple robotic manipulators," in *Proc. 30th Chinese Control Conference (CCC)*, Yantai, China, Jul. 2011, pp. 3705–3710.

[16] Y. Liu and N. Chopra, "Controlled synchronization of heterogeneous robotic manipulators in the task space," *IEEE Trans. Robot.*, vol. 28, no. 1, pp. 268–275, 2012.

[17] Y. C. Liu, "Distributed synchronization for heterogeneous robots with uncertain kinematics and dynamics under switching topology," *J. Franklin Inst.*, vol. 352, pp. 3808–3826, 2015.

[18] X. Liang, H. Wang, and Y. Liu, "Adaptive task-space cooperative tracking control of networked robotic manipulators without task-space velocity measurements," *IEEE Transactions on Cybernetics*, vol. 46, no. 10, pp. 2386–2398, 2015.

[19] S. Phukan and C. Mahanta, "Position synchronization control of multiple robotic manipulator systems using low pass filter based integral sliding mode," in *15th International Workshop on Variable Structure Systems (VSS)*, Graz, Austria, Jul. 2018, pp. 203–208.

[20] F. G. Ding, Y. Ma, J. Li, and Y. Zhou, "Adaptive synchronization control of multiple vessels with time delays," in *Proc. IEEE Int. Conf. Mech. Auto. (ICMA)*, Tianjin, China, Aug. 2014, pp. 1491–1496.

[21] H. Min, S. Wang, F. Sun, Z. Gao, and J. Zhang, "Decentralized adaptive attitude synchronization of spacecraft formation," *Systems & Control Letters*, vol. 61, no. 1, pp. 238–246, 2012.

[22] G. B. Dai and Y. C. Liu, "Distributed coordination and cooperation control for networked mobile manipulators," *IEEE Trans. Ind. Electron.*, vol. 64, no. 6, pp. 5065–5074, 2017.

[23] A. K. Bondhus, K. Y. Pettersen, and H. Nijmeijer, "Master-slave synchronization of robot manipulators: Experimental results," in *Proc. 16th IFAC World Congress*, vol. 38, Prague,Czech Republic, Jul. 2005, pp. 367–372.

[24] E. Kyrkjebo and K. Y. Pettersen, "Operational space synchronization of two robot manipulators through a virtual velocity estimate," in *Proc. 46th IEEE Conf. Decision Control*, New Orleans, LA, USA, Dec. 2007, pp. 1052–1057.

[25] A. K. Bondhus and K. Y. Pettersen, "Control of ship replenishment by output feedback synchronization," in *OCEANS, Proc. MTS/IEEE*, Washington, DC, USA, Sep. 2005, pp. 1610–1617.

[26] E. Kyrkjebo, K. Y. Pettersen, M. Wondergem, and H. Nijmeijer, "Output synchronization control of ship replenishment operations: Theory and experiments," *Control Engineering Practice*, vol. 15, no. 6, pp. 741–755, 2007.

[27] A. Rodriguez-Angeles and H. Nijmeijer, "Mutual synchronization of robots via estimated state feedback: A cooperative approach," *IEEE Trans. Control Syst. Technol.*, vol. 12, no. 4, pp. 542–554, 2004.

[28] Q. Yang, F. Zhou, J. Chen, X. Li, and H. Fang, "Distributed tracking for multiple lagrangian systems using only position measurements," in *Proc. 19th IFAC World Congress*, vol. 47, Cape Town, South Africa, Aug. 2014, pp. 287–292.

[29] Z. Bin, J. Yingmin, and M. Deyuan, "Distributed observer-based output feedback control for networked robot systems," in *Proc. of the 34th Chinese Control Conference*, Hangzhou, China, Jul. 2015, pp. 7463–7468.

[30] M. Fu, L. Yu, M. Li, Y. Tuo, and C. Ni, "Synchronization control of multiple surface vessels without velocity measurements," in *Proc. IEEE Int. Conf. Mech. Auto. (ICMA)*, Beijing, China, Sep. 2015, pp. 643–648.

[31] A. Marino, "Distributed adaptive control of networked cooperative mobile manipulators," *IEEE Trans. Control Syst. Technol.*, vol. 26, no. 5, pp. 1646–1660, 2018.

[32] E. Nuno and R. Ortega, "Achieving consensus of euler–lagrange agents with interconnecting delays and without velocity measurements via passivity-based control," *IEEE Trans. Control Syst. Technol.*, vol. 26, no. 1, pp. 222–232, 2017.

[33] M. S. de Queiroz, D. Dawson, and T. Burg, "Position/force control of robot manipulators without velocity/force measurements," in *Proc. IEEE Int. Conf. Robot. Auto. (ICRA)*, Minneapolis, Minnesota, USA, Apr. 1996, pp. 2561–2566.

[34] J. Kuvulmaz and E. Zergeroglu, "Robust output feedback controller scheme for a class of uncertain nonlinear systems," in *Proc. of the 17th World Congress The Int. Federation of Automatic Control*, Seoul, Korea, Jul. 2008, pp. 14 125–14 130.

[35] A. Abdessameud, I. G. Polushin, and A. Tayebi, "Synchronization of lagrangian systems with irregular communication delays," *IEEE Trans. Autom. Control*, vol. 59, no. 1, pp. 187–193, 2014.

[36] W. Ren, R. W. Beard, and E. M. Atkins, "A survey of consensus problems in multi-agent coordination," in *Proc. American Control Conference (ACC),IEEE*, Portland, Oregon, USA, Jun. 2005, pp. 1859–1864.

[37] E. Cicek and J. Dasdemir, "Output feedback synchronization of multiple robot systems under parametric uncertainties," *Transactions of the Institute of Measurement and Control*, vol. 39, no. 3, pp. 277–287, 2017.

[38] C. Meyer, *Matrix Analysis and Applied Linear Algebra*. Philadelphia, USA: SIAM: Society for Industrial and Applied Mathematics, 2000.

[39] F. Lewis, C. Abdallah, and D. Dawson, *Control of Robot Manipulators*. New York, USA: Macmillan Publishing Co, 1993.

[40] J. J. Slotine and W. Li, *Applied Nonlinear Control*. New Jersey, USA: Prentice-Hall, 1991.

[41] S. Niculescu, E. I. Verriest, L. Dugard, and J.-M. Dion, *Stability and Robust Stability of Time-Delay Systems: A Guided Tour*, L. Dugard and E. Verriest, Eds., ser. Lecture Notes in Control and Information Sciences: Stability and Control of Time-delay Systems. London, Great Britain: Springer, 1998.

[42] A. Loria, T. I. Fossen, and E. Panteley, "A separation principle for dynamic positioning of ships: Theoretical and experimental results," *IEEE Trans. Control Syst. Technol.*, vol. 8, no. 2, pp. 332–343, 2000.

[43] S. Nicosia and P. Tomei, "Robot control by using only joint position measurements," *IEEE Trans. on Automatic Control*, vol. 35, no. 9, pp. 1058–1061, 1990.

[44] P. Hsu, J. Hauser, and S. Sastry, "Dynamic control of redundant manipulators," in *Proc. 1988 IEEE International Conference on Robotics and Automation*, Philadelphia, PA, USA, Apr. 1988, pp. 183–187.

[45] *3d systems haptic devices*, `https://www.3dsystems.com/sites/default/files/2018-08/3d-systems-haptic-device-en-web-2018-08-03_0.pdf`, [Online; accessed 02-April-2019], 2019.

[46] *Openhaptics sdk*, `https://softwaresupport.3dsystems.com/knowledgebase/article/KA-01405/en-us`, [Online; accessed 02-April-2019], 2019.

[47] A. Mohammadi, M. Tavakoli, and A. Jazayeri, "Phansim: A simulink toolkit for the sensable phantom haptic devices," in *Proceedings of the 23rd Canadian Congress of Applied Mechanics 2011 (CANCAM 2011)*, Vancouver, BC, Canada, Jun. 2011, pp. 787–790.

[48] B. Xian, M. de Queiroz, D. M. Dawson, and M. McIntyre, "Output feedback variable structure-like control of nonlinear mechanical systems," in *Proceedings of the 42nd IEEE Conference on Decision and Control*, Maui, Hawaii USA, Dec. 2003, pp. 368–373.

[49] B. Xian, D. M. Dawson, M. S. de Queiroz, and J. Chen, "A continuous asymptotic tracking control strategy for uncertain nonlinear systems," *IEEE Transactions on Automatic Control*, vol. 49, no. 7, pp. 1206–1211, 2004.

[50] J. Dasdemir and E. Zergeroglu, "A new continuous high-gain controller scheme for a class of uncertain nonlinear systems," *International Journal of Robust and Nonlinear Control*, vol. 25, no. 1, pp. 125–141, 2015.

[51] E. Tatlicioglu, M. McIntyre, D. Dawson, and I. Walker, "Adaptive nonlinear tracking control of kinematically redundant robot manipulators with sub-task extensions," in *Proceedings of the 44th IEEE Conference on Decision and Control and the European Control Conference*, Seville, Spain, Dec. 2005, pp. 4373–4378.

[52] H. Seraji, "Configuration control of redundant manipulators: Theory and implementation," *IEEE Transactions on Robotics and Automation*, vol. 5, no. 4, pp. 472–490, 1989.

[53] E. Zergeroglu, D. Dawson, I. Walker, and A. Behal, "Nonlinear tracking control of kinematically redundant robot manipulators," in *Proc. of the American Control Conference*, Chicago, Illinois USA, Jun. 2000, pp. 2513–2517.

[54] E. Zergeroglu, H. Sahin, U. Ozbay, and U. Tektas, “Robust tracking control of kinematically redundant robot manipulators subject to multiple self-motion criteria,” in *Proc. of the 2006 IEEE International Conference on Control Applications*, Munich, Germany, Oct. 2006, pp. 2860–2865.

Publications From the Thesis

Contact Information: ecicek@yildiz.edu.tr

Papers

1. E. Cicek and J. Dasdemir, “Adaptive output-feedback synchronisation of electromechanical systems under time-varying communication delays,” *International Journal of Control*, pp. 1–12, 2018. DOI:10.1080/00207179.2018.1556809

Conference Papers

1. E. Cicek and J. Dasdemir, “Gemilerin Ağ Tabanlı Senkronizasyonu ve Yörünge Takip Denetimi”, *Otomatik Kontrol Türk Milli Komitesi Konferansı, (TOK’17)*, Istanbul, 21-23 Sept. 2017, pp. 65-71.

Projects

1. TUBITAK 3001 - Başlangıç AR-GE Projeleri Destekleme Programı, "Endüstriyel Robot Manipülatörlerinin Zaman Gecikmesi Altında Çıkış Geri Beslemeli Senkronizasyonu", Project No:217E084, 2018-2019.